Report on

River shifting analysis and flow modelling study of Ganga river from Rishikesh to Anupshahar

आपो हिष्ठा मयो भुवः

National Institute of Hydrology

Roorkee

March 2020

Study Group

Pankaj Mani, Scientist F

Rakesh Kumar, Scientist G,

J. P. Patra, Scientist D

Preface

In view of the directives of Governing Body of NIH, a 3-year comprehensive study to evaluate and understand the river dynamics and morphological characteristics is proposed during 16th RCC of CFMS, Patna. in the 2016. The site Anupshahar is facing continuous erosion threat on the right bank of river Ganga. Thus, the study entitled "River shifting analysis and flow modelling study of Ganga river from Rishikesh to Anupshahar" is included as internal study during 2016-2019. However, during 19th RCC, the duration of the study was extended for one more year upto March 2020. The various components of the study are; satellite image based river shifting analysis, evaluating flow hydrodynamics and morphological behaviour of river through suitable modelling. The temporal analysis of satellite data has been used river bank demarcation during various year between 1997 to 2015. In this study, the IRS images procured from NRSC, Hydrabad have been used. The entire study stretch is covered in four scenes of LISS III data. The locations of large shift are identified and the identified locations, detailed analysis have been carried out using high resolution LISS IV satellite data. GIS analysis is carried out to investigate the river shifting pattern and its year-wise trend analysis. The hydrodynamic (HD) modelling of the river provides the water surface profile and other flow characteristics corresponding to design basis flood near Anupshahar. For the flow model study, 103 surveyed river cross sections (between Rishikesh to Kachhalabridge in the stretch of 334 km) and hydrological data of the four gauging sites viz. Rishikesh, Gurumukteshwar, Narora and Kachhalabridge have been used. For a smaller stretch of river bwteen Garhmukteshwar to Kachala bridge, curvilinear grid based morpho-dynamic flow modelling has been carried out in MIKE 21C. The river stretch is divided into 1484x 107 grids and using the surveyed river sections, bathymetry has been developed. The model is

calibrated and validated with 2013 monsson data. The sediment balance analysis for 2013 flow model has been carried out and river stretches of erosion and sedimentation have been identified. MIKE 21C model is simulated for 25- and 100- year flood and various flow attributes like maximum flood level, flooding depth, sediment concentration, sheer stress etc have been estimated. For these two flooding conditions, the short term morphological behaviours of the river has also been simulated and reported.

Contents

List of Figures

List of Tables

1 INTRODUCTION

The flow in alluvial river is a dynamic process in temporal as well as spatial domain. River erosion (sedimentation) is a natural and inevitable phenomenon of river which involves the removal of materials from the banks/ bed of a river. It causes channel shifting, creation of channels during floods, bank slumping due to undercutting and local scour from turbulence. Irregular flooding and fast riverbank shifts seriously disrupt human settlement and activities. Erosion causes havoc in lives and livelihoods as loss of land is involved. River morphology changes with time and is affected by river discharge, velocity, sediment load, sediment characteristics and the composition of bed and bank material apart from varied geological controls. In response to various types of anthropological disruption, Indian rivers have also experienced a significant channel alteration during the last centuries, particularly in the last few decades following increase in population and consequently induced pressure on land for agricultural and other developmental activities. The rivers of India have certain unique features because they go through large seasonal fluctuations in flow due to uneven rainfall pattern during the year (Kale 2002). During the past ten years, in many fluvial systems, river dynamics have been considerably affected by human disturbances such as land use changes, urbanization, channelization, dams, diversions, gravel and sand mining (Gregory 2006). In India, flood affected area is first estimated by the Rashtriya Barh Ayog (RBA) in 1976 as 40 MHa. Further in 2006, the XI Plan Working Group on Water Resources compiled the area liable to floods as 45.64 MHa and subsequently in 2011 revised the assessment to 49.815 MHa (through XII Plan Working Group) based on the flood damage data reported by the States for the period 1953-2010 (GFCC, AR 2011). The erosion problem in the alluvial flood plain of the Ganges and the Brahmaputra River systems are chronicle due to meteorological and geological contentions. This study is specific to a reach of river Ganga and therefore discusses the genesis of erosion problem in Ganga basin. River Ganga is defined herein as comprising of six main head-streams originating in the Himalayas, namely the Alaknanda, Dhauli Ganga, Nandakini, Pinder, Mandakini and Bhagirathi rivers starting from their feeding glaciers up to their respective confluences at Vishnu Prayag, Nand Prayag, Karn Prayag, Rudr Prayag, Dev Prayag and Rishikesh (together comprising the Upper Ganga segment), the subsequent main stem of the river downstream from Rishikesh to Varanasi (the Middle Ganga segment) and the final stretch from Varanasi to Ganga Sagar (the Lower

Ganga segment). Among these segments, the headstreams are fast-flowing mountainous rivers cutting through deep gorges and narrow valleys, whereas the Middle Ganga stretch meanders through relatively flat plains, with annual floods often covering vast expanses on both sides of the river. The lowermost part of the Lower Ganga segment tends to be braided, especially in the delta region near the Bay of Bengal where sea tides affect the river flow (GRBM, 2013). The upper courses are noted predominantly for deep erosion i.e., bed retrogression. The scoured material is carried downstream by the flow and the middle courses have evidence of both erosion and aggradation. The lower reaches where the bed slope is flatter and velocities are low, accumulation process i.e., sedimentation and accretion of the river bed is predominant. At the same time due to meandering, erosion and sedimentation take place simultaneously. (GFCC, AR 2019). In the middle stretch of the Ganga, the river changes its course due to large seasonal variation of flow and sediment discharge on annual cycle and also extreme events in specific years. Bank erosion refers to the erosion of sediment from bank wall under turbulent flow conditions. The eroded bank materials move laterally towards the channel or in the downstream direction. The channel migration due to bank erosion, downcutting, and bank accretion is the natural adjustment mechanism of alluvial channels of dynamic non-equilibrium. When the flow velocity decreases, the suspended sediments deposit near or on the river banks known as riverbank accretion. Fluvial sediment transport dynamics, basin sediment yields, and floodplain destruction and construction are largely determined by bank erosion and accretion processes. Thus both of them play very significant role in the evolution of channel, especially along the alluvial reaches. Because of bank erosion, a series of environmental, socio-economic and engineering problems may occur, such as erosion of existing riparian, agricultural land, rural and urban land, damage to hydraulic structures, transport network, etc. So, understanding the nature of bank erosion and accretion is necessary to manage the alluvial rivers. Anupshahr is a major town in Bulandshahar district of Uttar Pradesh, located on right bank of the river Ganga. The town is facing continuous erosion threat from the right bank of river Ganga. Several flood protection and anti-erosion works have been carried out in the area to protect the township (GFCC, 2010, http://www.cwc.gov.in/sites/default/files/102%20to%20104meeting.pdf), although the problem still persists. Studies of river flow dynamics and geomorphological characteristics are important for understanding the river behaviour. The site specific understanding would be helpful in planning and designing of suitable anti-erosion works and the river training work for protection of the area. In the 76th Governing Body meeting of National Institute of hydrology (NIH) held on 7th January, 2016 and again in 35th meeting of

NIH Society held on 10th March, 2016, it was decided to take up a study to investigate the erosion problem of river Ganga at Anupshahar. Accordingly the study was planned with following objectives:

1. River shifting study-To evaluate location, magnitude and trend of shifting through delineation of river bank line using temporal satellite image through change detection.
2. Development of hydrodynamic river flow model – To estimate the river surface water profile for the design flood and computation of flow parameters like maximum flow velocity, flow depth etc.
3. Morphodynamic modelling for river sediment transport study and Sediment balance study in the river stretch.

2 LITERATURE REVIEW

Three major components study are (i) satellite data based river shifting analysis, (ii) development of river flow model and (iii) development of morphodynamic model for the study reach. Hence the literature review is also divided into three sections.

2.1 Satellite based river shifting analysis

Satellite remote sensing techniques have been used frequently for generating useful information related with river engineering. The remote sensing data are accurate and time and cost effective and can be obtained without human interventions which make it more reliable. High resolution images are used in delineating recent river configuration, temporal shifting of river course, identification of erosion/ deposition zone, drainage congestion area etc. These information, in turn, can be used for identification of vulnerable erosion reach, planning of bank protection work and drainage improvement work etc. Availability of temporal data over the same area are used for monitoring the performance of existing flood protection works and other morphological applications.

In earlier river morphological studies direct field measurements were done to measure bank erosion rate at specified time intervals. Subsequently, use of topographical maps and aerial photographs were adopted and now with availability of high resolution short interval multi-satellite data and advancement of GIS, it has been widely used for spatio-temporal monitoring of bank erosion and accretion phenomena (Mukherjee et al., 2017). Several researchers have carried out river shifting analysis using satellite remote sensing images and GIS technique. Some important studies are being summarised in following paragraphs.

Using temporal satellite data and GIS technique, Winterbottom and Gilvear; 2000 predicted the probability of river bank erosion in the Regulated River Tummel, Scotland. Mani et al. 2003 have carried out river bank erosion study of a part of the Majuli River-Island, India, using Survey of India (SOI) toposheets and Indian Remote Sensing (IRS) satellite data. Bhakal et al., 2005 carried out estimation of bank erosion in the river Brahmaputra near

Agyathuri using satellite data. Sharma et al. measured the sequential bankline migration due to the effect of bank erosion and accretion of Burhi Dihing River in India, applying SOI topo sheets and IRS satellite data. Bartley et al. (2008) monitored the rate of bankline erosion of Daintree River, Australia by employing the methods of erosion pins, bench marked cross sections and historical aerial photos. In the Western Gangetic Plain area, Rana et al. (2009) studied the nature of bank composition of Rapti river and its susceptibility to bank erosion as well as the different mechanisms for bank erosion on Rapti river. Similarly, Singh and Awasthi (2011) gave a detailed account of flood-induced bank erosion of Ghagra river. Ahmed and Fawzi (2011) investigated the evolution of meander bend and associated bank erosion of the Nile river between Sohag and El-Minia, Egypt. Yao et al. Baki and Gan (2012) measured the trend and rates of bank erosion and accretion of the braided Jamuna River using Landsat images from 1973 to 2003 and also established the impact of variable discharge and width of the river on the erosion and accretion processes. Sinha and Ghosh (2012) made use of IRS-LISS III data, SOI toposheets, Rennell's Map of 1776 and US Army survey maps for GIS-based assessment of temporal dynamics of channel morphology and bank erosion of the Ganga river. Sarma and Acharjee (2012) investigated the trend of bank erosion and explained the role of neotectonic activity on bank erosion of the Brahmaputra river around Kaziranga National Park, Assam, India. Thakur (2012) studied the bank erosion of the Ganga river in the upstream of Farakka barrage up to Rajmahal by using Landsat and IRS satellite images. Nardi et al. (2013) used the hydrodynamic models (1-D and 2-D) combined with shear stress model in order to estimate the bank erosion of the river Cecina in Tuscany. Bandyopadhyay et al. (2014) proposed a Remote Sensing-GIS based model for determining the bank erosion vulnerability zones of the Haora River, Tripura, India. Bhowmik and Pan (2014) identified the vulnerable areas of bank erosion by overlay analysis in GIS. Ashraf et al. (2016) determined the role of bank erosion on the evolution of river channel and also assessed the flood-induced bank erosion during the monsoon season in river Chenab . Pal et al. (2016) predicted the vulnerability of bank erosion along the meander bends of the Bhagirathi-Hugli river of lower Ganga plain, India, by applying channel avulsion modeling.

2.2 Hydrodynamic River flow modelling

Several authors have reviewed the computational methods which are commonly used for flood inundation and flow simulation based on the solution of relevant equations (Bates *et al*., 2005). The numerical models with 1D approximation are mostly based on the finite

difference method (Cunge *et al*., 1980) and the finite element method (Sen and Garg, 1998). The finite difference method is more popular due to comparatively less computational effort. The 1D models, though simple to use and provide information on bulk flow characteristics, fail to provide detailed information regarding the flow field. Hence, attempts have been made to model the 2D nature of floodplain flow. However, in the absence of sufficient, accurate and well distributed calibration and validation data sets, the 1D models predict the bulk flow characteristics comparable to the 2D models (Horritt and Bates, 2002). Dhondia and Stelling (2002) described the 1D-2D model SOBEK (Rural/Urban) developed by the laboratory at Delft Hydraulics. The MIKE 21 has been dynamically linked to the MIKE 11 model, into a single package called MIKE FLOOD developed at the Danish Hydraulic Institute is also widely used for river hydrodynamic modelling (Rungo and Olesen, 2003). Tingsanchali and Karim (2005) conducted flood hazard and risk assessment in southwest region of Bangladesh for flood mitigation. Usul and Turan (2006) studied the hydrodynamic characteristics of the Ulus basin in turkey by calibrating the hydraulic module of the MIKE 11 modeling system with the observed 1991 flood. Then, for the 25-, 50- and 100-year floods the highest water levels in the river are forecasted by integration of the MIKE 11 hydrologic and hydraulic modules. Chatterjee *et al*. (2008) compared the performance of MIKE 11 and MIKE FLOOD models in modelling floods with emergency storage areas. Forster *et al*. (2008) used emergency storage areas for controlled flooding to reduce risk of inundation for downstream areas with higher vulnerability. Patro *et al*. (2009) used MIKE FLOOD model for flood inundation modelling in Delta region of Mahanadi river basin. Pramanik *et al* (2010) carried out hydrodynamic modeling of deltaic reach of river Brahmani located in eastern India using SRTM extracted river cross sections in MIKE 11. Mani et al. (2014) used MIKE FLOOD model to simulate flow for regional and site-specific flooding scenarios considering PMP and PMF of the study area. The study was carried out at a proposed plant site in northern India. To identify the flood protection measures at the plant site, the authors further carried out flood hazard assessment taking into account the flooding characteristics obtained from MIKE FLOOD model output.

2.3 Morpho-dynamic modelling

Two-dimensional numerical models for turbulent flow and sediment transport can efficiently perform long-term simulations of river morphology including impact of river engineering structures. These tools have been used in numerous projects around the world for last three

decades or so. National Sedimentation Laboratory of ARS-USDA for the U.S. Army Corps of Engineers (Langendoen, 2001) carried out a bench marking research study of the present state of two-dimensional modelling tools for river morphology. The five modelling software that could fulfill the benchmarking criteria set out in their research are the following:

- **MIKE 21 C developed** by DHI in Denmark.
- **Delft2D-Rivers** developed by Deltares in the Netherlands.
- **CCHE2D** developed by NCCHE in the University of Mississippi in USA.
- **TABS-MD** developed by US Army Corps of Engineers in USA.
- **TELEMAC** developed by EDF in France.

Among the above only, MIKE 21 C and Delft2D generally fulfilled all the criteria of the terms of reference of bench marking. These two softwares contain most rigorous theoretical foundation for modelling, sediment transports and morphological change in curved channels and bank migration through bank erosion. The capabilities of a Morphodynamic Models are:

1. Model for bend: 2-d hydrodynamic model in curvilinear grid
2. Model for a meander: 2-d hydrodynamic and sediment transport model in curvilinear grid.
3. Model for meander and bifurcation: 2-d hydrodynamic and sediment transport model in curvilinear grid.
4. Computation of scour and deposition, bank erosion, change in river plan form.
5. Prediction of morphological changes in the stream.
6. To estimate the design criteria for the anti-erosion/ river training/ flood protection works such as design flow velocity, flow depth and erosion rates etc. for a river or stream.

Several researchers have carried out hydrodynamic and sediment transport analysis of alluvial river stream using MIKE 21 program. Some important works are summarised in following paragraph.

Christensen et al (2006) the author developed a quasi 3D generalized mathematical modeling system using MIKE 21 C for the hydrodynamic and morphological simulation for the River Loire and Labe. After the simulation the water level (H) vs. discharge (Q) graph is plotted and the relation between water level and discharge (Q-H) relation is found.

Rahman et.al (2014) have assessed the morphological changes of the major rivers of Bangladesh due to anticipated climate changes using the mathematical modelling tool MIKE 11 and MIKE 21 C. They found that the sea level rise will slow down and thus there is likeliness of large scale sedimentation. However, they used data for one monsoon season of only.

Mahmood Khan and Dr. Mohammad Mostafa Ali (2016) gave the correlation between the bank shear stress and river discharge and used this relation to predict the bank erosion rates (yearly). The author selected the Jamuna River as the study area and developed a 2-dimensional numerical model using MIKE 21 C and simulated for the return period 2.33 years, 10 years and 100 years to estimate the erosion rates. The bank shear stress is calculated by the bank erosion rates and then correlated it with the simulated hydrologic events (obtained from the model).

Tayade et al (2016) In this paper the author developed a 2D mathematical model for a braided river and uses this model to obtain the critical location of erosion and design parameters for the anti erosion works for a braided river. The curvilinear grid (500 X 120 cells) of braided river for a stretch about 42 km is developed using MIKE 21 C grid generator. The MIKE 21 C is used to create the hydrodynamic model and run for the different discharges from 10,000 m3/s to 60,000 m3/s without sediment inflow and the water surface profile and velocity profile is represented. Then the critical velocity is calculated at discharge and decided to design the anti-erosion works with velocity 3.5 m/s. After the analysis the author gave suitable design of revetment and launching apron using geobags using IRC: 89-1997, IS 14262:1995 and IS 13195:1991.

Morianou et al (2016) In this work the author developed a 2D hydraulic model for the simulation of water depth and flow velocity of the downstream section of the Koiliaris River in Crete (Greece). The orthogonal curvilinear grid of 6750 cells is made and then MIKE 21 C software is used for the simulation. 2D maps of water depth and flow velocities are presented. Manning coefficient (n) is used for the model calibration for the stretch from 1-10-2010 to 30-09-2011.

Morianou et. al (2017) used MIKE 21 C to obtain hydrodynamic and sediment transport changes separately for rectilinear and curvilinear grids for the 36 km stretch of the Koiliaris River, Crete. After comparison of these two models, they found that curvilinear grid modelling approach gives better results than rectilinear are and also the results are in better agreement with the final data. They also found that the curvilinear grid method provides good flow analysis near the bends of the river and requires less computation time and creates smaller size output files. In this paper the comparison between rectilinear and curvilinear grid modeling approach for river flow and sediment transport simulation is proposed by author. The curvilinear grid follows the bank lines accurately and shows better resolution near the bank boundary than the rectilinear grid. The MIKE 21 C is used to obtain the hydrodynamic and sediment transport changes in rectilinear and curvilinear grid separately. The 2D-mathematical model for hydrodynamic and sediment transport is developed for The Koiliaris River, Crete of length 36 km. by using a dense curvilinear grid (1000X25 cell) with using highly accurate DEM of resolution of 1mx1m. The results obtained from the simulation are then calibrated with the field observation data and these models are compared. After the analysis it is found by the author that the curvilinear gird modeling approach gives the better result than the rectilinear one and better agreement with the field observation data. In addition the curvilinear grid provide good flow analysis near the banks of river and requires less time of computation and it creates the smaller size output files.

Kourgialas et al (2017) developed a model to analysis of climate change impact on hydrodynamic and morphological parameter in Mediterranean stream. The variation of water depth, flow velocity and morphological characters i.e. sediment transport and bank erosion etc. are simulated using MIKE 21 C for orthogonal curvilinear grid with very high resolution DEM 1mx1m was used. Time series discharge data and suspended sediment concentration is used as input then model is developed and calibrated for the observed bank erosion measurement at different locations. Then this model is used to predict the flow and bank erosion for the next ten years (2017-2027).

The review shows that in most of the studies the behaviour of small alluvial streams is described. Most of the studies are confined to limited extent and intended for estimating design parameters for anti-erosion works. The calibration/ validation of the model are either missing or have been carry out using flow data only. A more realistic morphological model could be developed if the sediment data is used for calibration and validation. For Indian conditions, very limited studies are available. Thus, it is decided to carry out a comprehensive

study for Indian terrain condition through development of morphological model based on observed sediment and flow data.

In this background, this study has been carried out for a larger alluvial river of India having considerable silt load and a very long stretch of about 142 km is modelled. The model is used for quantitative estimation of erosion and deposition prone areas. The study also estimates the flow and morphological behaviour of river for three flooding condition including peak flood. Further, the model calibration and validation has been carried out with observed and simulated sediment load and discharge.

3 STUDY AREA

Geographical extent of the study area Anupshahr is located between 78°16'2.814"E and 28°21'25.226"N. It is located on the banks of the holy river Ganges. Anupshahr, also called Anoopshahr, is a small city and a municipal board in Anupshahr district in the state of Uttar Pradesh, India.

3.1 Climate

The climate in Anupshahr is warm and temperate. There is more rainfall in the winter than in the summer in Anupshahr. This climate is considered to be C_{sa} according to the Köppen-Geiger climate classification. The average annual temperature is 25.0 °C in Anupshahr. Precipitation here averages 826 mm. The driest month is April, with 4 mm of rain. With an average of 283 mm, the most precipitation falls in August. June is the warmest month of the year. The temperature in June averages 33.9 °C. January has the lowest average temperature of the year. It is 14.5 °C. There is a difference of 279 mm of precipitation between the driest and wettest months. During the year, the average temperatures vary by 19.4 °C.

3.2 Geography

The Ganga River is one of the most important rivers in the Indian subcontinent. It is a snow fed Himalayan River, heavily laden with detritus and flows sluggishly from west to east. The Ganga River has numerous large and small tributaries, of which the important ones are the Yamuna, the Gandak, the Kosi and the Mahananda. Together they comprise the Ganga river basin which covers the States of Uttar Pradesh, Bihar, West Bengal and parts of Haryana, Rajasthan, Madhya Pradesh and the Union territory of Delhi. The total length of the river Ganga is 2,506 km and its catchment area is 10,73,070 km^2. The average gradient of the river Ganga is 9.5 cm per km in the upstream reaches and slows down to 6 cm per km in Bihar. The normal annual rainfall of Ganga basin varies from about 600 mm to 1900 mm of which more than 80 percent occurs during the South-West monsoon. The rainfall increases from west to east and from south to north. It has an average elevation of 182 metres and area 15$km^{2.}$ The district has a total area of 4512 Km2 with a population of 34, 99,171 persons (Census 2011). The district is about 84 km in length and 62 km is breadth. The district is 237.44 meters above sea level. The location map of the study area is shown in Figure 3.1.

3.3 Extent of study area for river modelling

For hydrodynamic flow modelling the extent of river stretch is govern by the availability and location of hydrological data. For the study stretch, the hydrological data are available for Rishikesh and Kachalabridge tsdy For the river hydrodynamic flow model have been developed for a stretch of Rishikesh The river flow model extent of study

3.1 Data Availability

The study involves development of flow model and morpho-dynamic model for which different types of data have been used. The hydrological data nd river cross sections are required for development of hydrodynamic model while additional data of sediment are needed for morphodynamic modelling. Further, the satellite images have been used river bank shifting analysis. The details of data used in this study are discussed in following section.

3.1.1 Hydrological data

In the study stretch of river Ganga from Rishikesh to Kachalabridge site, several hydrological observation (HO) sites are maintained by Central Water Commission. (CWC). The data for Discharge (D) , Silt (S) and Water Quality (Q) are observed at few sites while gauge (G) data is observed for all the sites. The details of HO sites are shown in Figure 3.5 and extent of data available and used in the study are given in Table 3.1.

Table 3.1: Availability of hydrological data

Name of Site	Data type	Frequency	Period of availability
Rishikesh	GD Silt	Daily 10 daily	01 Jun 2010-31 Oct 2013
Dharamnagari	G	Daily	
Garhmukteshwar	GD S	Daily 10 daily	
Narora Barrage	G	Daily	
Kachalabridge	GD Q	Daily 10 daily	

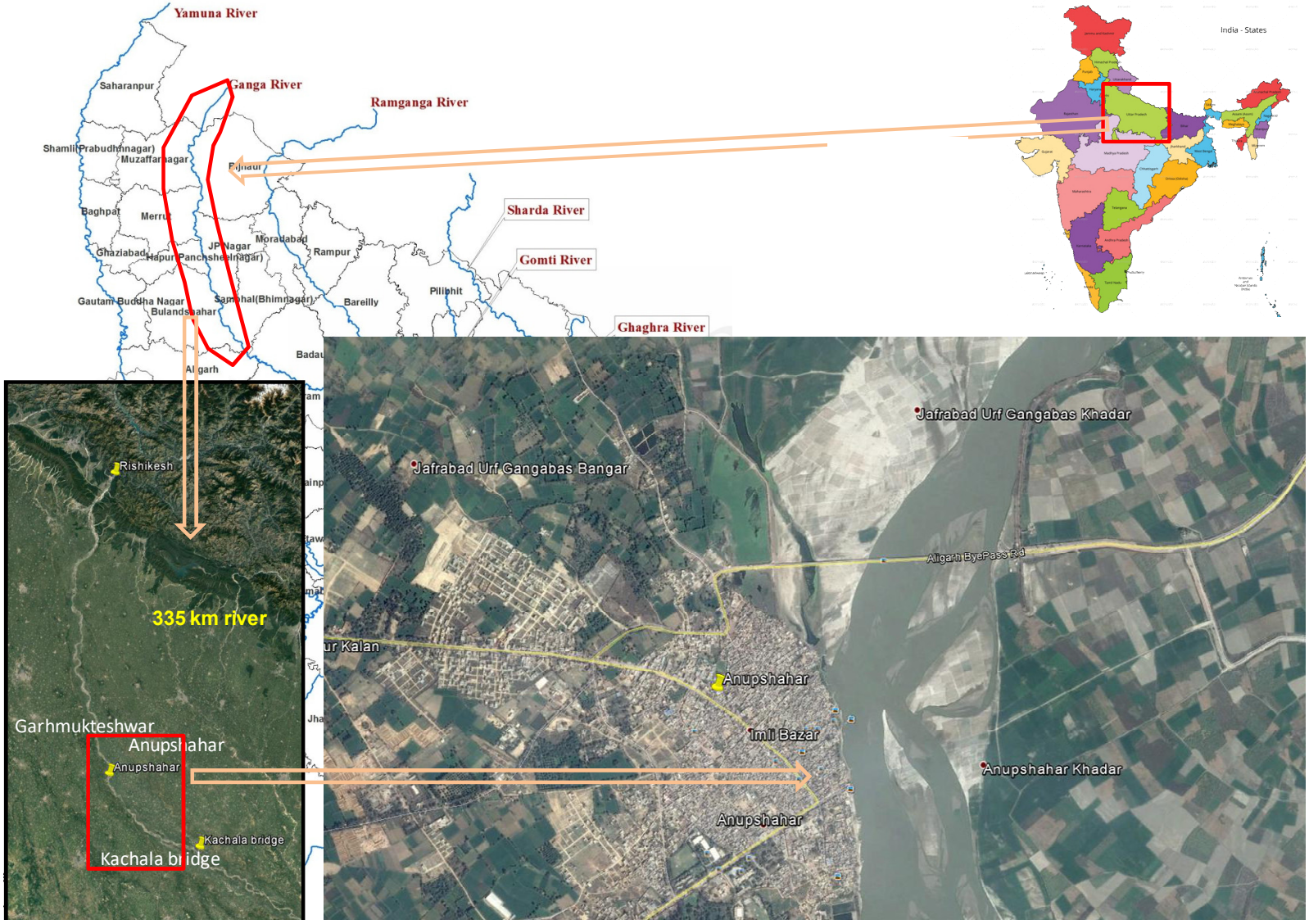

Figure 3.1: Location map of the study area

3.1.2 Design Flood Estimates

The design flood for the river Ganga in its various sub catchments up to Kachalabridge site has been adopted from a separate study carried out by NIH (Estimation of design flood and safe grade elevation for Narora Nuclear Power Plant). The peak floods at Rishikesh, Garhmukteshwar and Kachlabridge gauging sites for various return periods are estimated using the L-moments based flood frequency analysis of annual maximum rainfall data of various rain gauges in the study basin. The analysis gives the value of peak flood of various say 25 or 100 year return period. However, for propose of flood routing and flood inundation modelling the complete hydrograph at 1 hour interval is required. Therefore, PMF hydrograph at Rishikesh, Garhmukteshwar and Kachlabridge are derived from the SUH and PMP data obtained by IMD by dividing the basin in to 15 sub basins as shown in Figure 3.2. The basin model of the study area is prepared in HEC HMS as shown in Figure 3.3 for estimation of flood hydrographs at different locations. Hence with PMF analysis we estimate the shape of the flood hydrograph while with frequency analysis we estimate the magnitude of peak of the various flood estimates. Finally, the PMF flood hydrographs are proportionality multiplied to estimate the design flood hydrographs of various return periods at Rishikesh, Garhmukteshwar and Kachlabridge for various cases as shown in Figure 3.4.

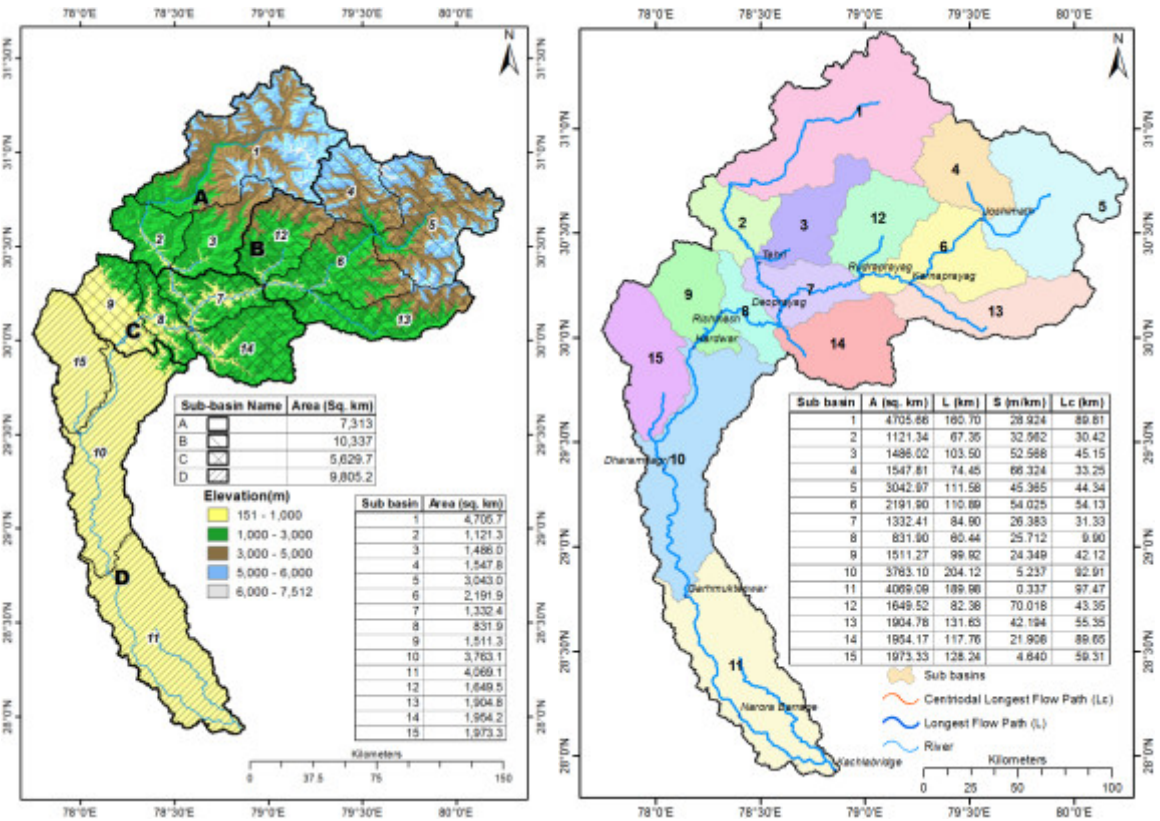

Figure 3.2: Various sub basins of the study area.

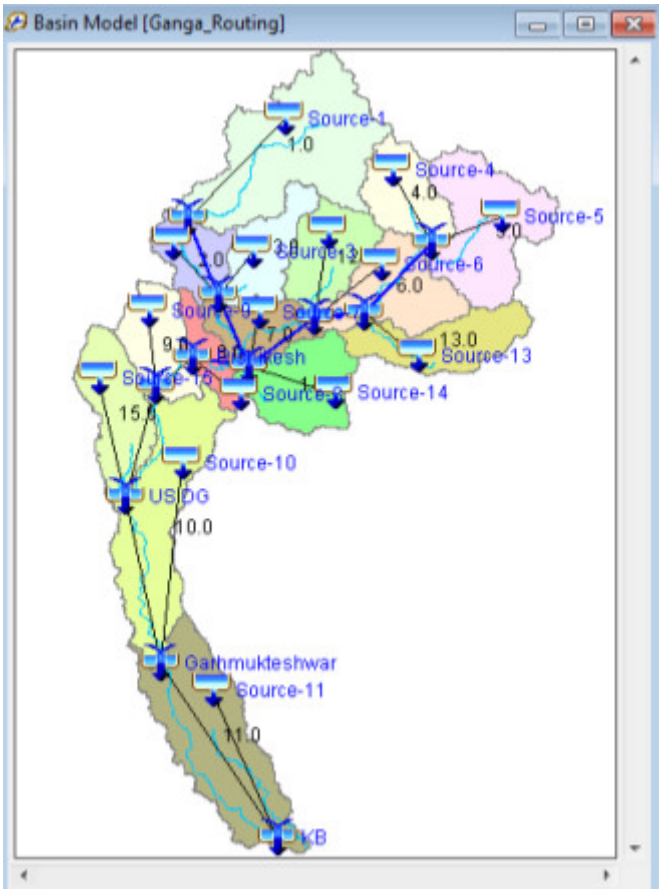

Figure 3.3: Basin model of the study area in HEC HMS

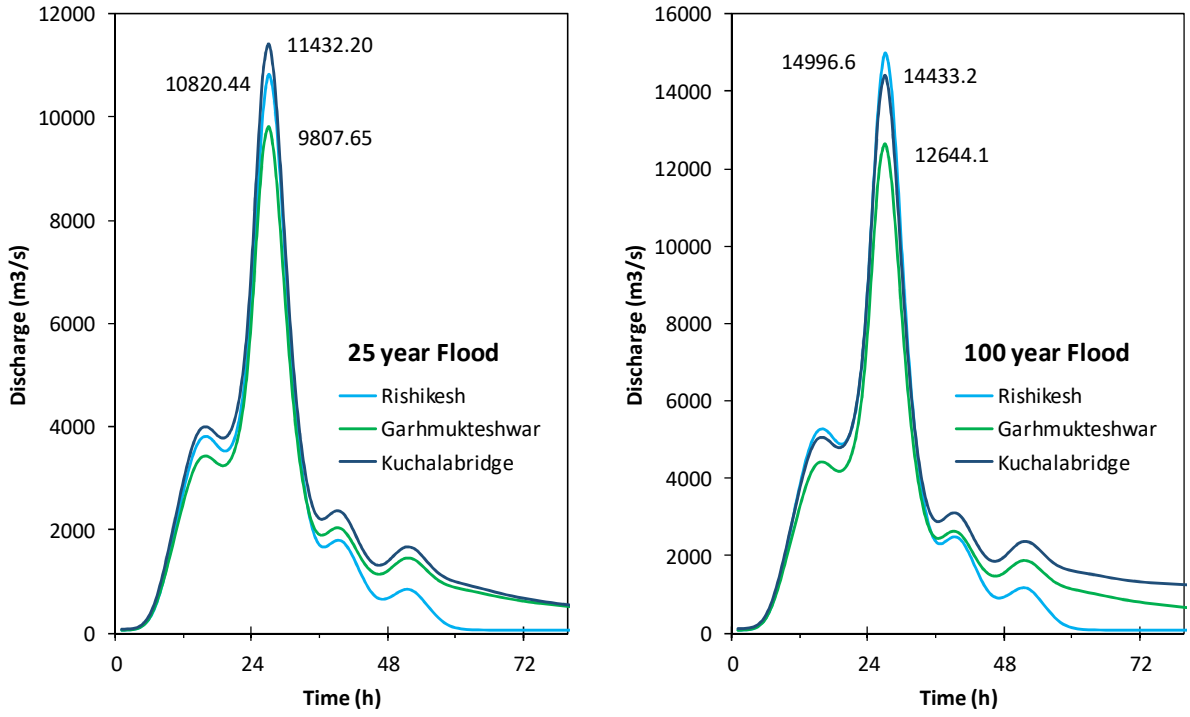

Figure 3.4: Design Flood for 25- and 100- year return period estimated at Rishikesh, Garhmukteshwar and Kachalabridge GD site

3.1.1 Data Availability for River Cross Sections and Digital Elevation Model

For the study reach of river Ganga from Rishikesh to Kachalabridge site, river cross sections data are obtained from CWC (at the GD sites) and data set available in project study of "Estimation of Design Flood and Safe Grade Elevation of Narora Nuclear Plant site carried out by NIH. In the project study, the river cross section was surveyed at an interval of 3-5 km from Rishikesh to Kachlabridge GD site in a stretch of 335 km as shown in Figure 3.5. For 1-dimeniosnal flow modelling from Rishikesh to Kachalabridge, the river sections are used to develop river flow modelling while for morpho-dynamic modelling between Garhmukteshwar to Kachalabridge site, DEM is needed for 2 dimensional modelling. Hence, in addition to river section data, the elevation information (contours and spot levels) available in Survey of India (SOI) toposheets for the study area are used to develop the DEM of the area. The details of SOI toposheets and DEM used in the study area are shown in Figure 3.6 and Figure 3.7.

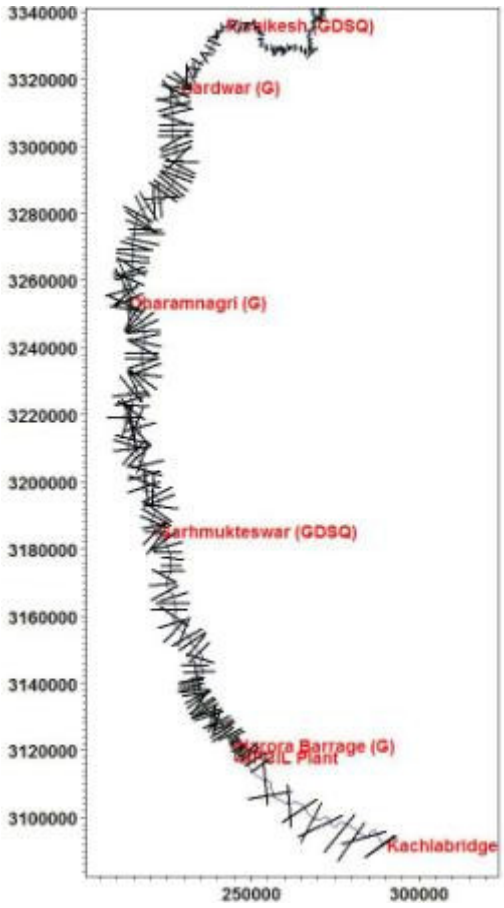

Figure 3.5: Surveyed river cross section between Rishikesh to KachlabridgeGD site.

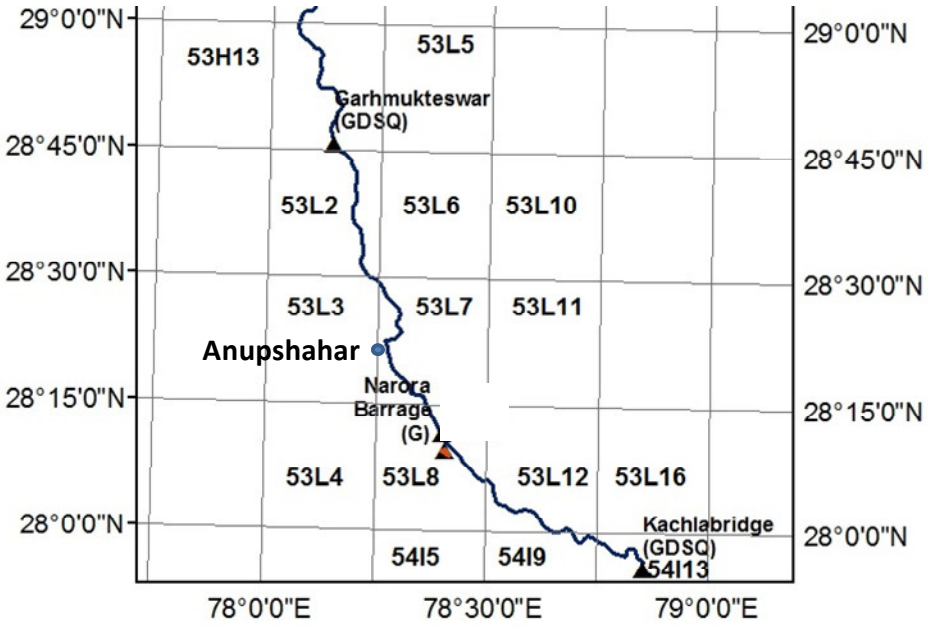

Figure 3.6: Details of SOI toposheet of the study reach for 2D morpho-hydrodynamic modelling

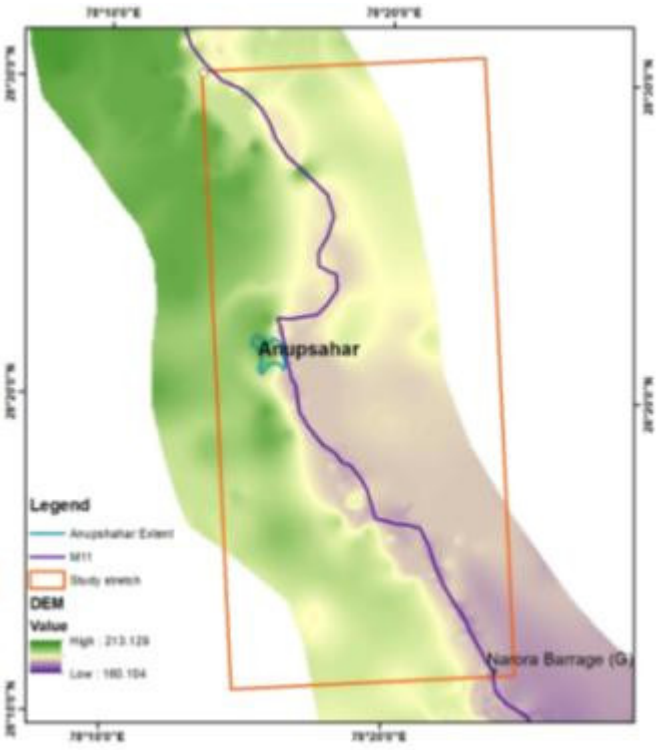

Figure 3.7: Digital elevation model of the study area

3.1.2 Satellite data

The satellite images from Indian Resources Survey (IRS) satellite in optical wavelength region is obtained from National Remote Sensing Centre, Hyderabad. The details of satellite data used in the study are given in Table 3.2.

Table 3.2: Details of satellite images used for river shifting analysis.

Date of Pass	Satellite (IRS)	Sensor	Path/Row/ subscene
30Sep1997	1C	LIS3	99/52/
09Oct1997	1C	LIS3	96/50/
09Oct1997	1C	LIS3	96/50/
14Oct1997	1C	LIS3	97/51/
14Oct1997	1C	LIS3	97/50/
19Oct1997	1C	LIS3	98/52/
19Oct1997	1C	LIS3	98/51/
07Nov1997	1C	PAN	97/50/C0
07Nov1997	1C	LIS3	97/51/
14Oct1998	1C	LIS3	98/52/
14Oct1998	1C	PAN	98/52/B0
08Oct2000	1C	LIS3	99/52/
15Nov2000	1C	LIS3	97/51/
20Nov2000	1C	LIS3	98/52/
04Dec2000	1C	LIS3	96/50/
04Dec2001	1C	LIS3	97/51/
20Aug2002	1C	LIS3	96/50/
01Oct2004	1C	LIS3	97/50/
30Oct2004	1C	LIS3	98/51/
10Oct2005	P6	LIS4	97/50/
23Nov2005	P6	LIS4	97/47/
26Sep2006	1C	LIS3	98/52/
01Oct2006	1C	LIS3	99/52/
10Oct2006	1C	LIS3	96/50/
10Oct2006	1C	LIS3	96/50/
15Oct2006	1C	LIS3	97/51/
15Oct2006	1C	LIS3	97/50/
09Oct2008	P6	LIS4	97/56/
16Nov2008	P6	LIS4	97/24/
08Oct2011	P6	LIS3	96/50/
30Oct2011	RS2	LIS4	98/52/B
30Oct2011	RS2	LIS4	98/52/B
30Oct2011	RS2	LIS4	98/52/B
06Nov2011	P6	LIS3	97/51/
11Nov2011	P6	LIS3	98/52/

Date of Pass	Satellite (IRS)	Sensor	Path/Row/ subscene
13Nov2011	RS2	LIS4	96/51/B
13Nov2011	RS2	LIS4	96/51/B
13Nov2011	RS2	LIS4	96/51/B
16Nov2011	P6	LIS3	99/52/
18Nov2011	RS2	LIS4	97/51/C
18Nov2011	RS2	LIS4	97/51/C
18Nov2011	RS2	LIS4	97/51/C
02Dec2011	RS2	LIS4	96/50/B
02Dec2011	RS2	LIS4	96/50/B
02Dec2011	RS2	LIS4	96/50/B
25Sep2012	RS2	LIS4	97/51/D
06Dec2012	RS2	LIS4	97/51/A
06Dec2012	RS2	LIS4	97/51/A
06Dec2012	RS2	LIS4	97/51/A
04Oct2015	RS2	LIS3	97/51/
04Oct2015	RS2	LIS4	97/51/D
04Oct2015	RS2	LIS4	97/51/D
04Oct2015	RS2	LIS4	97/51/D
09Oct2015	RS2	LIS3	98/52/
09Oct2015	RS2	LIS4	98/52/B
09Oct2015	RS2	LIS4	98/52/B
09Oct2015	RS2	LIS4	98/52/B
23Oct2015	RS2	LIS3	96/50/
23Oct2015	RS2	LIS4	96/50/B
23Oct2015	RS2	LIS4	96/50/B
23Oct2015	RS2	LIS4	96/50/B
01Dec2015	RS2	LIS3	99/52/
15Dec2015	RS2	LIS4	97/51/A
15Dec2015	RS2	LIS4	97/51/A
15Dec2015	RS2	LIS4	97/51/A
15Dec2015	RS2	LIS4	97/51/C
15Dec2015	RS2	LIS4	97/51/C
15Dec2015	RS2	LIS4	97/51/C

4 METHODOLOGY

The methodology for river shifting analysis using satellite images, 1D river flow modelling in MIKE 11 and morpho-hydrodynamic modelling is discussed in this chapter.

4.1 River shifting Analysis

The basic data used in river shifting analysis are digital satellite images obtain from NRSC, Hyderabad comprising of scenes between the years 1997 and 2015. The study reach is very extensive and therefore multiple of images are used to cover the entire stretch in a pspecific year (various images in nearby dates). The cloud free images are procured and image analysis and processing are carried out to delineate the river bank line. The digital analysis was carried out in the image processing software, 'ERDAS Imagine' and GIS analysis is carried out in ArcGIS 10.0, and finally the river bank line of river Ganga for the years 1997, 2001, 2005, 2011 and 2015 are delineated. The following aspects of methodology used for delineation of the river course using satellite remote sensing data are discussed as follows.

(a) Import and visualization,
(b) Geo-referencing,
(c) Reference System,
(d) Separation of area of interest (AOI),
(e) Delineation of river course from remote sensing data, and
(f) GIS analysis

4.1.1 Import and visualisation

The IRS data of LISS-III sensor have four spectral bands correspond to green (0.52 – 0.59μ), red (0.62 – 0.68μ), NIR (0.77 – 0.86μ) and MIR (1.55 – 1.70μ) while and LISS-IV have green (0.52 – 0.59μ), red (0.62 – 0.68μ), NIR (0.77 – 0.86μ) and MONO/PAN (0.4-0.7μ) band. The spatial resolution for LISS-III sensor is 23.5 m while the spatial resolution for LISS-IV (multi-spectral and MONO) is 5.8 m. The areal extent i.e. swath of the LISS-III scene is 141 km x 141 km and areal extent for LISS-IV is 70 km x 70 km. The study stretch from Rishikesh to Kachalabridge GD sites are covered in multiple scenes of IRS LISS III/ LISS IV images.

4.1.2 Geo-referencing

While using the temporal satellite data, it is required to geo-reference the imageries of different dates in a uniform reference system. These images were first registered using various control points from the Survey of India (SOI) toposheets. Some clearly identifiable features like crossing of roads, railways, canals, bridges etc. were located on both images and were selected as control points. Some points which generated big errors were deleted and replaced by other points so as to obtain satisfactory geo-referencing. The error in geo-referencing should be less than one pixel. Subsequently, other satellite images are geo referenced in respect to initially registered satellite images.

4.1.3 Separation of area of interest (AOI)

The sizes of the full scenes of the satellite remote sensing data were large in comparison to the study stretch along river Ganga, hence, the study area is separated from the full image using a utility in the ArcGIS software, namely, area of interest (AOI). A polygon was digitised which covered the entire study area including sufficient buffer around it. Separation of the area of interest from the full scene results in less computational time and computer storage.

4.1.4 Delineation of river course from remote sensing data

The remote sensing data are analysed to determine the water spread area and river sand which together represents the river course. There are two techniques of feature classification from satellite images i.e. visual and digital. The visual techniques are purely based on the interpretative capability of the analyst and it is not possible to use the information of different bands, after the visual product is generated. Around the periphery of the water spread area, the wet land appears very similar to the water pixels and it becomes very difficult for the eye to decide whether a pixel near the periphery is to be classified as water or land. Using digital techniques, the information of different bands can be utilised to the maximum extent and consistent analysis can be carried out over the entire area. In the present study, digital interpretation technique was used for delineation of the river bank line. Supervised classification of satellite images for identifying water pixel and sand pixel is carried out and two individual classes are identified. Later on, these two class (Water pixel and river sand) are merged together to represent, the river course. Entire image processing exercise is carried out in “ERDAS Imagine” software. In the visible region of the spectrum (0.4 – 0.7 μm), the transmittance of water is significant and the absorptance and the reflectance are low. The

absorptance of water rises rapidly in the near-IR where both, the reflectance and transmittance are low. At near-IR wavelengths, water apparently acts as a black body absorber. Deep water bodies have quite distinct and clear representation as compared to shallow water. Shallow water can be mistaken for soil while saturated soil can be mistaken for water, especially along the periphery of the surface water features. To differentiate water pixels from the adjacent wetland pixels, comparative analysis of the digital numbers in different band is usually carried out. The flow chart for supervised classification scheme for river is shown Figure 4.1.

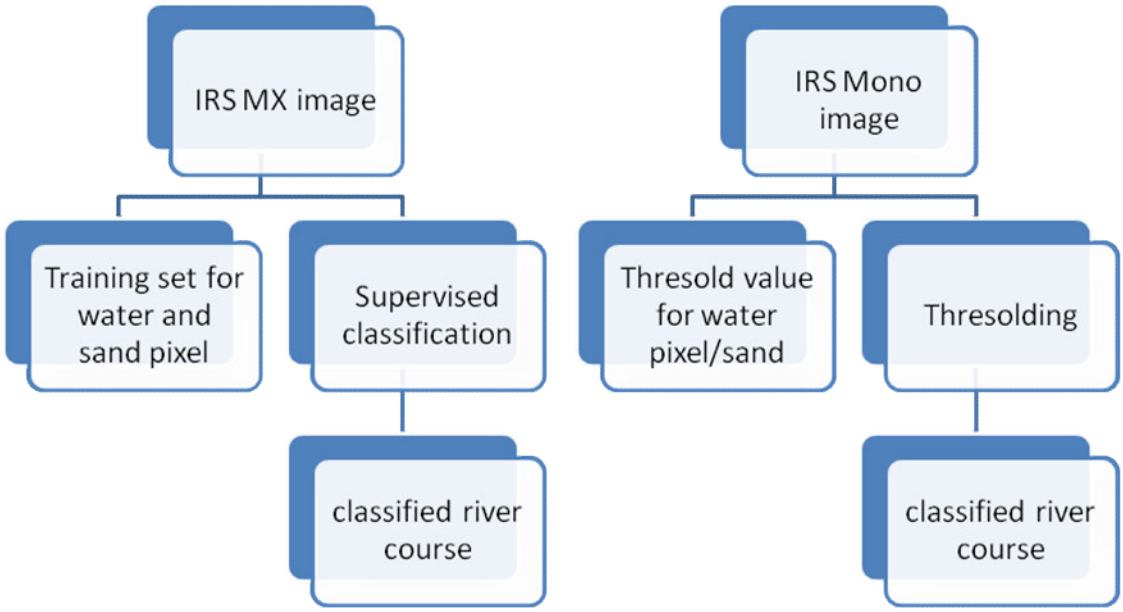

Figure 4.1: Flow chart for extracting river course using digital analysis of IRS satellite images

4.1.5 GIS Analysis

The various layers of river course for different years prepared using supervised classification of multi-spectral image or thresolding technique of monochromatic (PAN) images are analysed in GIS (ArcGIS). The road alignment extracted as linear feature from 1997 (the first image on temporal line) is verified in successive image. As all the images are geo-referenced in same projection system, the overlay are ready for shifting analysis. Through over analysis, the critical locations where shifting has taken place were identified. The details of the shifting characteristics of river Ganga at the critical locations are first identified. Further, detailed

studies were carried out for estimating the shifting pattern of river Ganga at these critical locations using the temporal satellite data. For study of shifting course of the river Ganga, a road running almost parallel to the river has been identified and used as reference line for estimating the shift of river bank line. Along this line, the position of both river banks at every half kilometer is measured (as Y coordinate). The difference of Y co-ordinates at a particular chainage in any two images gives the shift of the river bank during the acquisition dates of two images.

4.2 Flow modelling by Mike 11 hydrodynamic model

MIKE 11 is a versatile and modular engineering tool for modeling hydrodynamic conditions in rivers, lakes/reservoirs, irrigation canals and other inland water systems. It is a fully dynamic modeling tool for the detailed analysis, design, management and operation of both simple and complex river and channel systems (DHI, 2004). The hydrodynamic (HD) model is the nucleus of the MIKE 11 modeling system and forms the basis for simulation of flood inundation. The HD model is capable of simulating unsteady flow in a network of rivers. The result of HD simulation consists of a time series of water level and discharges at various points along the river system. MIKE 11 HD provides a choice among three different flow descriptions, namely kinematics, diffusive and dynamic wave approaches. MIKE 11 HD solves the Saint-Venant equations to obtain the hydrodynamic state of the river networks. The post-processor tool of MIKE 11 is the MIKEVIEW, which helps to view and analyze the results through graphical and animated interfaces.

4.2.1 Governing Equations

The governing equations in MIKE 11 are 1-D (one-dimensional) and shallow water type, which are the modifications of basic Saint-Venant equations. These are transformed to a set of implicit finite difference equations, and solved using double sweep algorithm (Abbot and Ionescu, 1967). The computational grid comprises of alternating Q and H points automatically generated by the model, on the basis of user requirements. Q points are always placed midway between neighbouring H points (Figure 4.2). H points are located at cross sections or at equidistant intervals, in between if the distance between cross-sections is greater than the maximum space interval, dx specified by the users (dx=1000 m in the present setup).

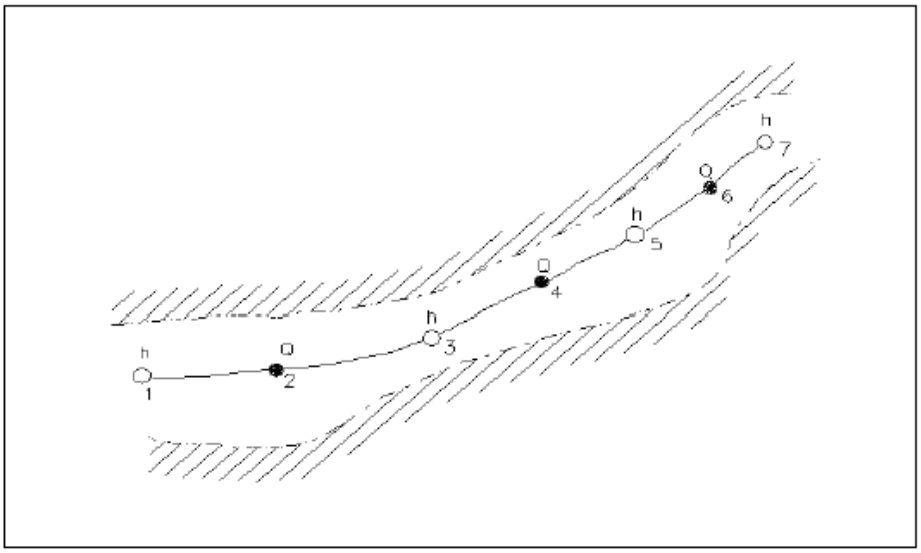

Figure 4.2: MIKE 11 computational grids

4.2.2 MIKE 11 model setup

In the present study, the MIKE 11 model setup is prepared by defining following five input parameters:

1. Layout of river network
2. Cross section data definition
3. Defining hydrodynamic boundary conditions
4. Setting the HD parameters
5. Fixing the simulation parameters

4.2.2.1 Layout of river networks

The layout of MIKE 11 river network is prepared from the digital SOI topographical map of the study area in the MIKE 11 network editor tool. The Ganga River extends from Rishikesh to Kachla bridge GD site. The catchment area draining directly to Ganga River between Rishikesh to Kachla bridge is modelled through lateral uniformly distributed inflow between the two river ends. While digitizing the drains in downstream directions, the length is computed automatically and accordingly Chainage of various points on the drains are defined. The chainage at Rishikesh GD site is 99678 m (Zero Chainage is considered at Tehri dam). The Ganga River is digitized upto Kachalabridge GD site where the Chainage is 433813 m. There are three barrages in this stretch; (i) Bhimgoda barrage (Upper Ganga Canal

System) at Chainage 124320 m, (ii) Raoli barrage (Middle Ganga Canal System) at Chainge 203325 m and (iii) Narora barrage (Lower Ganga Canal System) at Chainge 369251 m.

4.2.2.2 Cross section data definition

The topographical description of the area to be modelled is achieved through the cross-sections of the river, which lie approximately perpendicular to the direction of flow. Cross-sections are specified by a number of *x-z* co-ordinates where *x* is the transverse distance from a fixed point (often left bank top) and *z* is the corresponding bed elevation. Ideally there should be sufficient number of cross-sections to define adequately the variation in river shape. The *x-z* co-ordinates are entered as raw data in the cross-section editor. The raw data are then automatically processed into a form used in the hydrodynamic calculations, i.e. the hydraulic parameters; cross-sectional area, hydraulic radius and width are calculated for a number of elevations between a minimum and a maximum which are either determined automatically or may be user specified.

4.2.2.3 Hydrodynamic boundary condition definition

Boundary conditions are required at all model boundaries, i.e. upstream and downstream ends of model branch which are not connected at any junction. The boundary conditions may be internal or external. The internal boundary condition includes the specifications at nodal points and structures, whereas the external boundary condition includes the specification of constant values of *H* or *Q* or time varying values of *Q* or *H* at start and end points. In the present setup there are only one branch which generates two open hydrodynamic boundaries on the main river; flow boundary at Rishikesh and water level boundary at Kachalabridge. In addition, point sources at three barrage location are defined from where the flow is diverted for irrigation canal systems. Further, another HD point is defined as distributed source between Rishikesh to Kachalabridge to account for the later inflow in Ganga River in this stretch (Figure 3.2).

4.2.2.4 Setting the HD parameters

The HD parameters, in the present study, include the initial conditions of water level and discharge, friction coefficient (*n*) and output parameters options. Initial conditions are required to avoid the dry bed conditions. The extended 1D flow model is being set up for most part of the river stretch in the study; the bed resistance are specified considering the

river section as triple zone. The lowest zone defines the low flow condition, medium flow condition within river bank and high flow condition above the river bank. Thus three values of Manning's 'n' are defined. The final estimate has been finalised as 0.023, 0.04 and 0.055 after model calibration as discussed in section 4.2.3. The model is simulated for the monsoon flow during 2010, 2011 and 2013.

4.2.2.5 Fixing the simulation parameters

Before running the model simulation, control parameters such as simulation period, simulation time step, data to be stored and storage time have to be specified. The simulation periods are specified by start and end dates specified by year, month, day and hour and minute. MIKE 11 checks the actual time and reads all the data given in the time series during the simulation. There exists a versatile relationship between the time step and the computational distance (*dx)* to define the Courant number given below, which is widely considered to choose the time step for the model simulation.

$$\text{Courant number } (C_R) = \frac{\Delta t\left(V + \sqrt{gy}\right)}{\Delta x}$$

Where, Δt = time step, V= mean flow velocity (m/s), y = water level (m) and Δx = dx-max. If there is a large value of *dx,* the time step should be chosen so small that the C_R value should be low. Low value of C_R is needed to avoid instability during the model simulation. Mike 11 applies a 6-point Abbott scheme for solving the Saint Venant's partial differential equations where good results are obtained up to Courant numbers as high as 10-20 (DHI 2004).

4.2.3 Calibration and validation of MIKE 11

Calibration of a model is the process of adjusting model parameters to obtain a close agreement between the observed and the simulated outputs. Validation of the calibrated model is essential to check the calibration precision. In the present study, for calibration of MIKE FLOOD model, the manning's roughness coefficients of river network and flood plain are considered as calibrating parameter. The simulated and observed water level in the reservoir has been used for error estimation of the model computation. Correlation coefficient (R^2), maximum positive and negative difference, peak error (%) and peak time error (hour)

have been considered as goodness of fit criteria to verify the acceptability of MIKE FLOOD results.

4.3 Morpho-hydrodynamic Modelling

Sediment transport modelling in alluvial river can be simulated through river morphodynamic model. The morphodynamic modelling includes both hydrodynamic and morphological studies of a river, simultaneously. The hydrological and morphological parameters of a river describe the change in flow behaviour with space and time scale. In the morphodynamic modelling, flow dynamics like water levels and flow velocities are computed over a curvilinear or a rectangular computational grid by solving the vertically integrated St. Venant equations of continuity and conservation of momentum. In addition to main currents, the alluvial rivers also exhibit secondary flow/ currents (helical flow) which is developing in channel bends due to curved streamlines and it is defined through curvilinear 2D flow model and using suitable sediment transport models defined through various empirical formulas. Morphodynamic model is able to describe the variation in hydrodynamic characteristics i.e. water level and flow velocity and morphological characteristics such as helical flow, sediment transport, scour and deposition, bank erosion and plan form change of a river etc.

4.3.1 Numerical Modelling Tools (MIKE 21C)

Two-dimensional numerical models for turbulent flow and sediment transport can efficiently perform long-term simulations of river morphology including impact of river engineering structures. In the present study morphodynamic modelling for a stretch of river the Ganga between Garhmukteshwar to Kachalabridge GD site (142 km) is carried out using MIKE 21 C software. MIKE 21C is a curvilinear grid based morphodynamic model and its capabilities includes: (i) Model for bend, (ii) Model for meander and bifurcation**,** (iii) Computation of scour and deposition, bank erosion, change in river plan form, (iv) Prediction of morphological changes in the stream etc. and yield estimates for the design criteria for the anti-erosion/ river training/ flood protection works such as design flow velocity, flow depth and erosion rates etc. for a river or stream.

4.3.1.1 GIS processing for river bank line and DEM

The various pre-processing (for making the required input data of MIKE 21 C simulation data) and post-processing tools (to present the result data from output files that obtained from simulation through MIKE 21 C) are used in modelling. These tools are shown in Figure 4.3. In GIS, the river bank line from a recent satellite image (year 2015) is extracted and its shape file is created. The shape file in turn is used to create the X,Y coordinate of the river bank line.

Further, the elevation values for river cross section data (spot level and contours from SOI toposheet and cross section survey data) are converted into .dat or .xyz file format using MIKE Zero tool and used to generate curvilinear grid using MIKE 21 C Grid generator.

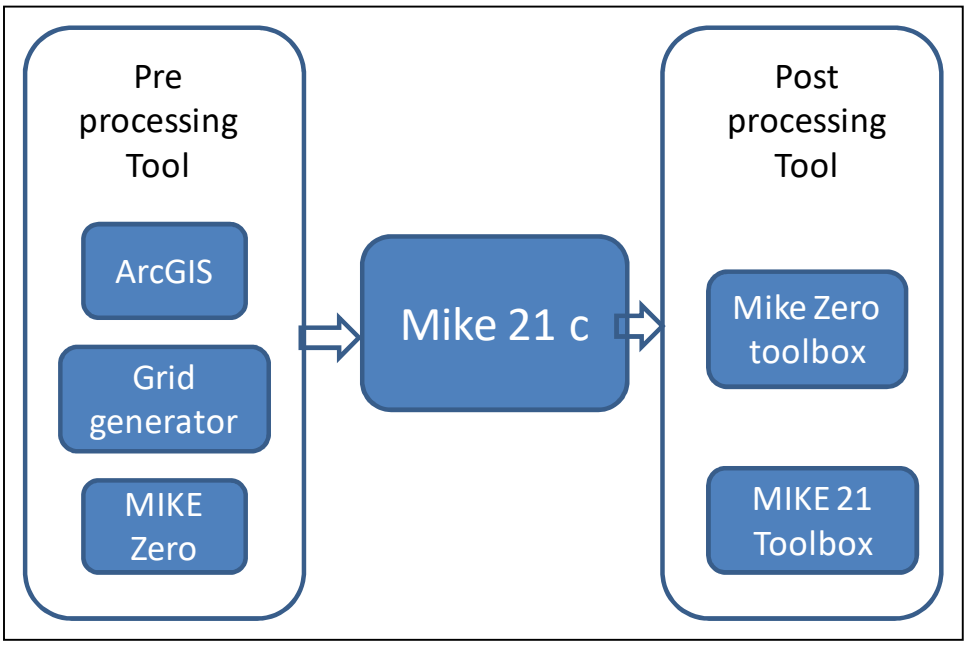

Figure 4.3: MIKE 21C tools used in morpho-hydrodynamic study

4.3.1.2 MIKE 21 C Grid Generator

An orthogonal curvilinear grid is used to cover the entire area of the model which is made by the grid generator tool provided in MIKE 21C software package. It requires the bitmap of the study area or the bank line polyline as the input. It follows the curvilinear co ordinate system which is shown in Figure 4.4. In the curvilinear grid co-ordinate system s represents direction along the river flow and n direction represents the direction transverse to flow. The generation of orthogonal curvilinear grid is an iterative process which consists of solving a

set of elliptical partial differential equation by using an implicit finite difference approximation. This tool can be also used to making other input (spatial varying for the study area) of MIKE 21 C such as bed elevation z (Bathymetry), bed resistance (Manning's number M, Chezy's number (C) and grain size (d_{50}) etc. These elliptical partial differential equations are as following:

$$\frac{\partial}{\partial s}\left[g\frac{\partial x}{\partial s}\right]+\frac{\partial}{\partial n}\left[\frac{1}{g}\frac{\partial x}{\partial n}\right]=0 \quad \textbf{(4.1)}$$

$$\left[g\frac{\partial y}{\partial s}\right]+\frac{\partial}{\partial n}\left[\frac{1}{g}\frac{\partial y}{\partial n}\right]=0 \quad \textbf{(4.2)}$$

Where, x, y are co-ordinates of Cartesian system; s, n are curvilinear co-ordinates (anti-clockwise system); g is the weight function

$$g=\sqrt{\frac{\left[\frac{\partial x}{\partial s}\right]^2+\left[\frac{\partial y}{\partial s}\right]^2}{\left[\frac{\partial x}{\partial n}\right]^2+\left[\frac{\partial y}{\partial n}\right]^2}} \quad \textbf{(4.3)}$$

In this work MIKE 21 C grid generator is used for making an orthogonal curvilinear gird of 1872x72 cells. As the stretch is longer multi block grid generation approach is used to generate the grid for whole model. The grid is adjusted such that it can fulfil both orthogonal and aspect ratio requirements. The data files store in the centre of grid points this is shown in Figure 4.5. The Bathymetry data (.dfs2/.dt2 format) is prepared from the available cross section data. This is the basic input of the MIKE 21 C software. The key criteria considered for grid generation are:

i) Grid has to be orthogonal - it should be in between within recommended tolerance range -0.05 to +0.05.
ii) Aspect ratio (dx/dy) should be between 2 to 8.
iii) dx and dy should be based on flow adaptation which is described in following sections.

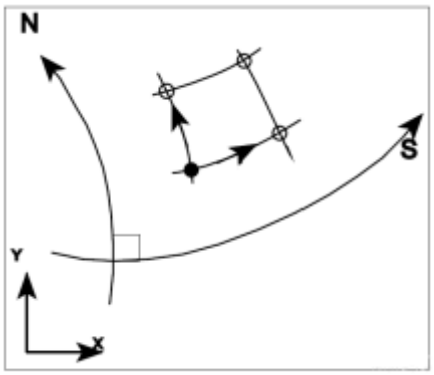

Figure 4.4: Curvilinear Grid Co-ordinate System

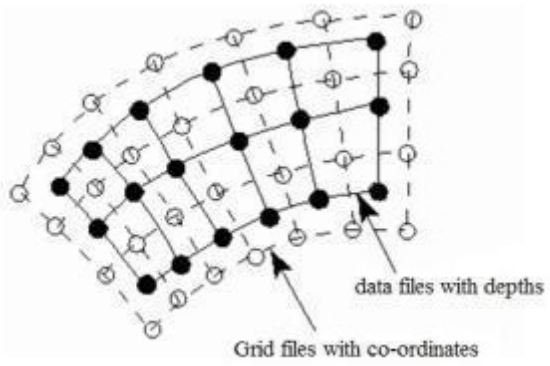

Figure 4.5: Example of Grid Files with Co–ordinates and Data Files with Depths Elevation

(Source: Grid Generator Users' Guide, DHI 2014)

Adaption length for main flow is the measures of the relative importance of the flow momentum compare to the bed friction and is defined by λ_w expressed by

$$\lambda_w = \frac{C^2}{2g} h \quad \textbf{(4.4)}$$

Where,

C is the Chezy's number, h is the flow depth, and g is the gravity. In a well developed model, grid size should be 3 times smaller than this adaption length in overall model domain except at bend, where grid size is to be much smaller to resolve secondary current.

Secondary flow adaption is the length scale adaption for secondary flow and is expressed by λ_{sf}

$$\lambda_{sf} \frac{1.2hC}{\sqrt{g}} \quad \textbf{(4.5)}$$

Where, h is the water depth. In a good model, grid size should be 3 times smaller than this adaption length to represent secondary current at bend. The primary and secondary flow in the river is shown in the Figure 4.6.

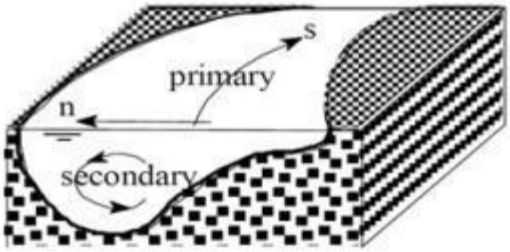

Figure 4.6: Representation of Primary and Secondary flow

4.3.1.3 MIKE Zero

MIKE Zero is a common interface modelling tool. In the present work this tool is used for developing the time series data (.dfs0) files and grid series data (.dfs2) files of various input parameters such as discharge, water level, initial water level, Chezy's / Manning's number and grain size etc. It has been also used to manipulate the time steps and start date of Hotstart file.

4.3.2 MIKE 21C Package

MIKE 21C is a mathematical modelling tool developed by the DHI (Danish Hydraulic Institute) it is generally suitable for the morphological studies (includes the hydrodynamic and sediment transport) and particularly suitable for river and channel. It computes over orthogonal curvilinear grid which is obtained from the MIKE 21 grid generator. The MIKE 21C has various modules which can run interactively and able to describe the dynamic nature of variation of morphological behavior of river. The solution techniques of various morphodynamic modeling components in MIKE 21 C is shown in Figure 4.7.

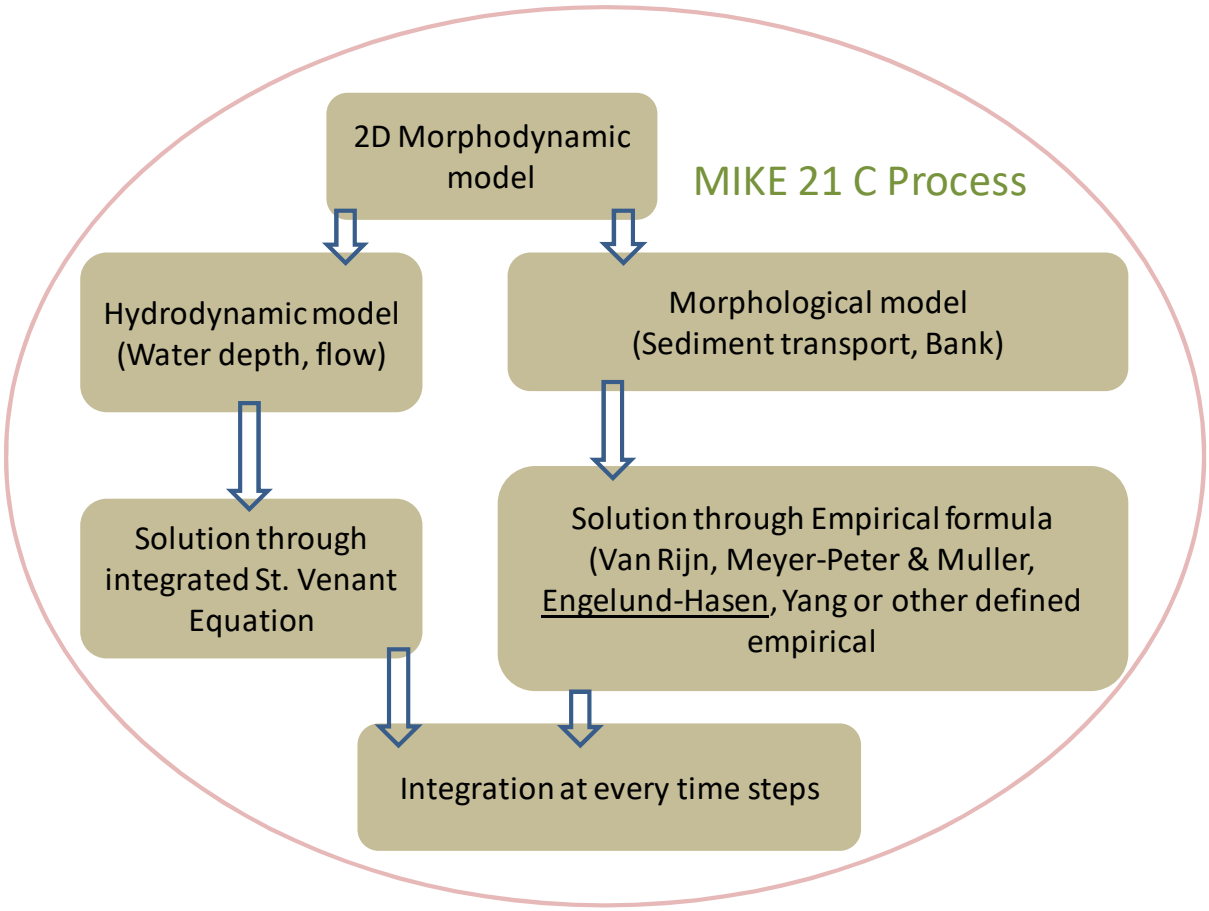

Figure 4.7: Solution techniques of various components of MIKE 21C model

The definition of various terms associated with MIKE 21C modeling are described as below:

Hydrodynamics - Computation of water level and flow velocities using vertically integrated St. Venant equations.

Helical Flow - Computation of Helical (secondary) flow intensity developed due to bends.

Sediment Transport - Based on different empirical formula e.g. Van Rijn, Engelund-Hansen etc.

Alluvial Resistance - Includes computation of skin friction from grain and drag force from bed forms

Bank erosion & Plan form - Includes computation of bank erosion rates and updating of curvilinear grid

Scour and Deposition - Computation of large – scale movement of bed material

4.3.2.1 2-Dimentional HD MODEL

Hydrodynamics of rivers is a complex 3D flow process that takes huge computations for exact modelling. The flow can be simplified by evolving Navier-Stroke equations and further,

it can be reduced to 2D equations of moment and mass conservation in horizontal direction. Helical flow component are described by depth average model with a separate model.
Governing equations are as follows:

$$\frac{\partial p}{\partial t}+\frac{\partial}{\partial s}\left\{\frac{p^2}{h}\right\}+\frac{\partial}{\partial s}\left\{\frac{pq}{h}\right\}-2\frac{pq}{hR_n}+\frac{p^2-q^2}{hR_s}+gh\frac{\partial H}{\partial s}+\frac{g}{C^2}\frac{p\sqrt{p^2+q^2}}{h^2}=RHS \quad \textbf{(4.6)}$$

$$\frac{\partial q}{\partial t}+\frac{\partial}{\partial s}\left\{\frac{pq}{h}\right\}+\frac{\partial}{\partial n}\left\{\frac{q^2}{h}\right\}+2\frac{pq}{hR_s}-\frac{q^2-p^2}{hR_n}+gh\frac{\partial H}{\partial n}+\frac{g}{C^2}\frac{q\sqrt{p^2+q^2}}{h^2}=RHS \quad \textbf{(4.7)}$$

$$\frac{\partial H}{\partial t}+\frac{\partial p}{\partial s}+\frac{\partial q}{\partial n}-\frac{q}{R_s}+\frac{q}{R_n}=0 \quad \textbf{(4.8)}$$

Where, p, q are mass flux in s and n directions respectively; s, n are co-ordinates of curvilinear coordinate system; H is the water level; h is water depth; C is Chezy's constant; g is the acceleration due to gravity; R_s, R_n are the radius of curvature in s and n directions; RHS is force balance includes Reynolds stresses, Coriolis force and Atmospheric pressure.

These partial differential equations are solved in MIKE 21 C by implicit finite difference technique. For development of HD model first grid and corresponding bathymetry data are defined in the input parameter. Then the time series (.dfs0) of water level or discharge are used as the boundary inputs.

4.3.2.2 Morphological Model

In MIKE 21 C river morphology includes the various parameters such as helical flow, sediment transport, plan form, alluvial resistance and morphological update etc. Morphological models are generally divided into coupled and uncoupled models. Combined equation of stream flow and sediment transport is used as principle equation in the coupled model while in the uncoupled model the HD simulation is solved at some time step prior than the sediment transport equations for the working model.

Sediment Transport

The flowing water in the river has tendency to scour its banks and bed level. In this process the different sediment particles are transported from bed or suspension to another place by the power of flowing river which is known as sediment transport. The classification of sediment

load by Jansen et al. (1979) is shown in Figure 4.8. For the study of river morpho-dynamics, the role of dissolved load and wash load is generally negligible. he

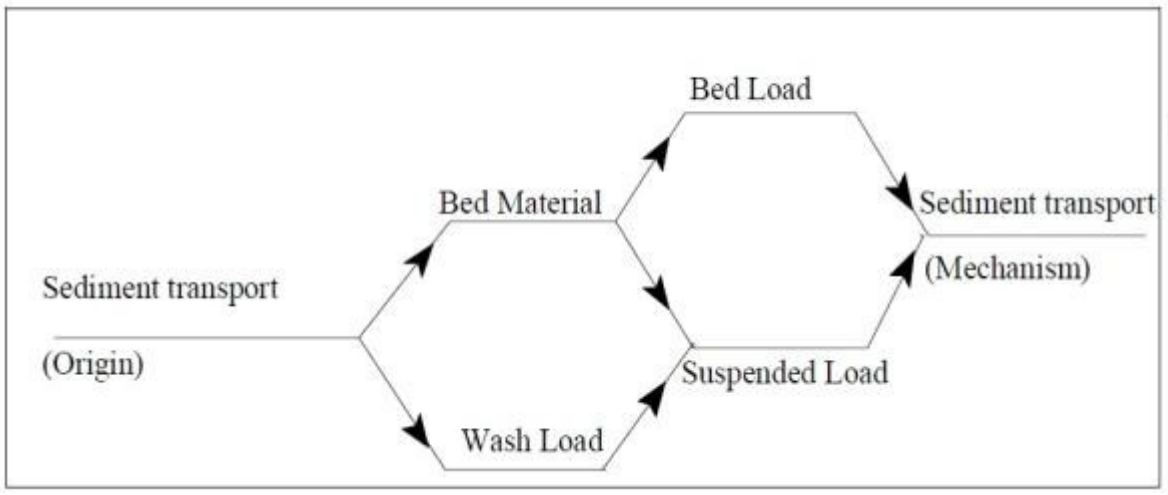

Figure 4.8: Various Types of Sediment Load
(Source: Mike 21 C Scientific documentation, DHI 2014)

The various types of sediment are defined as below:

Bed Load - This fraction of sediment load moves along the bed, roll and slides and sometimes it may comes in the suspension due to the turbulence or occasionally jump of water in the river. The characteristics of the bed material is similar to the river bed material, and the material in transport can therefore be actively interchanged with the bed. For this reason, bed material load exerts a control on river channel morphology.

Suspended Load - It is the component of the sediment which maintain in suspension due to the turbulence of the flowing water in the stream. The particles are finer than the bed load. The study of suspended sediment transport mechanism is more complex than bed load transport due to its 3dimensional movement in river.

Wash Load - It is the material that is not present in the river bed. It is carried in suspension without interaction with the river bed and thus has negligible influence on the river channel morphology**.** It is the part of suspension load is very fine so that it remains in the suspension by the molecular agitation (Brownian motion) even without any turbulence.

Governing Equations:

a. Sediment Continuity Equation:

The sediment continuity equation used in MIKE 21 C can be written as following:

$$(1-\eta)\frac{\partial z}{\partial t}+\frac{\partial Sx}{\partial x}+\frac{\partial Sy}{\partial x}=\Delta S_e \quad \textbf{(4.9)}$$

Where, η is porosity of River bed material (usually between 0.3 to 0.7); (x, y) is the co-ordinate in Cartesian coordinate system; S_x is the total sediment load transport in x – direction; S_y is the total sediment load transport in y – direction; and z is the bed level. This equation is solved over curvilinear grid using numerical solution technique.

b. Helical Flow

It is also known as secondary flow. It is generally occurs due to curved flow of stream especially at the river bends. For the helical flow α is used as the input parameter in MIKE 21 C. It varies from 0.4 to 1.2 for the Chezy's number of 40 $m^{1/2}/s$. The representation of the primary and secondary flow is shown in the Figure 4.9.

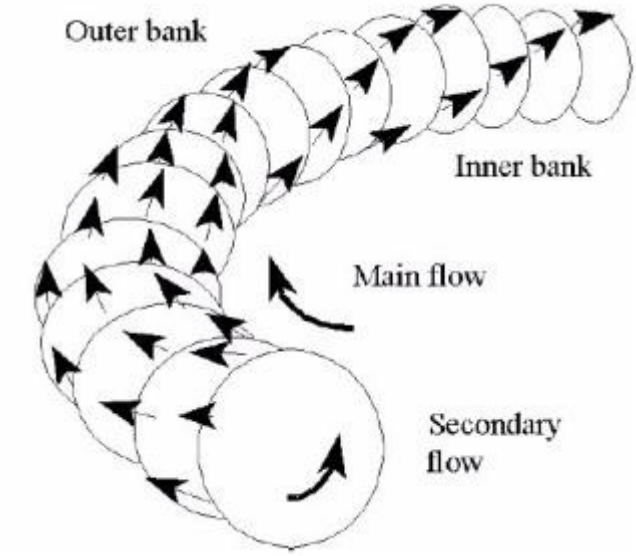

Figure 4.9: Representation of Helical Flow (Secondary flow) in Bends
(Source: MIKE 21 C Users' Guide, DHI 2014)

The equation which is adopted for the helical flow is as following:

$$i_s = u\frac{h}{Rs} \quad \textbf{(4.10)}$$

Where, i_s is the helical flow intensity; u is the velocity of main flow; R_s is the radius of curvature of streamlines; h is the depth of main flow.

$$tan\delta_s = \beta\frac{h}{Rs} \quad \textbf{(4.11)}$$

Where $\beta = 2\alpha.\left\{1 - \frac{\sqrt{g}}{\kappa c}\right\}/\kappa^2$ **(4.12)**

Where, δ_s is the angle between the bed shear stress and depth averaged shear stress; κ is the von karman constant, (0.4); g is the acceleration due to gravity; C is the Chezy's number; α is the model input (used as calibration parameter).

c. Bank Erosion

The bank erosion is calculated by the continuity equation for the sediment transport model. The various parameters of bank erosion adopted in the MIKE 21 C are shown in Figure 4.10.

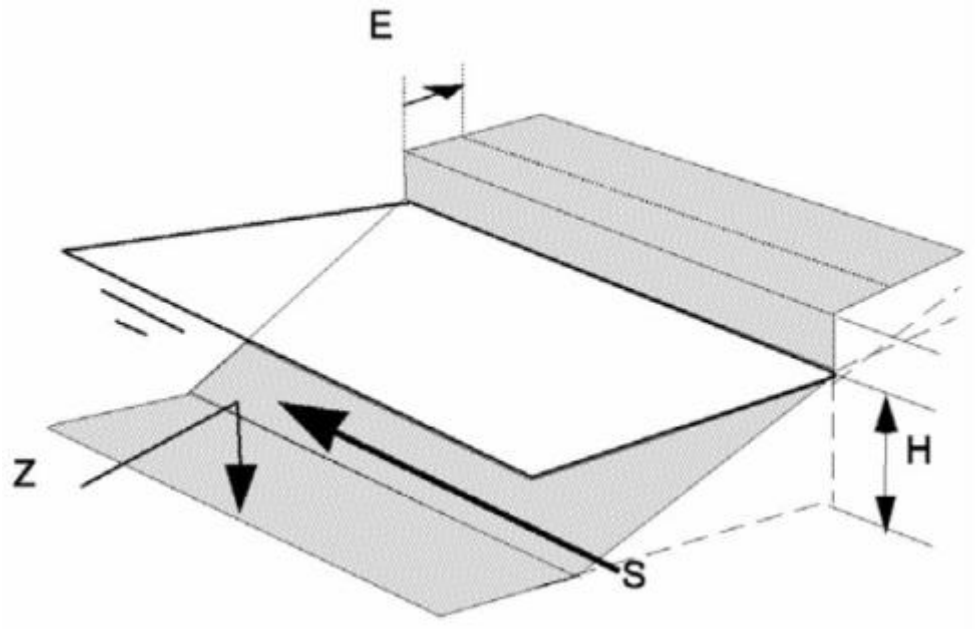

Figure 4.10: Representation of Governing Parameters of Bank Erosion

The adopted bank erosion rate is given by:

$$E_b = \alpha\frac{dz}{dt} + \beta\frac{S}{h} + \gamma \quad \textbf{(4.13)}$$

Additional **sediment is given by**

$$\Delta S = E_b(h_b + h) \quad \textbf{(4.14)}$$

Where, Z is the River bed level (local); S is the sediment transport of near bank; h is the local water level of River; α, β, and γ are the model input parameters; The α, and β are found from

the observed from bank erosion rates of the model area or sometimes the time constant bank erosion rate (γ) is applied for the model in case of lack of data.

d. Sediment Transport Formulas

There are number of empirical formula available in MIKE 21 C for the computation of sediment transport. The selection of the suitable formula depends upon its applications and limitations. In the present work Engelund & Hensen Formulae (1967) is used for the model as the literature shows that the formula can be applied in alluvial river with all range of sandy bed and suspended load material. The empirical formulation is described below.

Engelund & Hensen (1967) - It is based upon the Shear stress approach. They give a model for total load and then it is further divided into bed load and suspended load. The equation for total load is given by:

$$S_{tl} = 0.05\frac{C^2}{g}\Theta^{\frac{5}{2}}\sqrt{(s-1)gd_{50}^3} \quad \textbf{(4.15)}$$

$$S_{bl} = k_b S_{tl} \quad \textbf{(4.16)}$$

$$S_{sl} = k_s S_{tl} \quad \textbf{(4.17)}$$

Where, S_{tl} = total sediment load transport per unit width; S_{bl} = Bed load sediment load transport per unit width; S_{sl} = Suspended sediment load transport per unit width; C = Chezy's coefficient; Θ = Shield parameter; s = specific gravity; d_{50} = Grain size (50% particles are finer than this size); k_b = bed load calibration factor; k_s = suspended load calibration factor; g = acceleration due to gravity.

The comparisons among these formulas are shown in Table 4.1.

5 RESULT AND DISCUSSION

The study and analysis with respect to three major objectives of the study namely (i) Analysis of river bank shifting using temporal satellite data, (ii) river flow modelling of river Ganga from Rishikesh to Kachalabridge using MIKE 11 program and (iii) morpho-hydrodynamic modelling of river Ganga between Garhmukteshwar to Kachalabridge using MIKE 21C program have been discussed in this chapter in different section. The output from the one objective has become the input for the next analysis. The flow chart of the derivable from various components of the study is shown in Figure 5.1. The analysis of all three components is discussed in details in separate sections individually in the following sections.

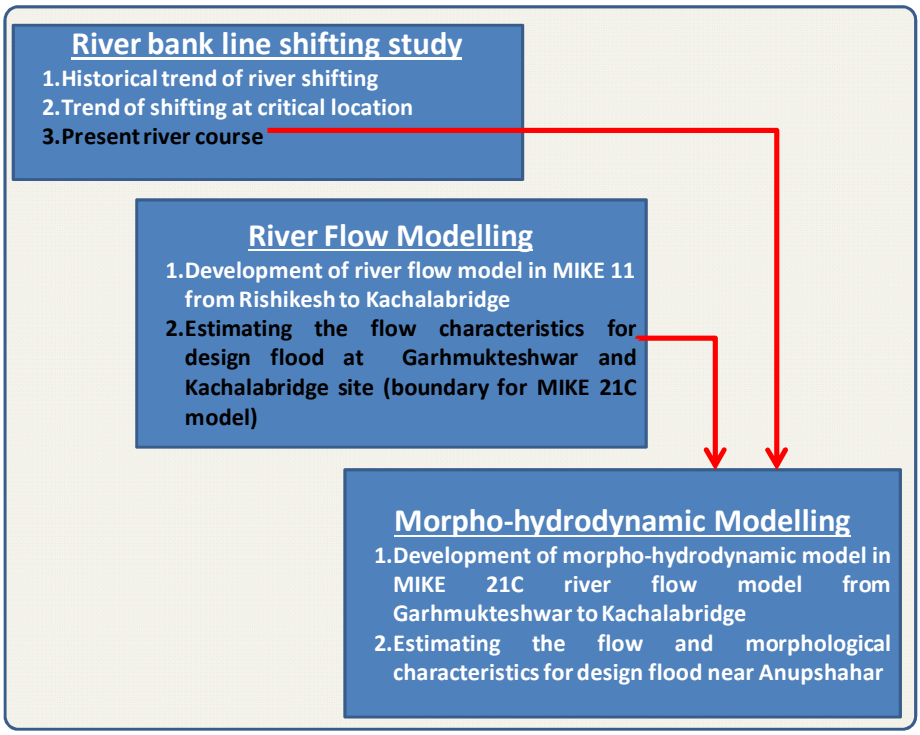

Figure 5.1: Flow chart of various components and sequence of derivable of the study

5.1 River shifting analysis

The course of the river Ganga from Garhmukteshwar to Kachalabridge site (near Anupshahar) along with the major roads, railways and important places were delineated from SOI toposheet. Also, the course of river Ganga near Anupshahar is delineated from the IRS

1C satellites images from LISS-III/ PAN data for the year 1997, 2001 and 2005 and using P6 satellite (RESOURCESAT-1) and RESOURCESAT-2 LISS-IV digital data for the years 2011 and 2015. All the images are geo-referenced in UTM-N44 projection system and then the shifting course of the river Ganga was studied in a GIS environment in ArcGIS through overlay analysis. The analysis carried out and results of the study for following aspects are presented below.

1. Shifting course of river Ganga near Anupshahr from 1997 to 2015 and identification of the critical locations where shifting has occurred,
2. Details of the shifting characteristics of river Ganga at the identified critical locations using temporal satellite data

5.1.1 Identification of critical locations of river shifting

The satellite images of the study area are geo-referenced with SOI toposheet at 1:50,000 scale. The coverage of toposheet from Garhmukteshwar GD site to Kachalabridge GD site is shown in Figure 5.2. The control points for geo-referencing are selected on the wider coverage while the supervised classification for river sand and water has been carried out for a limited area around the river bank shown by the red line polygon. Further, the permanent linear feature (road and major canals) of the area running along the right bank of the Ganga river has been taken as reference line along which the distance of left or right bank of river has been measured from the classified images of different year. Figure 5.3 shows the extracted river bank line from 1997 satellite images and the measurement (of distance) of bank line from permanent linear feature (road and canal alignment) shown by blue line. Along this line, points at every 1 km (along the line) is drawn and the distance of left bank, represented through magenta line arrow is computed. Similarly, the distance of right bank from this permanent linear feature, represented by black line arrow is estimated. Thus, we compute the river bank lines; left and right bank at every 1 km interval along permanent linear feature from all the images and the shifting of river is estimated.

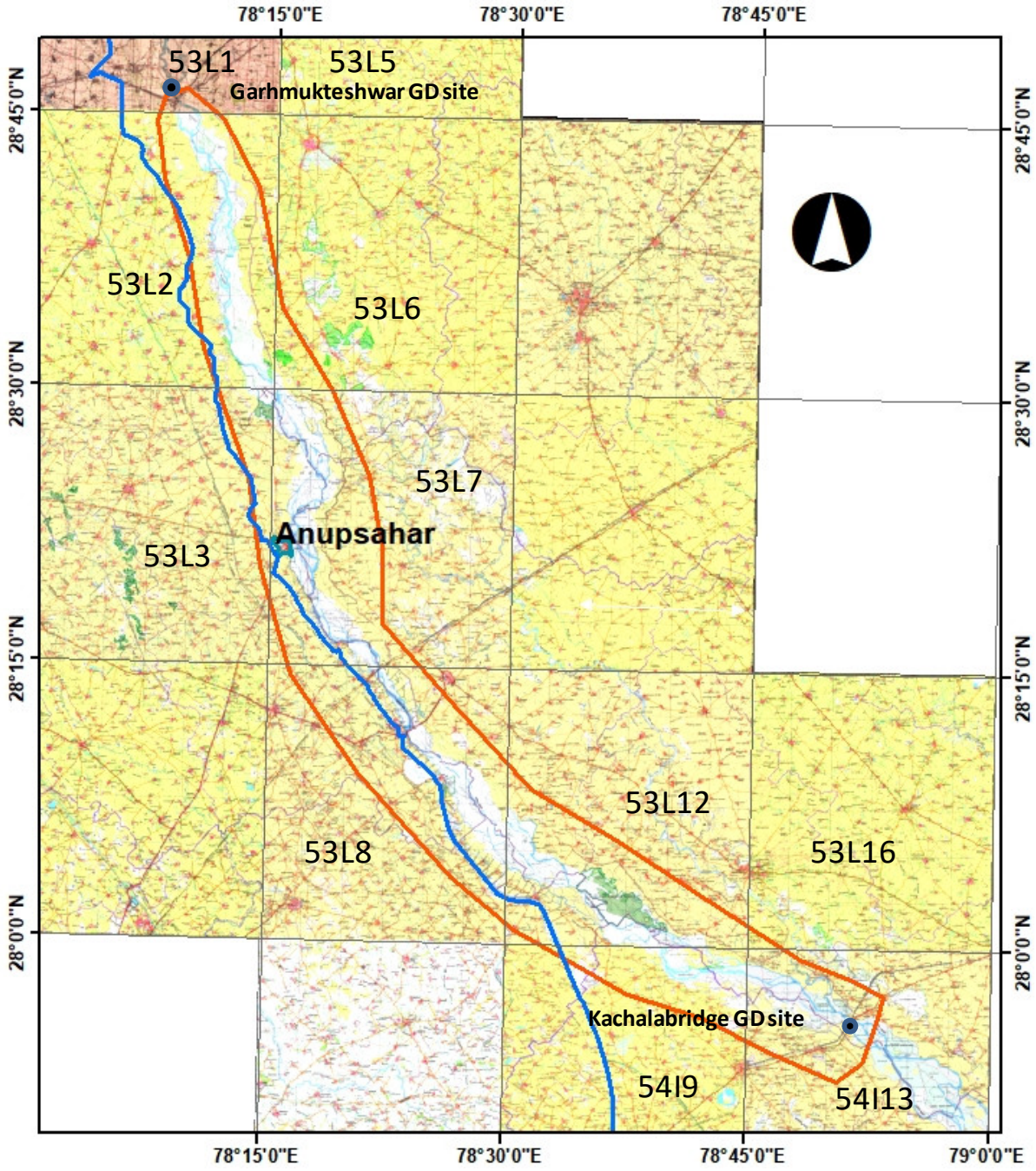

Figure 5.2: Coverage of SOI toposheet at 1:50000 scale for river stretch for river shifting analysis.

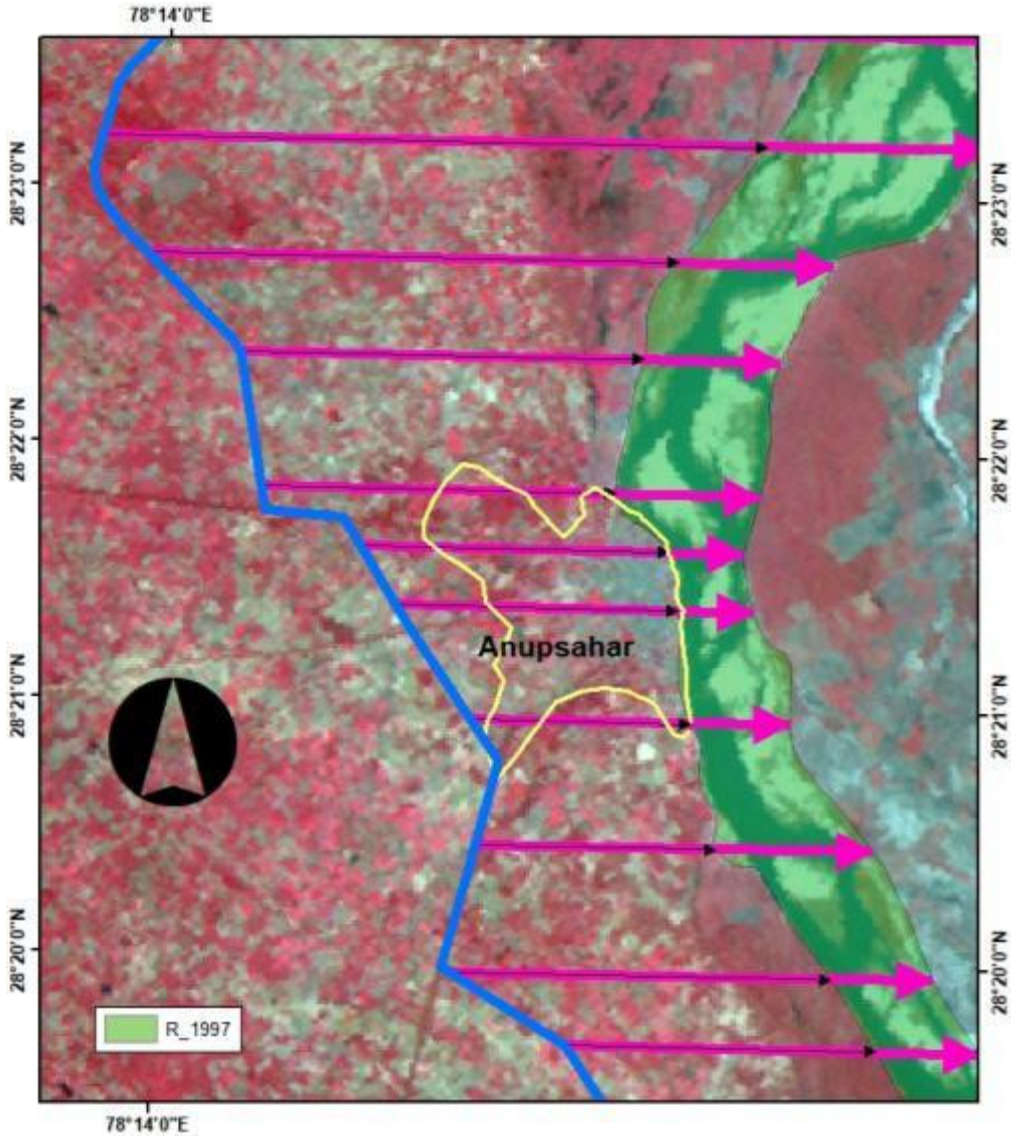

Figure 5.3: Extracting river bank line from classified image and measurement of bank line from reference line.

The river bank line for the year 1997, 2000, 2005, 2011 and 2015 is developed by mosaic of satellite images of respective years, classifying for river and river sand and then preparing the river layer. These river layers for various years are superimposed over each other in ArcGIS and shifting is analysed. The overlay of river bank line is shown in Figure 5.4. The distance of left bank and right bank from permanent linear feature at 1 km interval during different year is given in Table 5.1. The Point Id in the table is to define the point at which the distance of bank is computed. It is to mention that the coverage of river in different years are slightly varying due to use of different satellite/ sensor image and its varying swath area. Hence, the river stretch for which the data is available for the entire period is reported in the table. Further, the shifting of bank at each Point Id is computed by subtracting the distance between

two successive periods of analysis. The analysis shows that shifting has occurred at several places but major shifting is reported based on two criteria:

i) The site is located near some major settlement
ii) The shifting is significant, more than 150 m in two successive periods.

Based on the above criteria, eight locations have been identified where major shifting has been reported. These locations are Alampur, Pooth, Alapur, Mandu, Ahar, Anupshahar Sherpur and Karanwas as shown in Figure 5.4. The detailed shifting analyses at these locations are carried out and reported in following section.

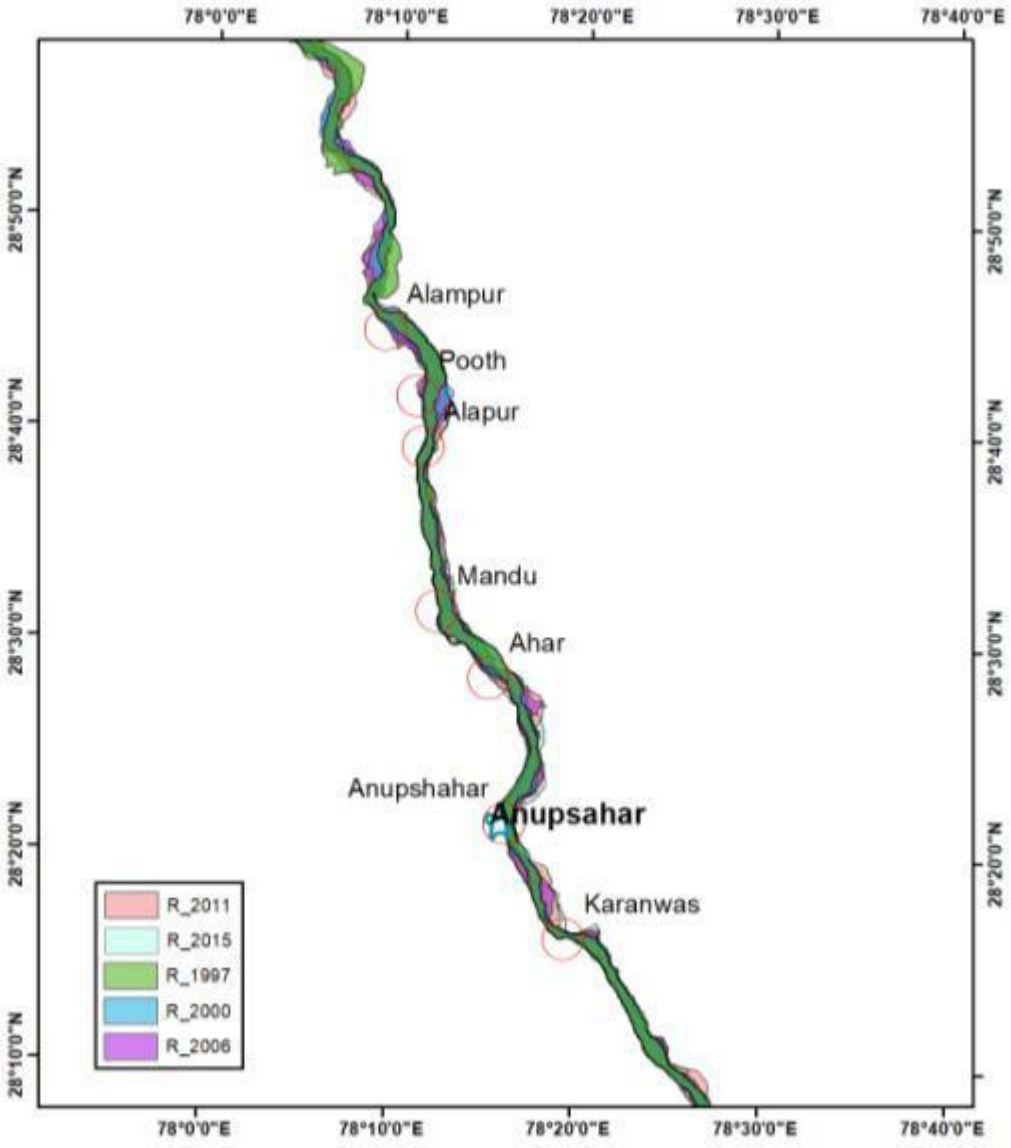

Figure 5.4: Bank line developed from multiple images for various year

Table 5.1: Distance of left bank of river from permanent linear feature during various years of analysis.

Point Id	Year of analysis				
	1997	2000	2006	2011	2015
	Distance of left bank in meter				
29	9823.13	9877.34	9679.35	9830.97	9770.49
30	10567.51	10570.90	10584.83	10588.13	10152.50
31	10066.84	10097.80	10051.04	9906.95	9256.44
32	9354.51	9452.72	9469.77	9489.32	8708.16
33	9622.05	9623.19	9645.90	9652.86	8832.00
34	8650.82	9492.92	9154.36	9209.96	9025.03
35	7785.32	9030.37	8594.08	8660.42	8744.08
36	6890.21	8095.96	8294.18	8577.55	8574.06
37	6586.85	6891.41	7429.62	7767.11	7788.74
38	6002.42	5978.05	7632.64	6942.76	6919.47
39	5067.49	5260.45	5273.90	5836.02	5798.00
40	4757.43	4649.31	4768.34	4918.12	4916.15
41	4197.38	4059.45	4364.65	4049.70	4233.35
42	3354.11	3308.60	3413.34	3439.09	3602.34
43	2850.83	2818.96	2903.28	3168.27	3891.06
44	3113.33	2923.34	3011.95	3187.28	3191.90
45	3743.84	3216.68	3491.09	3992.55	4019.97
46	3860.65	3901.63	4056.03	4179.12	4240.17
47	4124.35	4317.59	4400.54	4543.24	4558.16
48	4841.78	4870.16	5109.74	5206.21	5238.27
49	5242.89	5372.13	5524.83	5802.58	5858.55
50	4877.54	4966.91	5149.45	5388.39	5508.97
51	4623.32	4642.42	4638.40	4994.53	5086.28
52	4724.41	4817.46	4904.12	5090.07	5353.29
53	4209.72	4263.11	4439.27	4638.10	4716.73
54	3880.27	3784.60	4392.92	3967.34	3935.77
55	3318.97	3250.59	3451.33	2717.91	3250.60
56	3346.35	3400.55	3574.48	2843.40	2951.91
57	3083.20	3514.93	3506.23	2710.47	2383.78
58	3727.18	3876.93	3944.19	3666.70	3670.63
59	3907.24	4017.34	4189.41	4382.39	4406.59
60	5737.62	5747.55	4887.24	5294.76	5399.21
61	6900.72	6975.07	5312.31	5979.84	6076.37
62	7196.25	7218.30	5951.65	6116.27	6301.28
63	7968.04	7920.89	8055.12	8150.06	6721.69
64	8278.18	8286.86	8715.96	8672.11	7207.10
65	7828.69	8406.80	8884.74	9596.19	7786.43

Point Id	Year of analysis				
	1997	2000	2006	2011	2015
	Distance of left bank in meter				
66	8123.55	8420.45	9129.13	9569.86	8357.44
67	7950.37	8034.08	8150.74	8895.81	8915.74
68	7598.93	7794.88	7818.52	7888.06	8538.74
69	7383.80	7383.80	7450.16	7628.16	7946.60
70	6766.36	6685.85	6817.24	6675.88	7256.15
71	6904.07	6597.49	6738.10	6880.54	6730.20
72	6563.60	6607.07	6779.47	6960.57	6844.96
73	6024.55	6287.31	6827.51	6823.81	7046.92
74	6394.47	6609.39	6714.87	6925.21	7428.38
75	4944.25	5331.85	5474.05	5580.95	6395.03
76	3898.37	3889.95	4028.37	4272.71	4548.92
77	3597.75	3556.24	3638.09	3710.12	3721.53
79	2756.27	2768.62	2885.89	3763.46	2934.70
80	2575.89	2629.11	2622.11	2755.64	2728.51
81	2302.00	2290.98	2357.88	2338.57	2464.37
82	2868.33	2877.92	2235.60	2217.72	2499.74
83	3496.88	3759.44	2996.83	3303.17	2954.48
84	2997.57	3035.00	2775.42	3300.79	2416.52
85	3017.14	2948.88	3090.76	3954.57	1840.08
86	2720.35	2640.59	3025.25	3675.26	2040.90
87	2232.94	2274.46	3374.93	1366.53	3412.46
88	1933.72	1966.79	2861.73	3340.26	3208.81
89	1596.32	1634.43	2226.18	2795.03	2983.17
90	1062.30	1208.91	1416.54	2301.70	2731.37
91	1592.10	1511.81	1437.94	1752.12	2327.74
92	1737.31	1960.44	1960.27	1585.19	2049.18
93	3591.35	4262.51	4488.23	4489.38	4424.04
94	4031.98	4152.32	4017.98	4154.69	4021.30
95	4134.79	4159.64	4249.71	4210.37	4230.18
96	3661.58	3780.38	3556.76	3525.11	3495.85
97	3540.41	3620.39	3713.20	3641.98	3481.44
98	3217.28	3270.03	3277.24	3256.53	3279.72
99	2942.54	2928.89	3028.93	2954.13	2904.27
100	2555.36	2555.15	2575.45	3374.17	2465.08
101	2715.22	2732.62	2732.62	2742.34	2724.38
102	2734.43	2701.19	2730.32	2606.95	2343.79
103	2823.25	2662.67	2704.91	2433.52	2433.52
104	2636.86	2503.31	2528.09	2449.62	2401.27
105	2137.55	2102.47	2173.77	2014.08	1985.47

Point Id	Year of analysis				
	1997	2000	2006	2011	2015
	Distance of left bank in meter				
106	1881.17	1928.06	1989.21	1892.61	1880.48
107	2589.42	2789.16	3116.48	2916.87	2655.21
108	2365.43	2548.39	2785.71	2861.57	2518.85
109	2647.80	2620.34	2723.47	2741.32	2624.99
110	2317.69	2310.35	2514.03	2820.83	2973.28
111	2844.59	2765.30	2688.71	4175.38	3140.41
112	2572.12	2613.91	2967.81	3975.14	2470.82
113	2479.79	2495.63	2609.40	3348.05	1839.51
114	2570.08	2816.75	2723.25	2503.97	1577.79
115	2775.35	2778.79	2196.62	2202.30	1774.24
116	3501.52	3371.88	2401.93	2423.04	2665.76
117	4119.78	3926.25	3772.07	3628.28	3446.19
118	5124.72	10722.46	4489.02	6312.24	4216.14
119	8700.12	10741.66	4691.66	6525.06	4948.24
120	9376.18	10068.15	9728.10	6446.09	6703.39
121	9477.27	9543.05	9391.37	5980.73	7043.04
122	8983.28	9084.72	9060.53	6019.08	6585.67
123	9412.86	8689.57	8167.48	7112.57	6176.53
124	9473.02	8129.49	7900.50	6564.10	5861.80
125	10552.43	8215.84	8483.07	8480.65	5992.85
126	10368.84	8238.73	8423.81	8475.72	5704.26
127	9958.10	8492.75	8553.10	8263.13	6066.43
128	9713.29	8365.37	8467.42	8803.57	6125.83
129	9775.30	9609.92	8559.03	10327.93	7009.37
130	9425.77	9561.71	9865.63	9892.12	10406.14
131	7046.07	7168.85	7549.24	7700.92	7986.07
132	7062.37	7218.03	7447.61	7910.02	8022.29
133	7741.55	7938.88	7937.88	12086.74	8329.15
134	8115.04	8736.71	8499.04	12598.38	9422.23
135	8596.02	8812.91	9859.72	14108.43	21960.72

Table 5.2: Distance of right bank of river from permanent linear feature during various years of analysis.

Point Id	Year of analysis				
	1997	2000	2006	2011	2015
	Distance of right bank in meter				
29	7959.41		7012.79	7081.96	7920.21
30	9158.13	8995.41	8260.96	8580.95	8527.68
31	8444.97	8263.97	8215.51	8047.98	8021.10
32	7883.66	7835.85	7784.83	7829.21	7421.13
33	7976.98	7915.46	7714.55	7622.68	7895.08
34	7292.87	7238.34	6825.15	6586.88	7279.26
35	6468.54	6392.85	6102.09	6147.99	6134.09
36	6029.23	5930.68	5893.31	5930.68	5923.47
37	5438.40	5394.01	5321.77	5394.01	5406.23
38	5009.89	5007.35	4965.33	5009.89	5035.20
39	4649.25	4593.91	4585.13	4618.01	4640.27
40	4052.06	3940.44	3842.04	3881.65	3933.90
41	3156.53	3062.94	3156.53	3146.55	3146.55
42	2540.18	2513.73	2503.25	2524.58	2570.63
43	2306.08	2259.12	2273.49	2286.23	2306.08
44	2260.92	2232.92	2260.92	2294.34	2281.73
45	2644.43	2609.99	2598.77	2588.19	2612.84
46	3198.28	3163.98	3198.28	3198.28	3207.21
47	3099.45	3048.13	3048.13	3496.06	3159.59
48	3551.78	3528.85	3577.47	4609.24	3578.60
49	4157.89	4142.46	4135.48	4807.87	4190.50
50	4150.38	4151.03	4111.91	4434.96	4195.18
51	3792.61	3760.06	3940.82	3821.29	3817.64
52	3748.63	3727.21	3727.21	3828.75	3850.78
53	3438.58	3371.31	3333.83	3413.66	3371.31
54	2596.70	2561.49	2511.31	2511.31	2615.32
55	2125.39	2124.83	2104.05	2158.44	2145.54
56	2119.97	2103.70	2052.31	2119.97	2131.04
57	2021.93	2027.46	1979.12	2021.93	2037.64
58	1895.63	1875.61	1855.42	1696.58	1682.92
59	1925.13	1966.01	1693.91	1795.64	1901.36
60	3498.63	3530.59	3660.52	3830.98	2590.61
61	4856.64	4682.76	4543.68	4649.71	4632.42
62	5276.16	5156.47	4964.94	4858.71	4820.46
63	6497.46	6068.25	5801.32	5549.01	5565.72
64	6990.25	6955.88	7046.54	6307.60	6214.37
65	7139.56	7108.81	7070.02	7139.56	6922.67

Point Id	Year of analysis				
	1997	2000	2006	2011	2015
	Distance of right bank in meter				
66	7374.71	7369.30	7501.47	7450.30	7449.75
67	7032.23	6923.67	6947.48	6895.53	6870.60
68	6821.26	6570.05	6507.47	6429.23	6445.21
69	6537.41	6432.01	6388.83	6354.30	6256.26
70	6188.92	6106.33	6023.40	5878.95	5831.32
71	5765.49	5697.74	5900.96	5860.04	5718.45
72	5311.97	5265.22	5641.76	5483.46	5302.31
73	4746.76	4626.92	4830.21	5142.36	4987.90
74	4784.97	5208.01	4962.81	5226.96	5191.95
75	3831.09	3780.35	4145.73	4177.70	4091.75
76	2913.72	2619.80	2879.14	3022.73	2659.71
77	2548.97	2510.10	2826.55	2787.36	2699.34
79	2213.91	2170.47	2192.32	2235.25	2213.91
80	2026.40	2016.25	2047.37	2044.53	2066.11
81	1584.39	1547.32	1584.39	1584.39	1584.39
82	1729.42	1803.19	1626.69	1658.92	1644.74
83	2758.96	2541.11	2089.49	2047.82	2040.60
84	2242.55	2177.78	1612.54	1623.83	1612.54
85	2166.39	2116.40	1420.03	1405.84	1383.43
86	1593.68	1779.58	1296.57	1273.27	1267.29
87	1366.53	1503.35	1400.34	1424.88	1359.09
88	1198.26	1212.21	1302.48	1312.41	1696.31
89	926.05	935.43	1004.68	968.02	1588.79
90	539.88	533.56	576.13	575.44	996.28
91	653.25	647.42	713.57	723.97	812.41
92	534.80	539.85	506.13	534.80	606.56
93	656.28	710.33	738.56	735.82	738.27
94	2334.61	2552.51	2505.88	2358.89	2117.97
95	2117.32	2031.38	2079.58	2053.12	2065.17
96	2016.57	2052.55	2125.61	1976.34	1976.34
97	2497.01	2557.50	2644.11	2358.57	2188.61
98	2357.54	2318.11	2408.33	2333.51	2333.51
99	1987.81	1962.67	2095.57	2051.09	2038.57
100	1611.51	1492.43	1575.03	1627.21	1611.51
101	1769.03	1731.15	1832.40	1797.50	1769.03
102	1640.50	1639.96	1700.53	1694.76	1671.15
103	1555.52	1555.52	1567.25	1535.27	1555.52
104	1273.66	1292.35	1316.36	1292.33	1309.65
105	967.37	988.40	1054.37	1007.50	949.34

Point Id	Year of analysis				
	1997	2000	2006	2011	2015
	Distance of right bank in meter				
106	723.96	744.39	790.39	723.96	726.36
107	1084.80	1084.80	1084.80	1069.38	1079.54
108	642.63	703.23	676.25	642.63	642.63
109	1179.84	1295.66	1275.56	1191.74	1234.13
110	1395.09	1468.86	1452.64	1260.07	1395.09
111	1443.98	1490.38	1867.99	1475.48	1351.22
112	1343.72	1399.76	1789.68	1547.12	1343.72
113	1541.17	1503.79	1242.08	1189.51	1041.26
114	1491.41	1457.16	1360.98	1147.77	984.54
115	1597.86	1554.42	1481.94	1190.27	1204.84
116	2102.11	2034.12	1582.41	1342.79	1352.51
117	2579.00	2530.54	2358.93	1854.80	1672.50
118	2829.30	2773.14	3065.33	2415.30	2671.56
119	3084.55	2959.22	3385.03	2623.03	3519.83
120	6526.69	3635.60	3705.44	3840.23	4072.32
121	7955.80	7935.20	8028.99	5980.73	5325.64
122	7154.48	7897.82	7881.57	5104.08	5060.36
123	6626.48	7357.59	7286.38	4905.51	4717.83
124	5799.42	6642.66	6777.14	4460.06	4235.22
125	5658.14	6755.32	6408.61	4111.55	3993.02
126	5584.67	7033.12	6789.56	4238.83	4128.33
127	5639.94	7082.76	7577.76	5512.12	4919.15
128	7317.41	7246.54	6513.65	5417.83	5280.94
129	7863.66	7552.35	7182.83	5317.99	5425.55
130	7876.55	7177.23	6362.62	5996.59	5980.69
131	5731.30	5667.08	6918.85	4043.22	4013.95
132	5901.66	5885.17	6959.79	7024.00	7531.48
133	6258.33	6094.32	6868.58	7138.37	7631.73
134	6420.69	7196.54	6575.74	6719.10	7823.66
135	6564.29	7803.90	6564.29	6185.76	9466.03

5.1.2 Shifting trend at critical locations

The detailed shifting analysis at all eight critical locations namely; Alamgirpur, Pooth, Alapur, Mandu, Ahar, Anupshahar, Sherpur and Karanwas are carried out. The shifting of river Ganga at these locations are shown in Figure 5.5 and Figure 5.6. The shifting of river in different years are shown by white arrow line and its magnitude is written over it. The shift of river at critical locations with respect to 1997 river base line in various years are also tabulated in Table 5.3. It can be seen that the shift at various locations are as high as ~ 950 m. As these locations are near well developed settlement, the small river shift may result into serious flood hazard. At Anupshahar the shift during 1997-200 was 423 m which reduces to 1787 m (may be following some anti-erosion work at the location). However, the shift of 442 and 407 m again computed during 2011 and 2015. Hence, it is inferred that the anti-erosion work if any carried out to check the erosion of right bank remains ineffective.

Further, the shifting pattern at Anupshahar shows the shift of right bank of river towards settlement (Anupshahar urban area) and what is alarming is that the left bank is also shifting towards the settlement area. Similar river pattern is also observed at Karanwas. Thus at these locations, not only one bank is shifting towards settlement area but the entire river is shifting towards the settlement side.

Table 5.3 also shows the yearly rate of river shifting at each critical location. The average per year shift at Anupshahar is computed as 23 m, however this shift is not uniform and varies year to year.

The trend of river shift at various locations is shown in Figure 5.7. In the figure, the shift of river during various year of satellite data are shown by the continuous line and its path shows the year-wise shift. However, using the computed shift of various years, the trend of the shift is also estimated for each site and is shown by dashed line (of same colour). The trend line shows that the rate of shifting is maximum at Ahar, followed by Pooth, Sherpur and Alamgir and then Anupshahar. However, out of these settlement, Anupshahar is important due to major urban centre and due to its association with religious and cultural heritage.

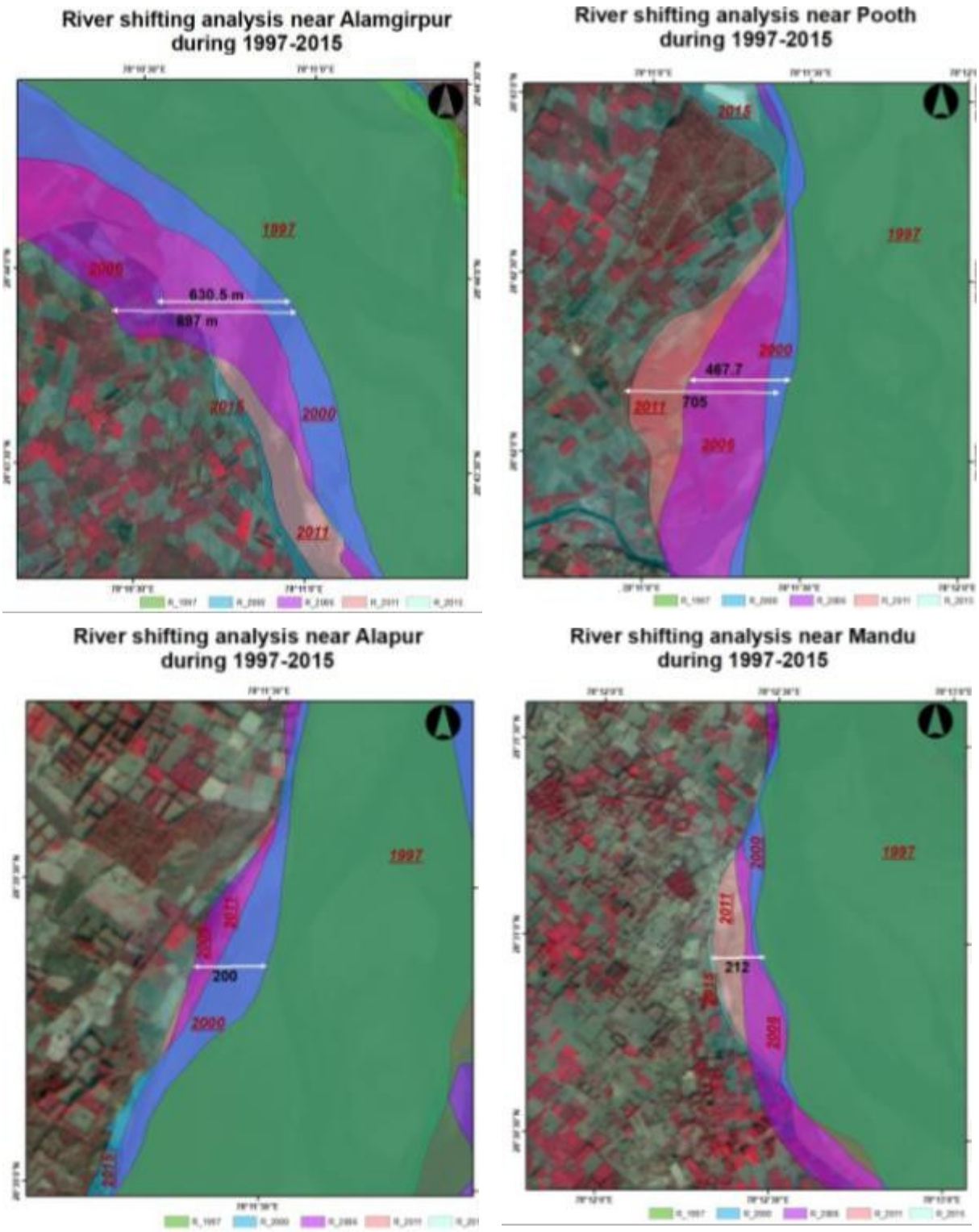

Figure 5.5: Shifting of river Ganga near Alamgirpur, Pooth, Alapur and Mandu during 1997-2015

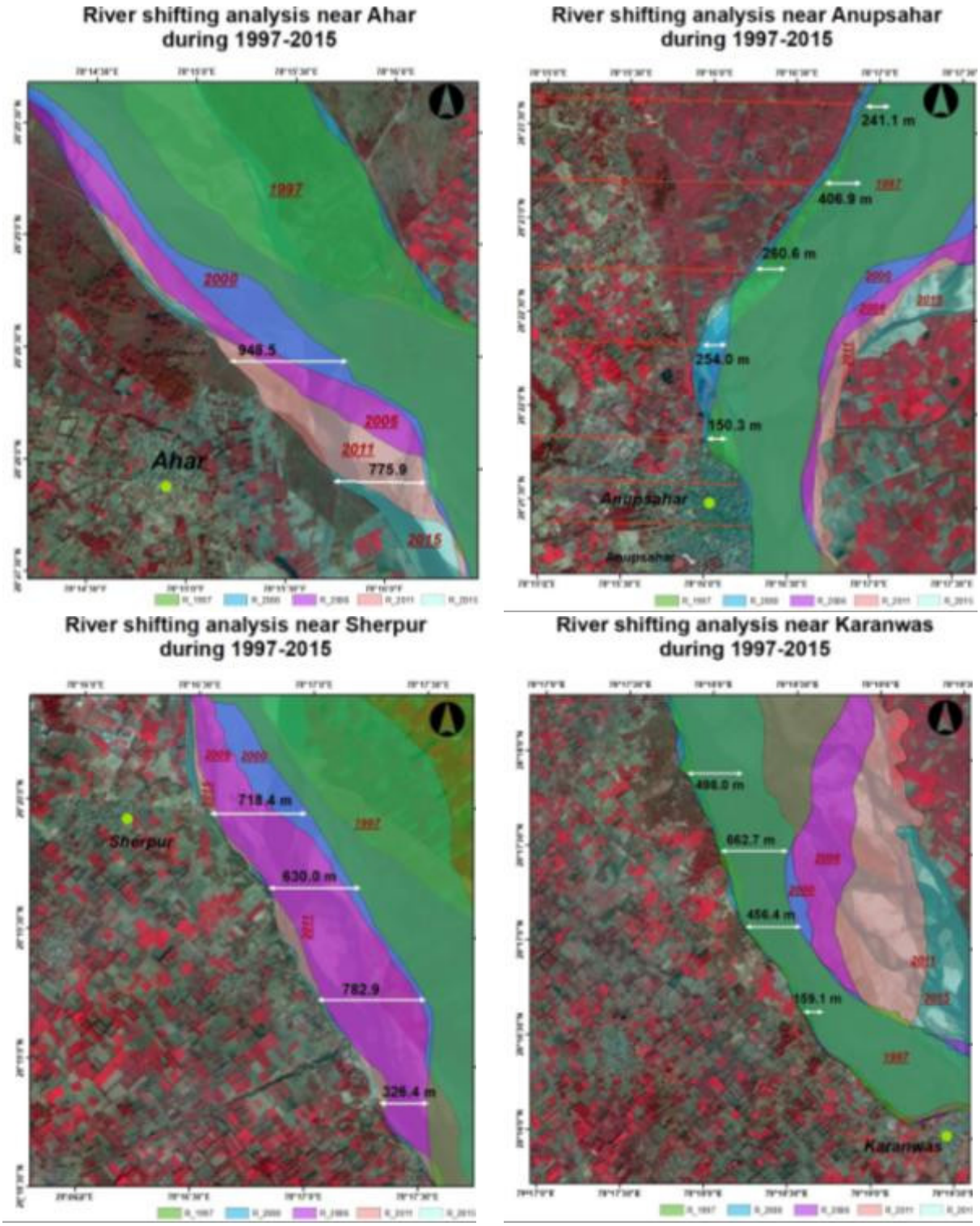

Figure 5.6: Shifting of river Ganga near Ahar, Anupshahar, Sherpur and Karanwas during 1997-2015

Table 5.3: Shift of river bank at critical locations in different year considering 1997 as base line

Year	Shift of river bank in meter							
	Alamgirpur	Pooth	Alapur	Mandu	Ahar	Anupshahar	Sherpur	Karanwas
1997	0	0	0	0	0	0	0	0
2000	163	55	112	20	429	423	50	9
2006	897	468	210	40	696	178	746	79
2011	577	706	170	199	948	442	761	42
2015	630	14	118	213	932	407	783	663
Shift/ year	35	1	7	12	52	23	43	37

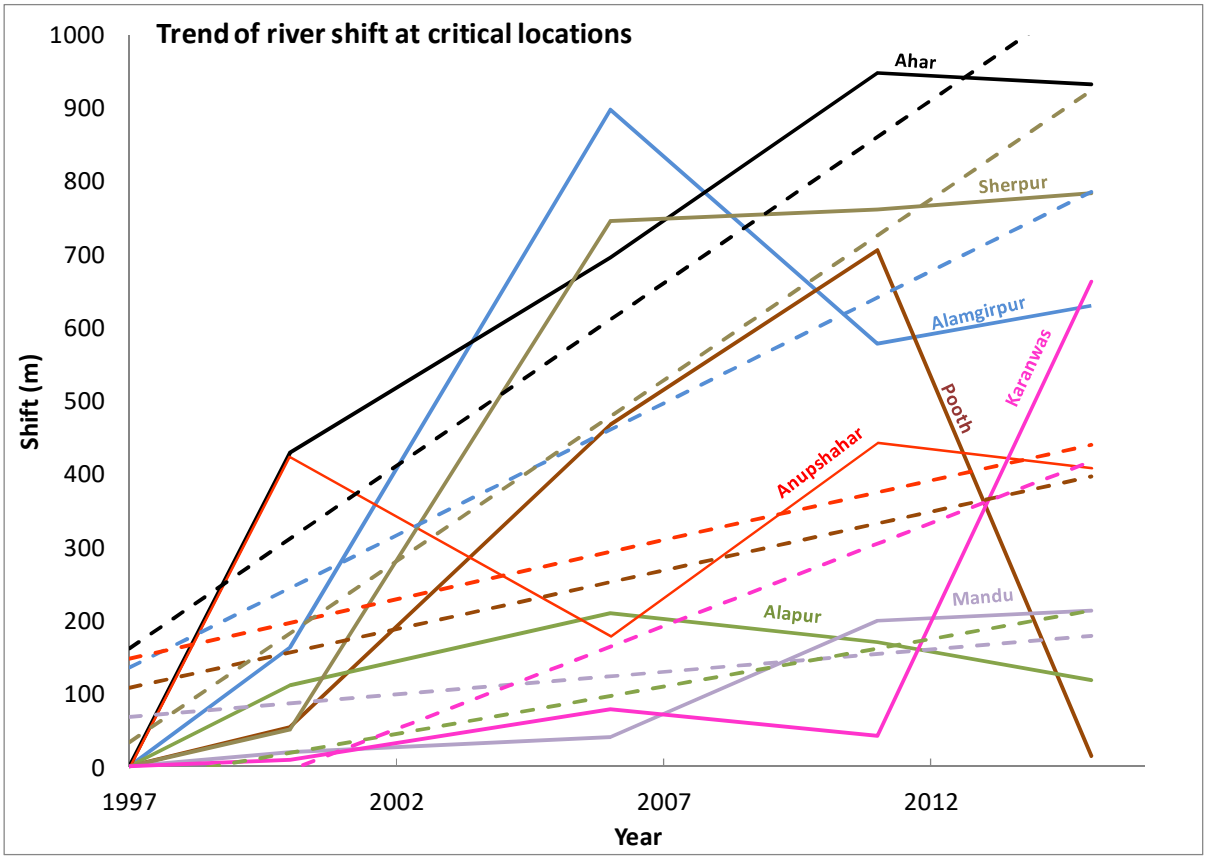

Figure 5.7: River shifting trend at critical locations

5.2 Hydrodynamic modelling of river flow

For simulation of design basis flood, a flow model has been setup from Rishikesh to Kachla bridge. The extended cross sections have been used to develop the model in 1D. The river network is extracted from satellite images and river sections are defined. In this reach, there are three gauge discharge (GD) sites, namely; Rishikesh, Garhmukteshwar and Kachla bridge

site for which hydrological data were obtained from CWC and used in model development. In addition, there is a Gauge site near Narora barrage and its levels are used for calibrating/ validating the flow model. Three barrage locations, namely, Bhimgoda, Raoli and Narora from where river flow is diverted for Irrigation projects have also been included in the model. The upstream boundary condition for the flow model is inflow at Rishikesh and the downstream boundary condition is water level at Kachla bridge GD site. To account for the catchment flowing directly to river Ganga a distributed lateral flow has also been considered.

5.2.1 MIKE 11 Model Setup for Flow Simulation

The model simulations are carried out for calibration and validation with the observed flow for the monsoon period (July to October). The simulated water level at Narora gauging site is compared with the observed level. Figure 5.8 shows the observed and simulated values for 2010. Further, the flow model is validated with 2011 and 2013 observed data and shown in Figure 5.9 and Figure 5.10. The error estimation in simulated and observed levels with respect to correlation coefficient, peak error and peak time error for calibration and validation runs are summarised in Table 5.4 below:

Table 5.4: Error estimated in flow model calibration and validation

SN	Error Parameter	Values		
		Calibration (2010)	Validation (2011)	Validation (2013)
1	Correlation Coefficient	0.849	0.736	0.695
2	Peak error (%)	-0.002	0.001	-0.001
3	Volume error (%)	0.002	0.002	0.004
4	Peak time error	0	-2.000	-2.500

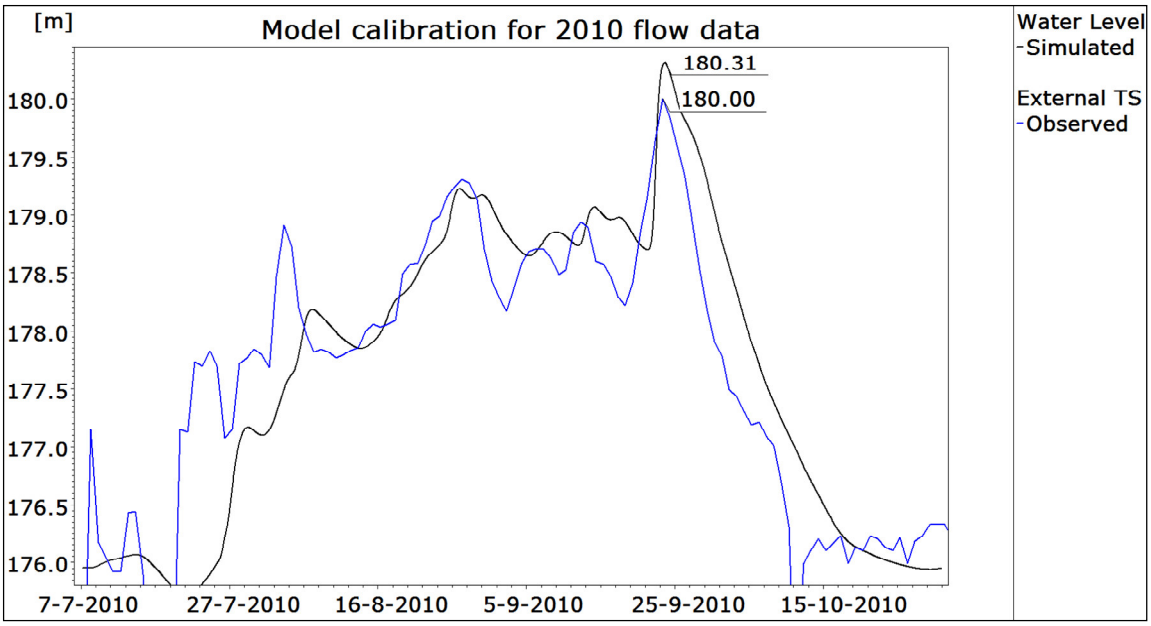

Figure 5.8: Comparison of simulated and observed reservoir level for 2010

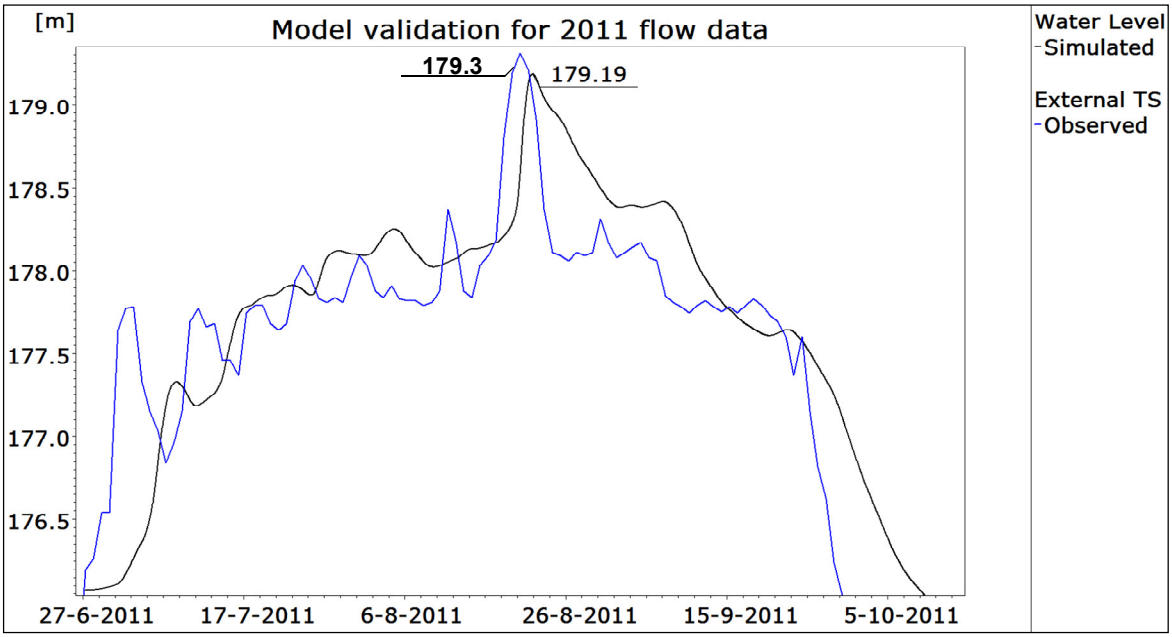

Figure 5.9: Comparison of simulated and observed reservoir level for 2011

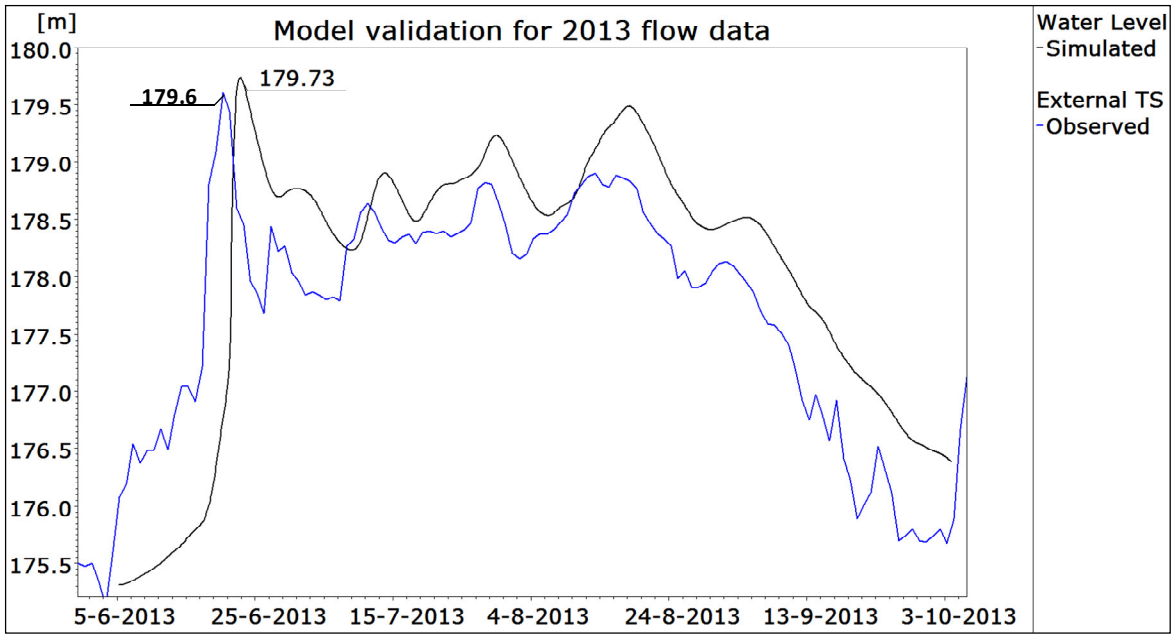

Figure 5.10: Comparison of simulated and observed reservoir level for 2013

5.2.2 Estimation of flood attributes for design flood at Anupshahar

The recommended design flood for flood protection work is defined as 25 year flood for agricultural land and 100 year flood for township/ industrial area (CWC, 2012). Hence, the design flood, 25- and 100- year return period flood at Rishikesh is simulated in the MIKE 11 model and the corresponding flood attributes near Anupshahar are computed. The design flood is considered as inflow at Rishikesh and from intermediate catchments (between Rishikesh to Kachlabridge, as shown in Figure 3.2) along the river stretch as distributed flood.

5.2.2.1.1 Simulation of 25 year return period flood

The design flood of 25 year return period is simulated in MIKE 11 model and the attenuation of flood is computed. Figure 5.11 shows the inflow hydrograph at Rishikesh and its attenuation at Anupshahar. The 25-year return period flood at Rishikesh is shown in Figure 3.4 and have peak flow of 11432.20 m^3/s and duration of about 80 hours. For simulation of design flood, an arbitrary start time of simulation has been adopted as 01 Jan 2017 08:00:00 (date and time in hour minute and second format) and hourly ordinate of design flood is defined. However, considering the longer stretch of model domain, the flood is simulated for a longer duration (about 10 days). At Anupshahar, the design flood is attenuated to peak flood of 4517.73 m^3/s and reaches after about 5th day from start of simulation. The maximum flood level at Anupshahar due to 25 year flood is computed as RL 182.07 m.

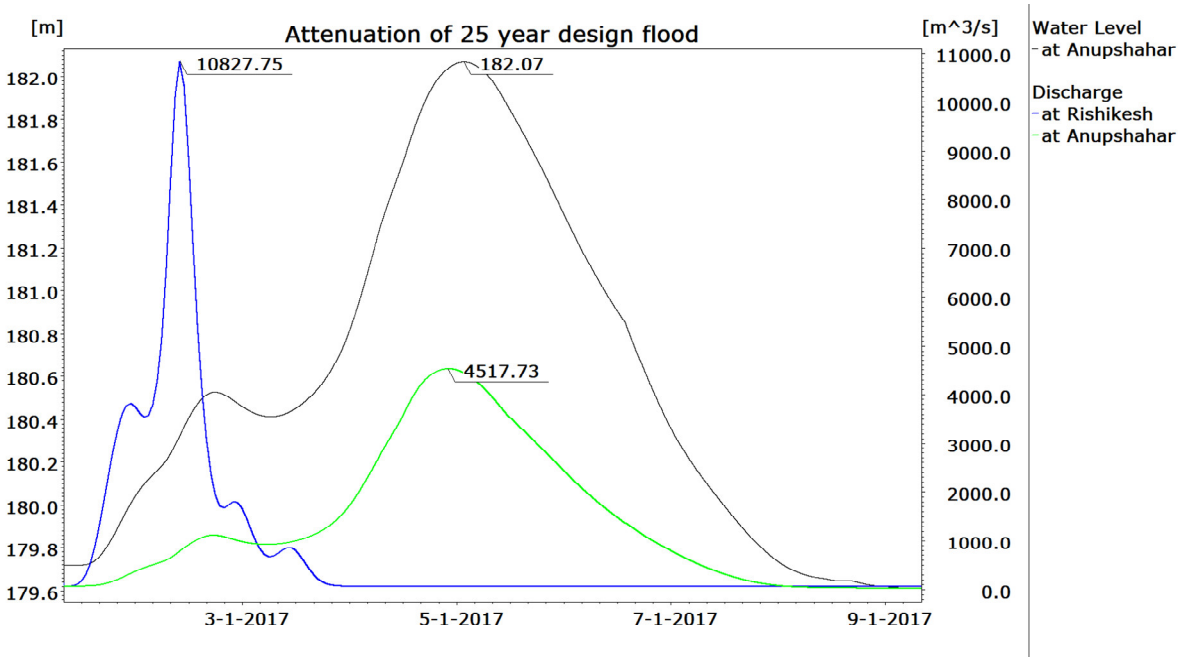

Figure 5.11: Attenuation of 25 year flood and stage hydrograph at Anupshahar

Further, the maps of flood attribute namely maximum flood level and flow velocity are also developed for this 1D flow simulation in the geographical extent of Anupshahar along river reach. In one dimensional flow modelling, the flow attributes are computed at each section and considered as uniform throughout the river section. The mapping of water levels, water depths, velocities etc. from the one-dimensional results to two-dimensional maps are done internally in MIKE 11 through a couple of steps:

i) Interpolation of cross sections at all digitised points and all interpolated water level grid points.

ii) Linear interpolation of results from the numerical grid to the interpolated cross sections.

iii) Spatial interpolation of the bed level from the cross sections to all intermediate cells in the two-dimensional grid within the river bed.

iv) Determination of the velocity profile at all cross sections based on conveyance distribution.

v) Spatial interpolation of the required results from the cross sections to all intermediate cells in the two-dimensional grid within the river bed.

For 25 year flood simulation, the maps of the maximum flood level and the maximum flow velocity have been generated, as shown in Figure 5.12 and Figure 5.13, respectively. These

maps show the variation of flood attributes in spatial domain near Anupshahar. The boundary of Anupshahar Township is overlaid over these maps. The velocity map shows that velocity as high as 1.4-1.6 m/s develops on the north of township area and therefore should sediment have induce higher erosion on this area. This estimation is in line with the real erosion observed through satellite images as shown in Figure 5.6 where major bank line shift has been observed on the north of Township on the right bank of river Ganga.

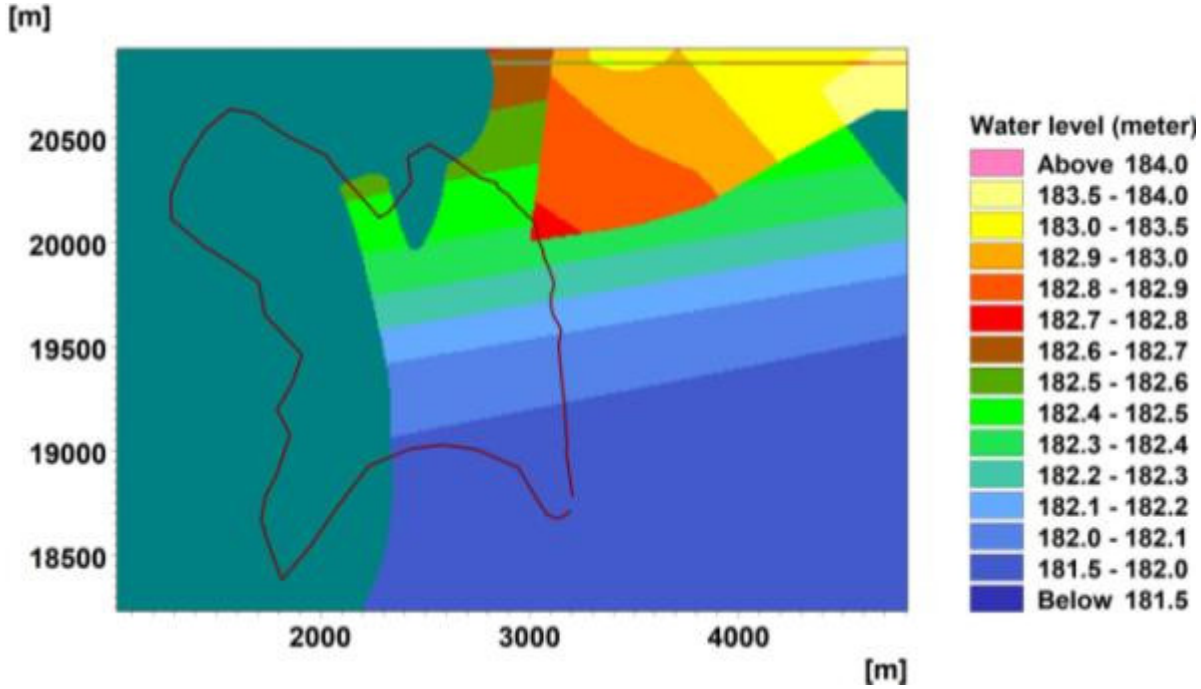

Figure 5.12: Maximum flood level map near Anupshahar for design flood

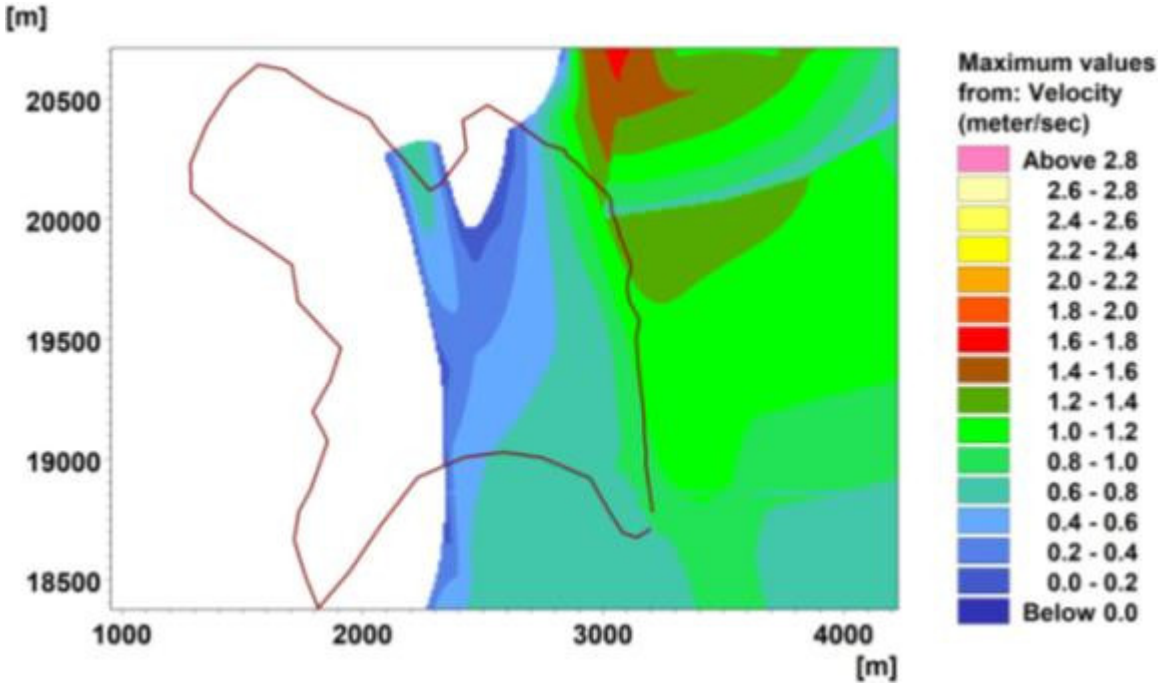

Figure 5.13: Maximum flow velocity map near Anupshahar for design flood

5.2.2.2 Simulation of 100 year return period flood

Similarly, 100 year design flood is simulated in MIKE 11 model and the flow attributes are estimated. The attenuation of 100 year design flood is shown in Figure 5.14. At Anupshahar, 100- year flood is attenuated to peak flood of 6243.88 m^3/s while the maximum flood level at Anupshahar is computed as RL 182.68 m.

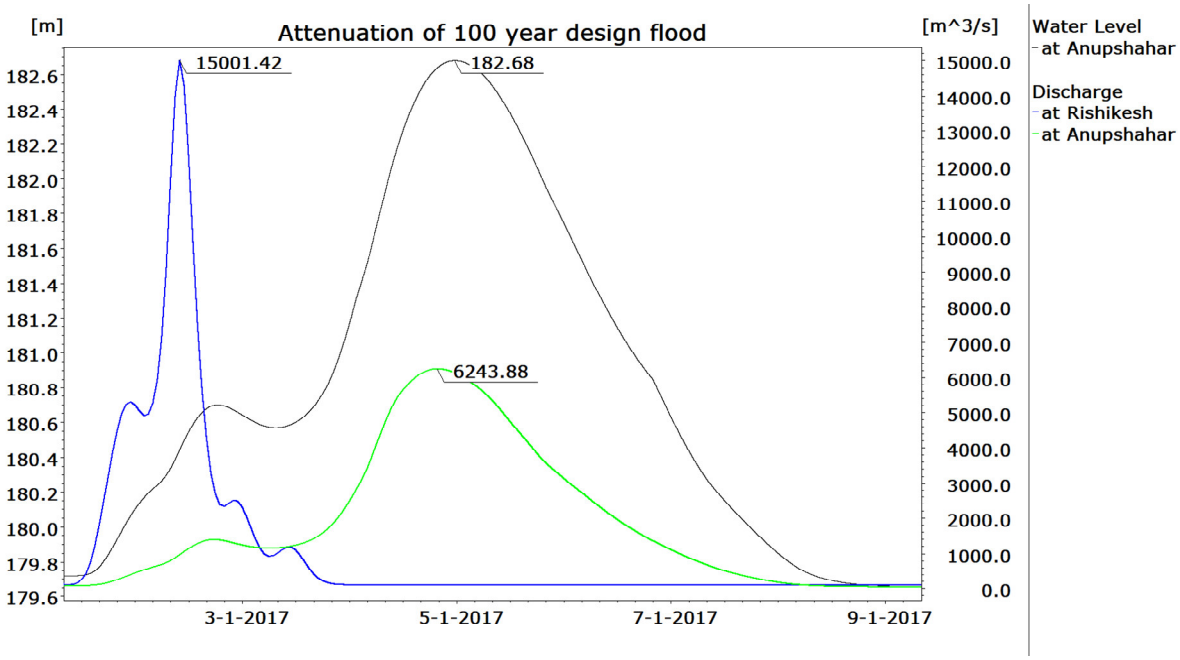

Figure 5.14: Attenuation of 100 year flood and stage hydrograph at Anupshahar

Further, for 100- year flood simulation, the maps of the maximum flood level and the maximum flow velocity have been generated, as shown in Figure 5.15 and Figure 5.16, respectively. In this case also, the velocity as high as 1.4-1.6 m/s is developed on the north of township area and therefore causes bank erosion.

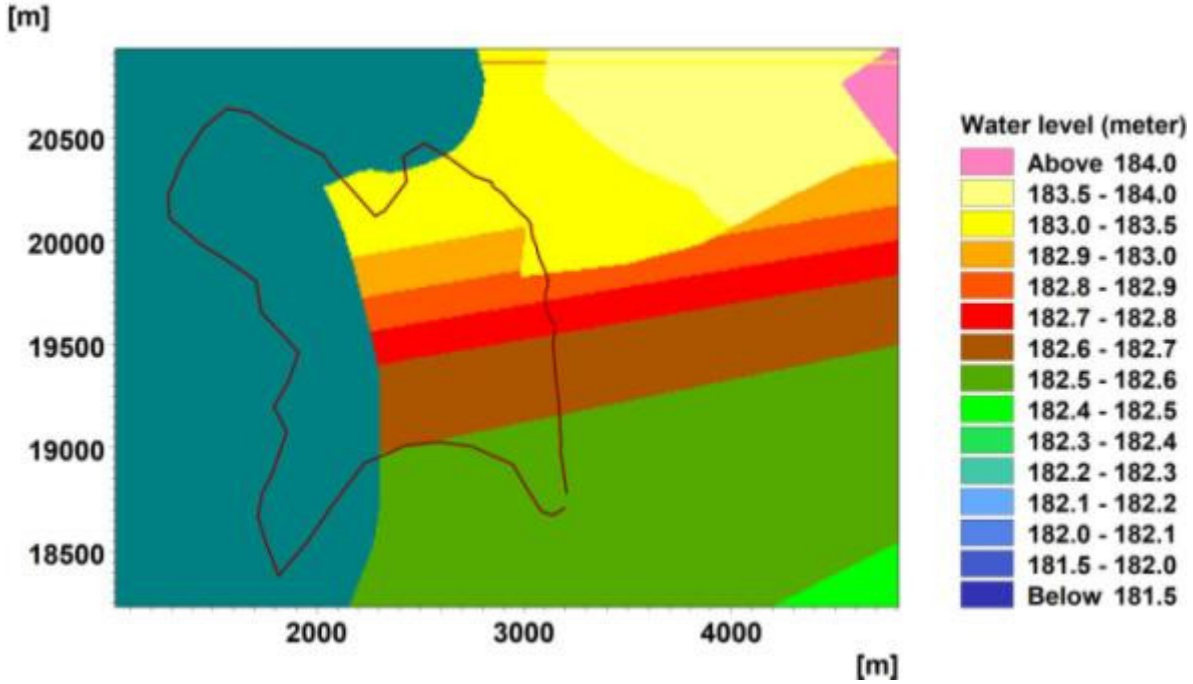

Figure 5.15: Maximum flood level map near Anupshahar for design flood

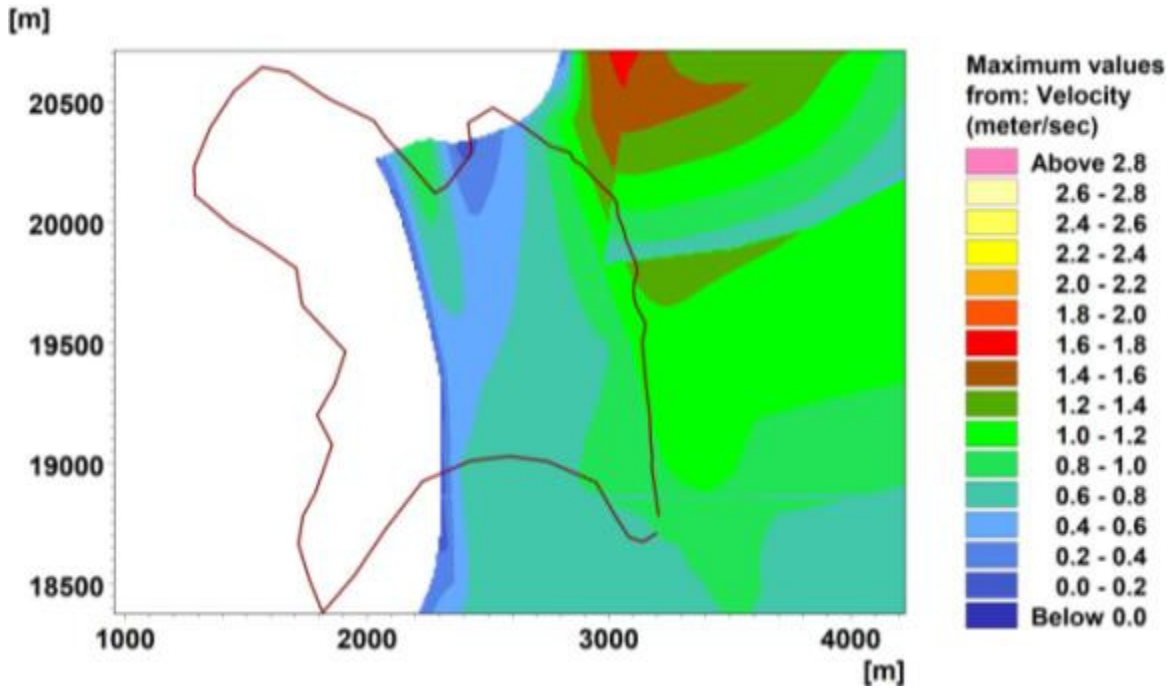

Figure 5.16: Maximum flow velocity map near Anupshahar for design flood

5.3 Morpho-dynamic modelling of river flow

The basic requirement for development of the morpho-dynamic model is the development of curvilinear grid for the study stretch. Subsequently, bathymetry for this curvilinear grid is defined. In the next step, 2D hydrodynamic model is developed with grids on the upstream river reach is defined for inflow and the grids on the most downstream river reach is defined for water level. Thereafter, morphological parameters are added to develop the morpho-dynamic model. The development of each component of the model is described in following sections.

5.3.1 Development of curvilinear grid

The study stretch from Garhmukteshwar to Kachalabridge (142.79 km) is defined through plan form of active river course as extracted from the recent satellite image of 2015. The polygon of the river bank line defines the extent of the curvilinear grid. Through curvilinear grid, the lines along flow line and normal to flow line are defined for the entire study stretch. As this is a cumbersome task, an additional tool of MIKE Grid Generator is available with MIKE 21C program. Using this tool, curvilinear grid for the study stretch is developed through 1468x108 cells. Here, 1468 grids are along the flow line defined through 's' cell as shown in Figure 4.4. These grids are defined in MIKE 21C grid as 'j' grid and its range varies from 0 to 1467; 0 at the most upstream end and 1467 at the most downstream end. Similarly, 108 grids are across the flow line (normal to flow line) defined through 'n' cell (Figure 4.4). These cells in the MIKE 21C model are defined through k grid and its range varies from 0 to 107, 0 at the right bank edge and 107 at the left bank edge at any of the j grid. Thus, the most upstream boundary corresponding to GD site at Garhmukteshwar is defined through j=0, k = 0 to 107. Likewise, the most downstream boundary at Kachalabridge GD site is defined through j=1467, k= 0 to 107. The curvilinear grid of the model stretch is checked for the Orthogonality and found within the range of ± 0.05. Further, the aspect ratio is also evaluated and found within the range of 2-7 with the average value of 4. The bathymetry (Digital elevation model for the river bed) of the study reach have been developed using elevation values obtained from river cross section survey data and spot and contours levels from SOI toposheets at 30 m rectangular grid and has been used to generate the curvilinear grid bathymetry as shown in Figure 5.17. The 'j' line for the stretch of Anupshahar is laying in the

range of 570 to 600, however the analysis of flow characteristics is carried out for longer stretch say j= 440 to j= 717 to have comprehensive effect of flow on the area of interest.

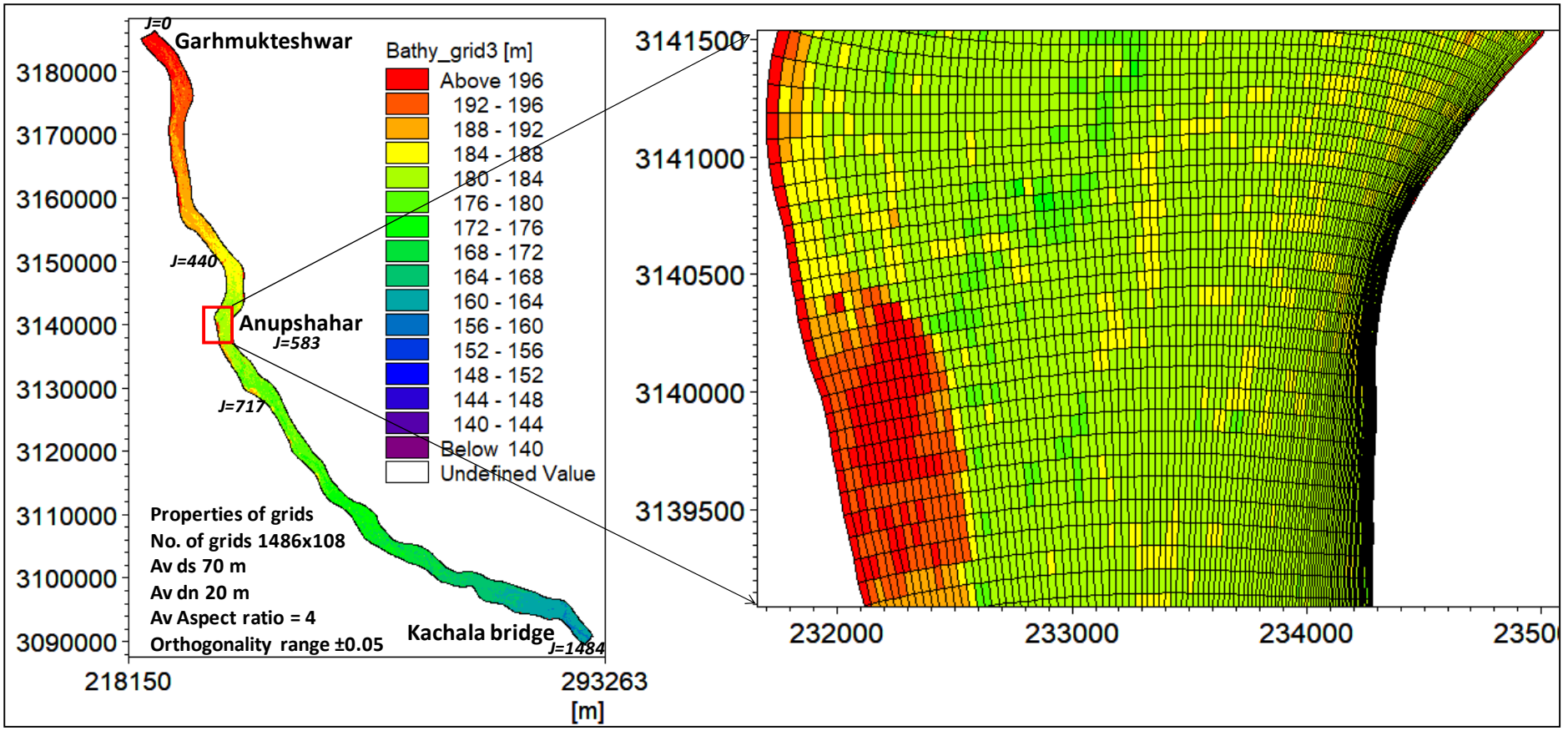

Figure 5.17: Bathymetry of the study area with curvilinear grid

Three grid locations namely j=440, 583 and 717 is selected to compute and compare various flooding attributed.

5.3.2 Development of morpho-dynamic model

For the bathymetry defined in earlier section, the morpho-dynamic model has been developed in MIKE 21C with the definition of flux inflow boundary condition at the upstream river end, i.e. at Garhmukteshwar and water level boundary condition at downstream river end at Kachalabridge site. The model is initially simulated for the monsoon flow of the year 2013, i.e 15 June-15 October 2013. The flow resistance is defined as Chezy number as a function of water depth. In the model, there is an option to use an alluvial roughness coefficient, which is a function of the local depth at every time-step. Inclusion of the resistance updating effects simulate scour and deposition patterns. Flow is deflected more over shallow parts, and sediment transport increases due to increased bed shear stresses. In general, this reduces overshoot effects when bed scour commences, and causes the topography of a point bar crest to become more rounded (as reported by Talmon, 1992). A 2D map of bed resistance (for the HD) is specified initially in the simulation to implement alluvial resistance as shown in Figure 5.18. The Chezy's number adopted in morphological simulation is shown in Table 5.5.

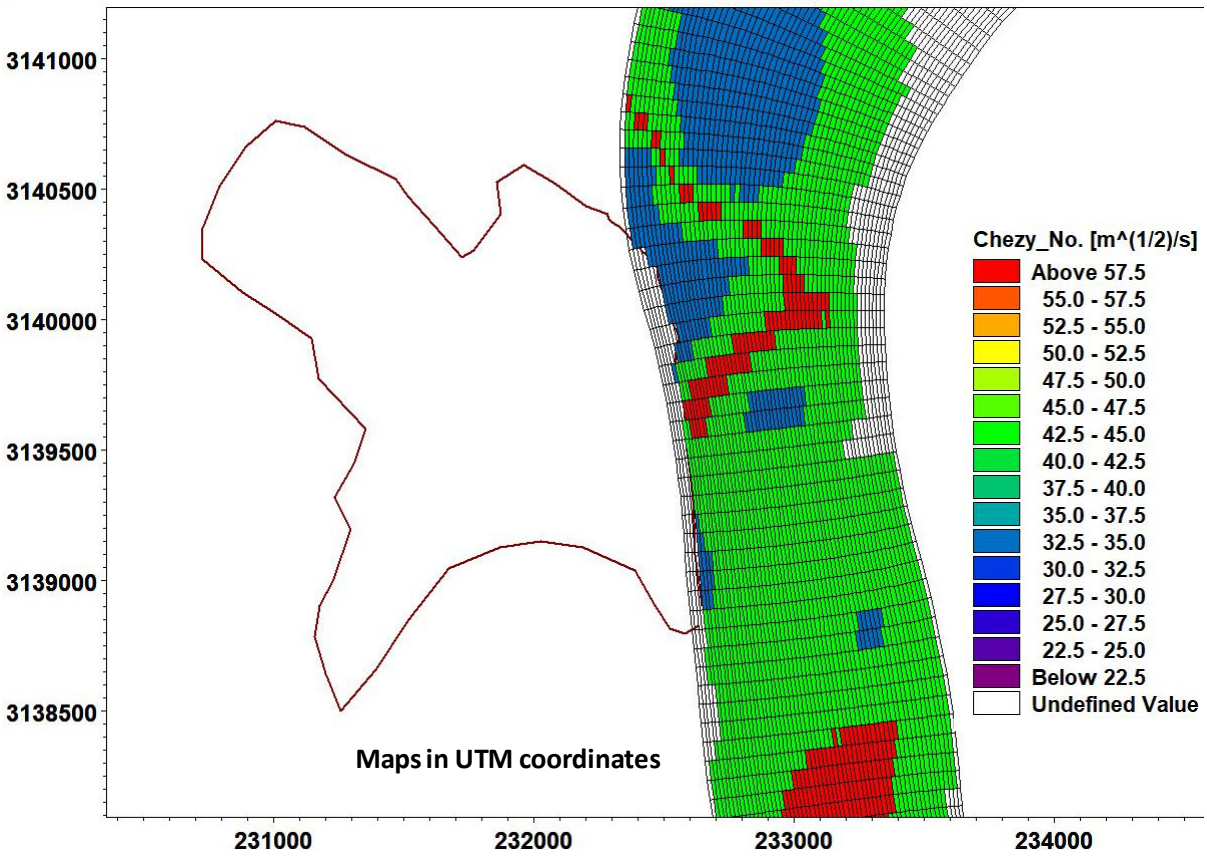

Figure 5.18: Inital Chezy number definition in spatial domain.

Table 5.5: Flow depth varying Chezy's number used in study.

Water depth (m)	Chezy's Number in $m^{1/2}/s$ (adopted for calibration)
0-1	25
1-3	30
3-6	35
6-10	45
10-15	60

5.3.2.1 Calibration and Validation

To calibrate and validate the model, the monsoon data set for 2013 is split in two parts; (i) 15 June 2013 to 14 August 2013 and (ii) 15 August 2013 to 15 October 2013. The second data set (16 August 2013 to 15 October 2013) is used to calibrated the model while the first data set (from 15 June 2013 to 15 August 2013) is used to validated the model. The calibration/ validation of the model have been done with the two data sets; (i) the observed gauge data at Narora barrage and (ii) the ratio of observed sediment load and discharge data at Kachalabridge GD site. The simulated and observed water depth at Narora gauging site for calibration and validation period is shown in Figure 5.19. The model is also calibrated and validated with the ratio of sediment load and discharge at Kachalabridge GD site as shown in Figure 5.20. The performance of model is evaluated through Nash-Sutcliffe efficiency as shown in Table 5.4.

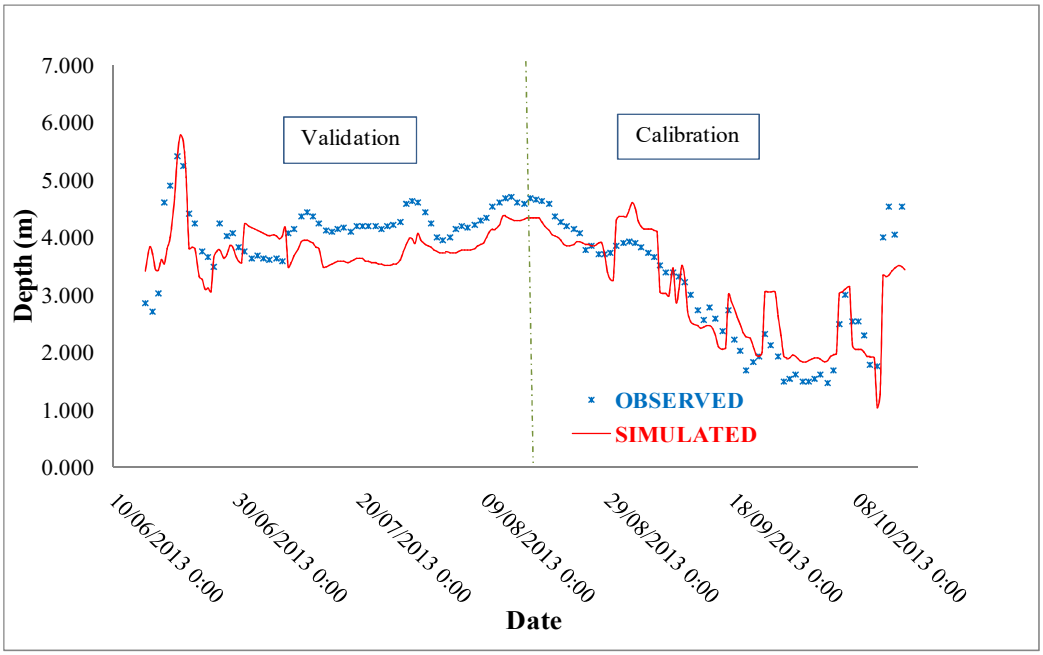

Figure 5.19: Calibration and Validation of flow model with gauge data of Narora Site

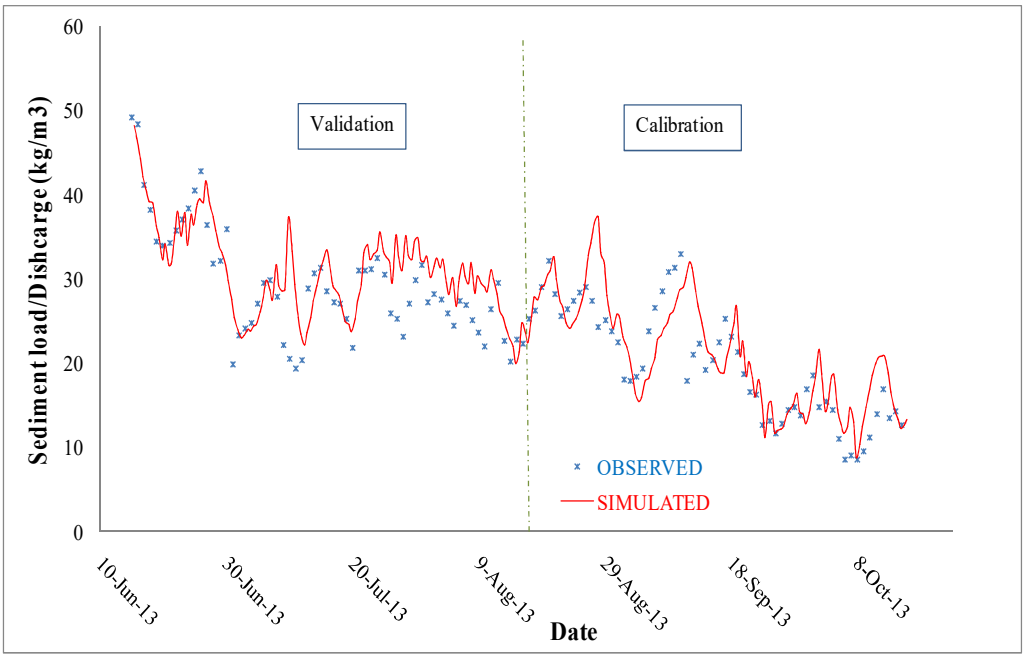

Figure 5.20: Calibration and Validation of flow model with ratio of sediment load and / discharge data at Kachalabridge site

Table 5.2 Nash – Sutcliffe Efficiency of the Model

Data Set	Nash -Sutcliffe Efficiency		
	Calibration	Validation	Overall
Water depth at Narora	0.86	0.53	0.76
Sediment Load / discharge at downstream	0.79	0.76	0.78

5.3.3 Identification of Erosion and Deposition Prone Area (net erosion map)

The result of the sediment transport model is used to compute the total sedimentation load passing through a specific cross section. The sediment laod (in MT) is computed at J= 200, 375, 550, 700, 850, 1000, 1150, 1125, 1250 and 1400. The tentative location of these cross section are shown in Figure 5.21. The computed sediment load is also shown in the figure. Between a stretch, if the sediment inflow is higher than the sediment outflow, the stretch is assigned as sedimentation reach. Similalrly, if the sediment inflow is smaller than sediment outflow, the reach is assigned as erosion reach.

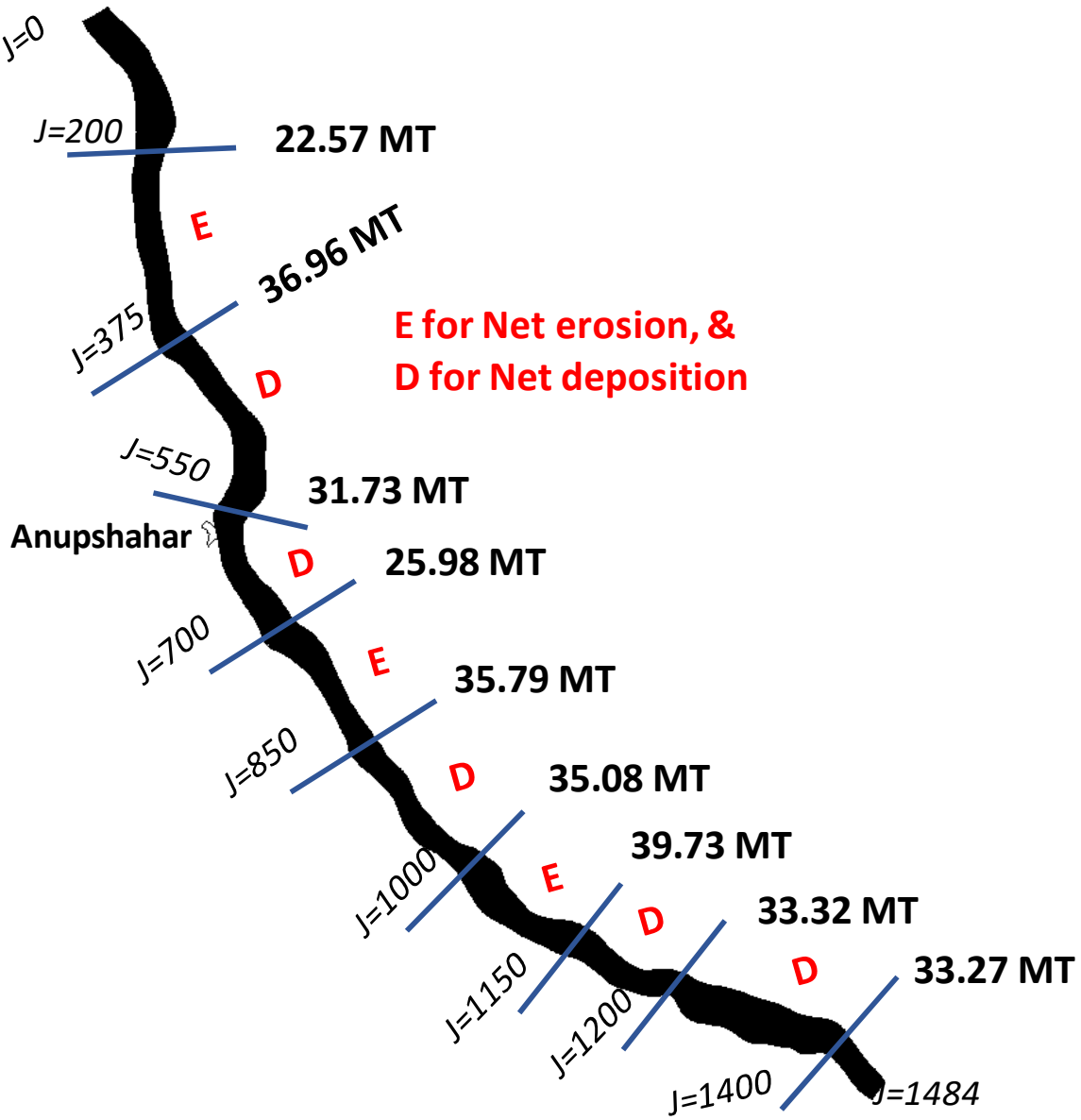

Figure 5.21: Estimation of river stretch of net erosion and deposition.

5.3.4 Simulation of Design Flood

The flow model is simulated for design flood condition of 25- and 100- year return period flood. However, as stated earlier, the duration of the design flood is about 80 hours only while the river stretch under study is longer (142.79 km), the time of travel would be higher. Further, the initial condition of the design flood may not meet with the simulation of isolated design flood. For morphological condition, the design flood as well as the flooding condition for longer duration (may be the flow during other period of monsoon of the specific year when design flood occurs) is influencing. Moreover, it would be difficult and almost impractical to estimate the entire monsoon flood along with the design flood. However, flow data for entire monsoon is available for the year 2013 and therefore using proportionality

method (ratio of peak of design flood/peak of 2013 flood at Garhmukteshwar), the flow for the entire monsoon for the design flood is estimated and simulated in the morpho-dynamic model. The computed flood for 25- and 100-year flood is shown in Figure 5.22. It is to mention that the start time of this synthesized flood is taken as 01 June 2018 and daily data is computed for the entire period, however, the morpho-dynamic model is simulated for monsoon period from 15 June to 15 October only. The inflow hydrograph shows three prominent peak on dates; 27 July, 11 Aug and 23 Aug, respectively. The flow characteristics would be analysed and discuss during the entire simulation period especially during these periods.

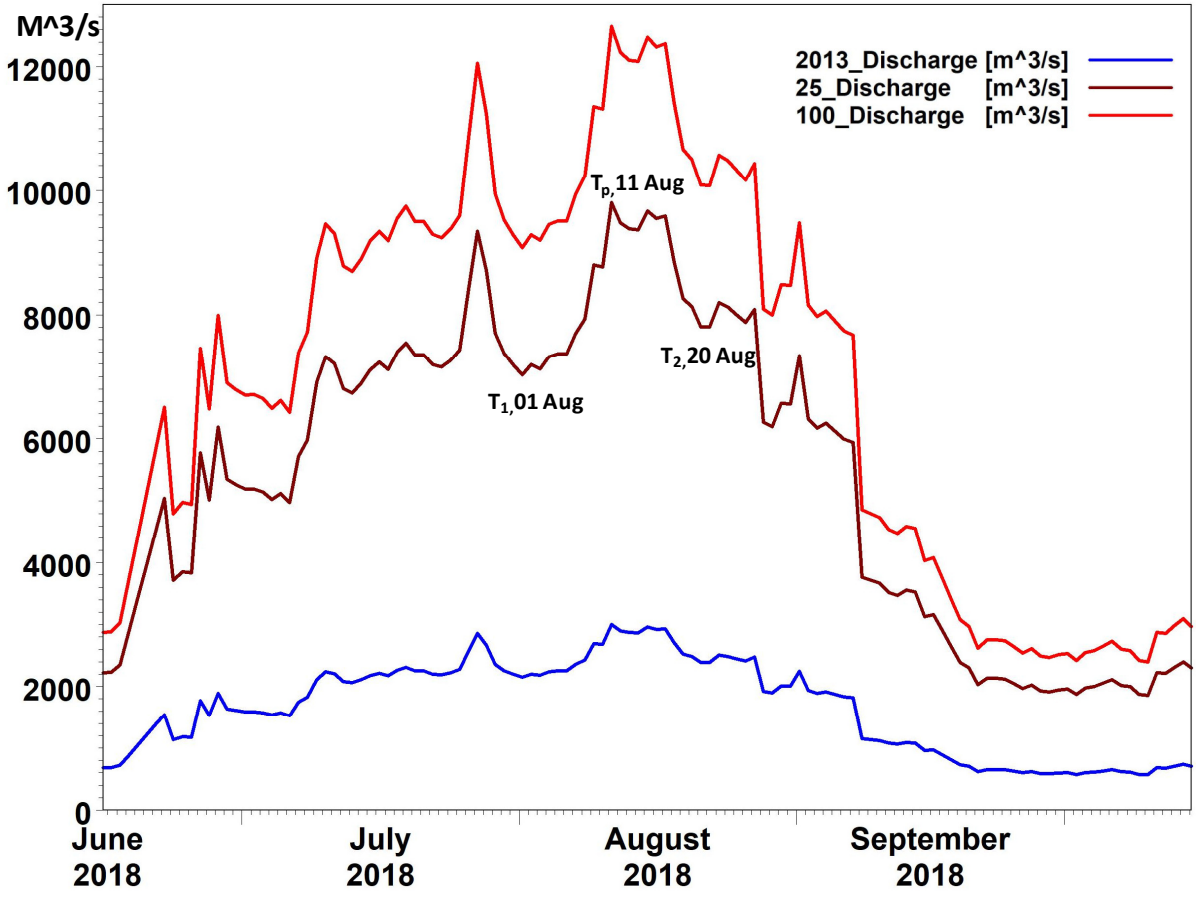

Figure 5.22: Synthesized flow at Garhmukteswar during design flood of 25- and 100-year return period flood.

5.3.5 Morpho-dynamic modelling for 25 year flood hydrograph

The MIKE 21C model computes various flow attributes like water level, flow depth, velocity, sediment concentration, total sediment load, Net sediment/ erosion in spatial domain study reach. The flow characteristics are evaluated for two design flood condition as mentioned

above. In this section we would discuss various flow attributes for 25 year flood. The attenuation of 25- year flood at various cross sections (grid location) is shown in Figure 5.23.

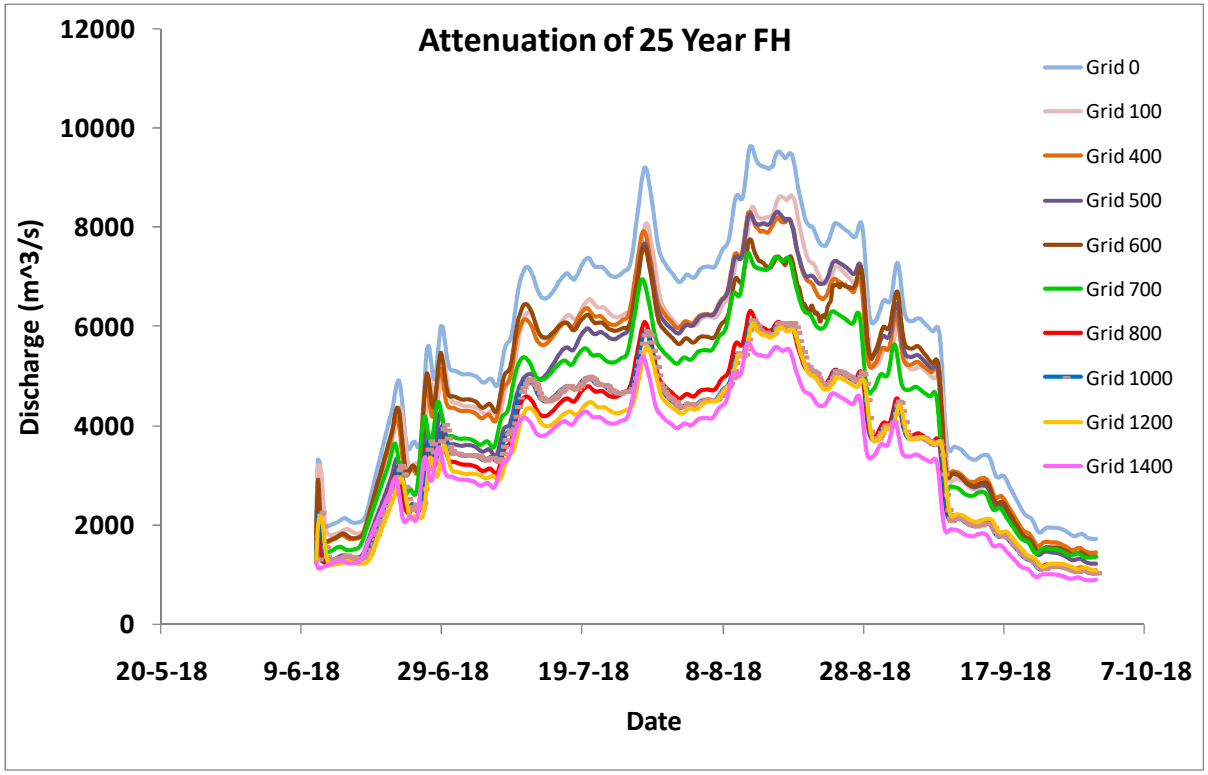

Figure 5.23: Attnuation of 25-year flood hydrograph at various locations in study stretch.

In morphodynamic model, dynamic river bed is considered. With the progress of flow either erosion or deposition makes the changes in the bed level. To illustrate the changing bed level, three locations have been identified, one upstream of Anupshahar (grid j=440), second at Anupshahar (grid j=583) and third downstream of Anupshahar (grid j=717). The river cross section profiles at these locations are plotted for an average interval of 10 days during the simulation. The river bed level profile for an upstream location (grid j=440) is shown in Figure 5.24. The figure shows the temporal changes of river bed level and flood level at this location. The movement of flow from right bank (grid k=0) towards left bank (grid k=107) can be visualised by comparing the temporal river section.

Similar movement of river flow from right bank towards left bank can be visualised for Anupshahar (grid j=583) and the downstream location (grid j=770) in Figure 5.25 and Figure 5.26, respectively.

The MIKE 21C flow model is simulated for two condition, initially without considering the sediment flow and later on considering the sediment flow with mobile river bed. For both the cases, the maximum flood level maps for the area around Anupshahar are plotted as shown in Figure 5.27. The figure shows with hydrodynamic (HD) flow simulation the maximum flood level near Anupshahar is higher (of the order of 189-191 m) compared to maximum flood level (of the order of 185 m) for flow simulation with sediment transport (ST) and mobile bed consideration. With sediment transport model, the scouring of the river bed at every grid and time steps are included in the simulation and therefore lower value of the maximum flood level is estimated.

The maps of maximum flooding depth and maximum current (flow velocity) are also computed from HD simulation and are shown in Figure 5.28 and Figure 5.29, respectively.

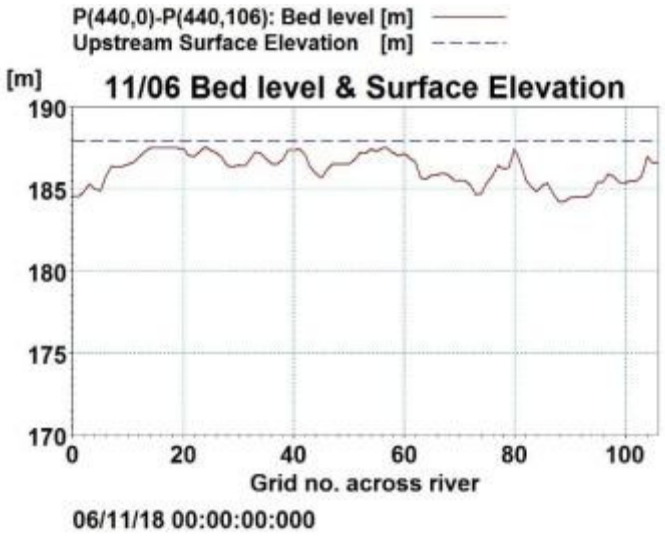
P(440,0)-P(440,106): Bed level [m]
Upstream Surface Elevation [m]
[m]
11/06 Bed level & Surface Elevation
190
185
180
175
170
0
20
40
60
80
100
Grid no. across river
06/11/18 00:00:00:000

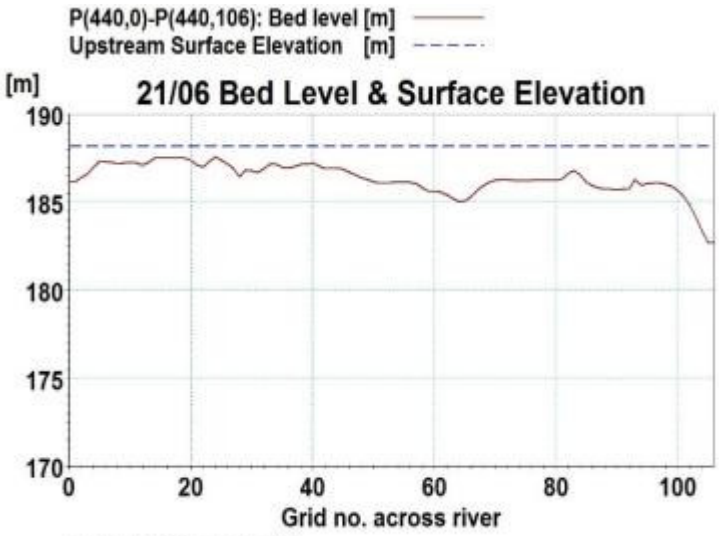
P(440,0)-P(440,106): Bed level [m]
Upstream Surface Elevation [m]
[m]
21/06 Bed Level & Surface Elevation
190
185
180
175
170
0
20
40
60
80
100
Grid no. across river
06/21/18 00:00:00:000

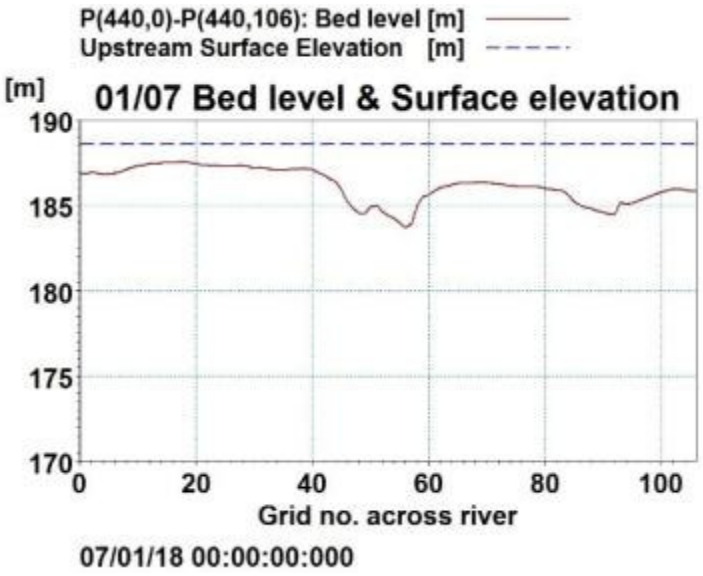
P(440,0)-P(440,106): Bed level [m]
Upstream Surface Elevation [m]
[m]
01/07 Bed level & Surface elevation
190
185
180
175
170
0
20
40
60
80
100
Grid no. across river
07/01/18 00:00:00:000

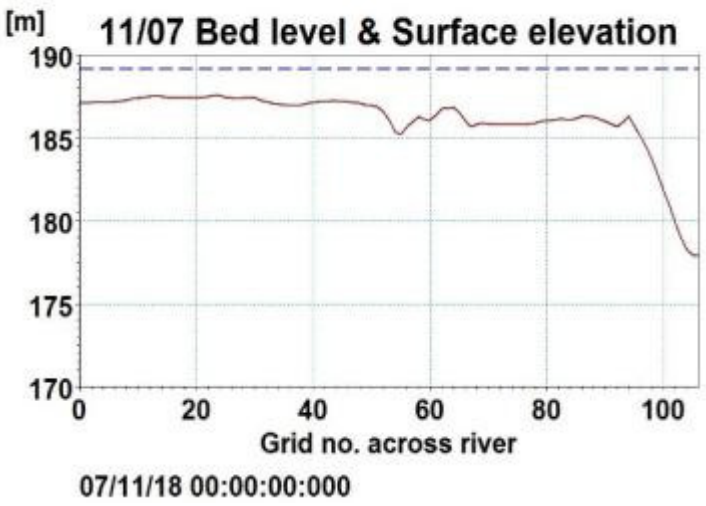
P(440,0)-P(440,106): Bed level [m]
Upstream Surface Elevation [m]
[m]
11/07 Bed level & Surface elevation
190
185
180
175
170
0
20
40
60
80
100
Grid no. across river
07/11/18 00:00:00:000

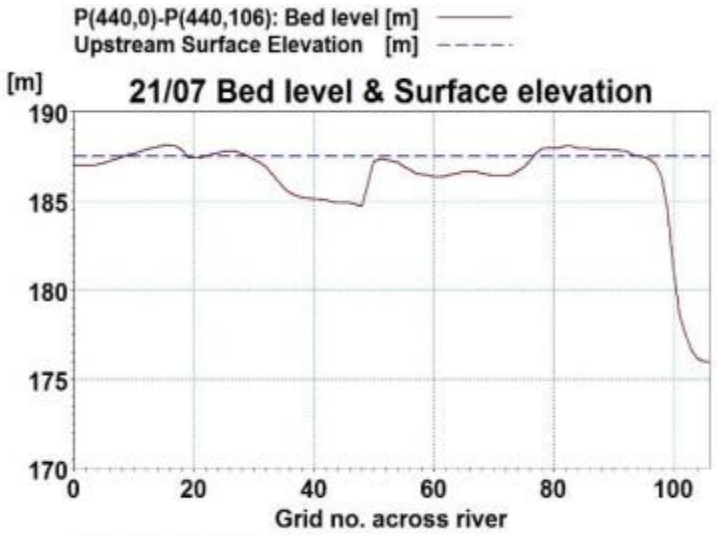
P(440,0)-P(440,106): Bed level [m]
Upstream Surface Elevation [m]
[m]
21/07 Bed level & Surface elevation
190
185
180
175
170
0
20
40
60
80
100
Grid no. across river
07/21/18 00:00:00:000

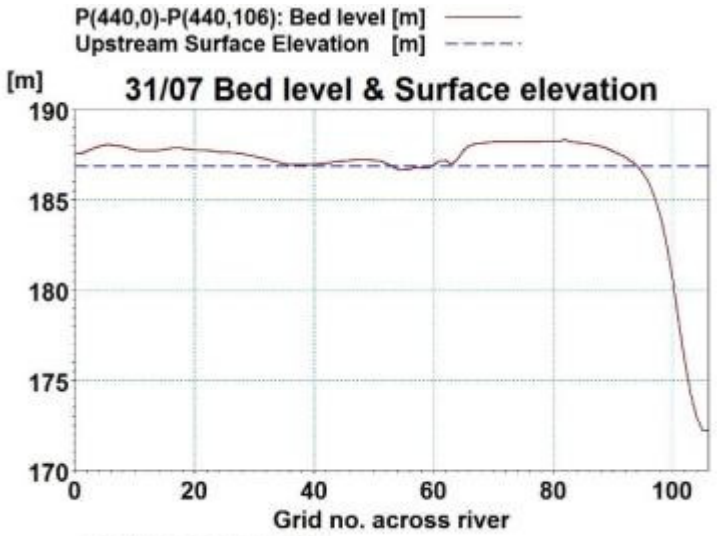
P(440,0)-P(440,106): Bed level [m]
Upstream Surface Elevation [m]
[m]
31/07 Bed level & Surface elevation
190
185
180
175
170
0
20
40
60
80
100
Grid no. across river
07/31/18 00:00:00:000

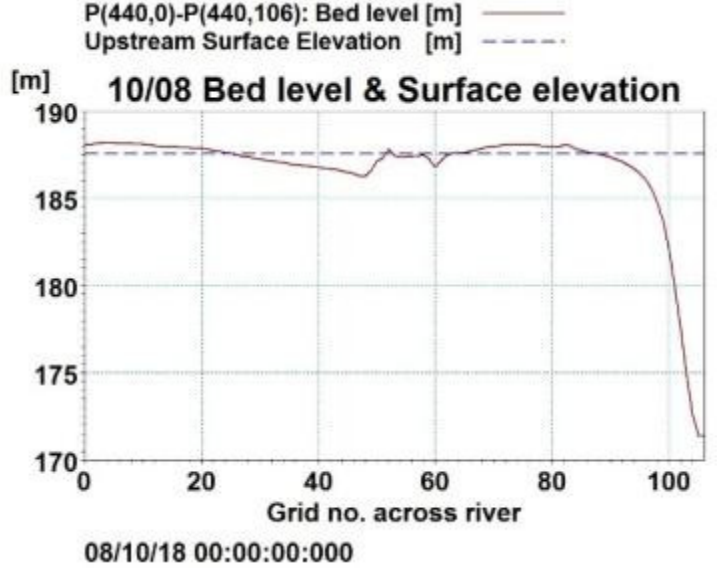
P(440,0)-P(440,106): Bed level [m]
Upstream Surface Elevation [m]
[m]
10/08 Bed level & Surface elevation
190
185
180
175
170
0
20
40
60
80
100
Grid no. across river
08/10/18 00:00:00:000

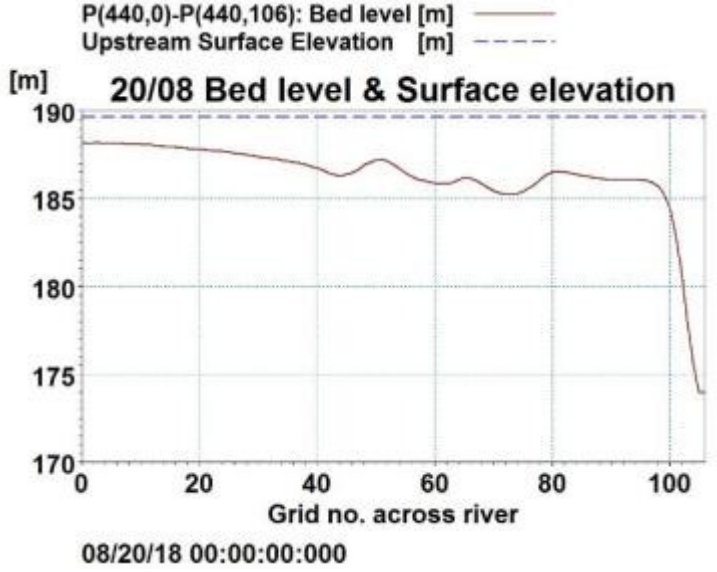
P(440,0)-P(440,106): Bed level [m]
Upstream Surface Elevation [m]
[m]
20/08 Bed level & Surface elevation
190
185
180
175
170
0
20
40
60
80
100
Grid no. across river
08/20/18 00:00:00:000

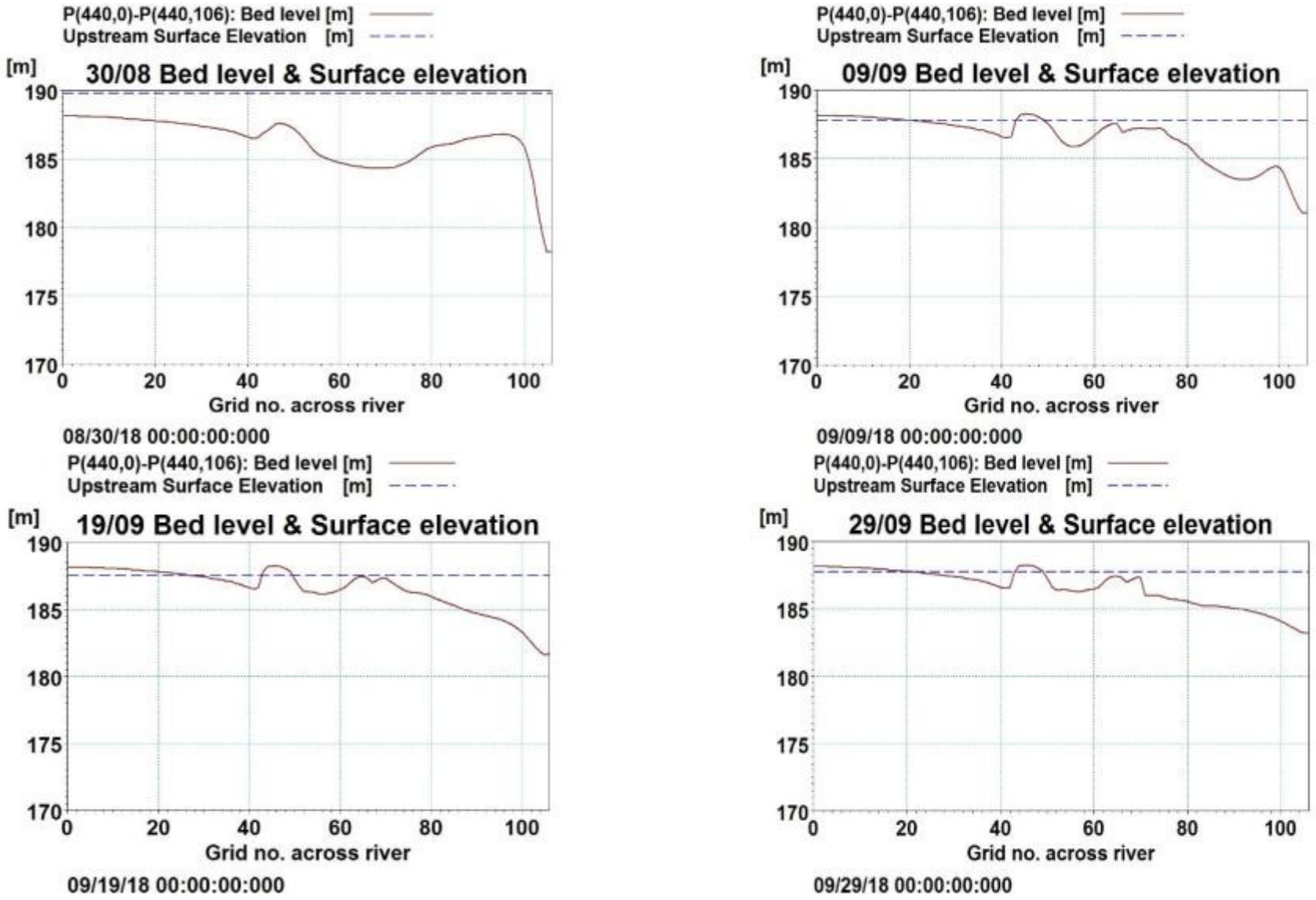

Figure 5.24: Temporal variation at 10 days interval of river section at upstream location (j=440) for 25-year flood.

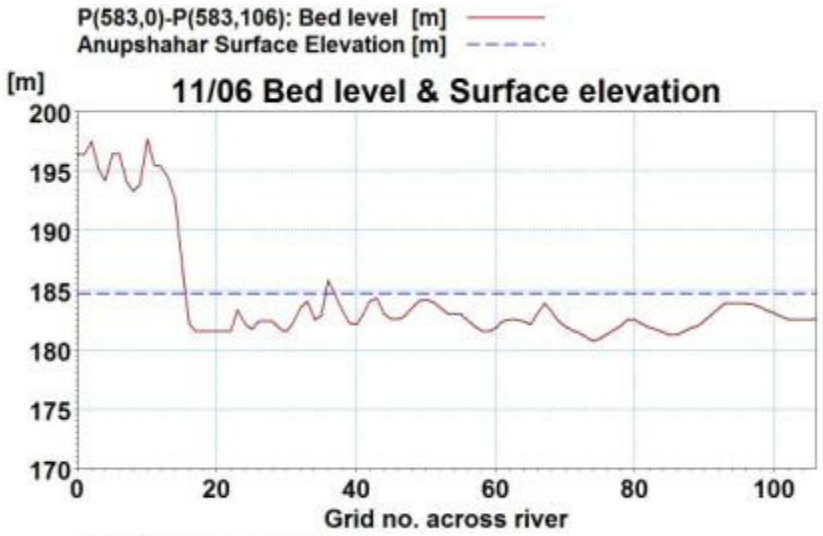
P(583,0)-P(583,106): Bed level [m]
Anupshahar Surface Elevation [m]
[m]
11/06 Bed level & Surface elevation
200
195
190
185
180
175
170
0
20
40
60
80
100
Grid no. across river
06/11/18 00:00:00:000

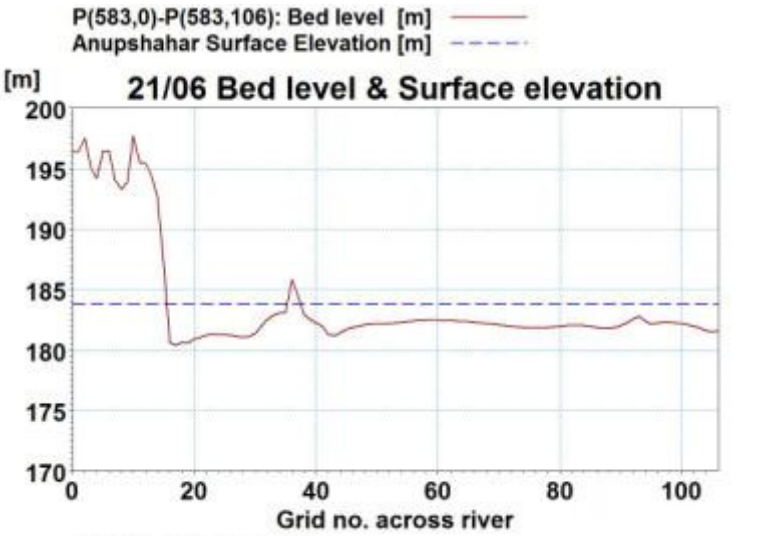
P(583,0)-P(583,106): Bed level [m]
Anupshahar Surface Elevation [m]
[m]
21/06 Bed level & Surface elevation
200
195
190
185
180
175
170
0
20
40
60
80
100
Grid no. across river
06/21/18 00:00:00:000

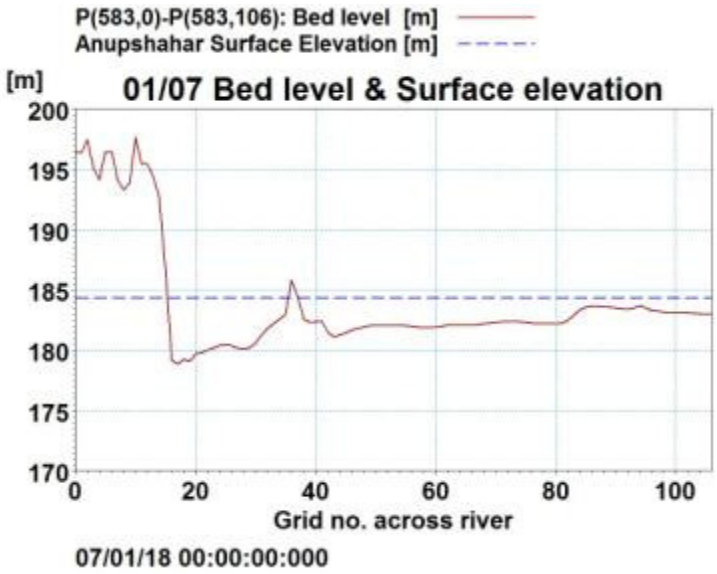
P(583,0)-P(583,106): Bed level [m]
Anupshahar Surface Elevation [m]
[m]
01/07 Bed level & Surface elevation
200
195
190
185
180
175
170
0
20
40
60
80
100
Grid no. across river
07/01/18 00:00:00:000

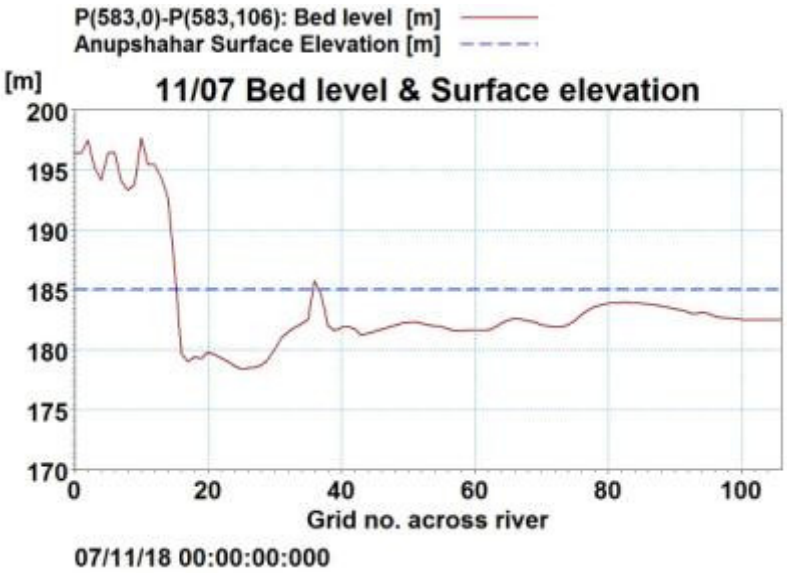
P(583,0)-P(583,106): Bed level [m]
Anupshahar Surface Elevation [m]
[m]
11/07 Bed level & Surface elevation
200
195
190
185
180
175
170
0
20
40
60
80
100
Grid no. across river
07/11/18 00:00:00:000

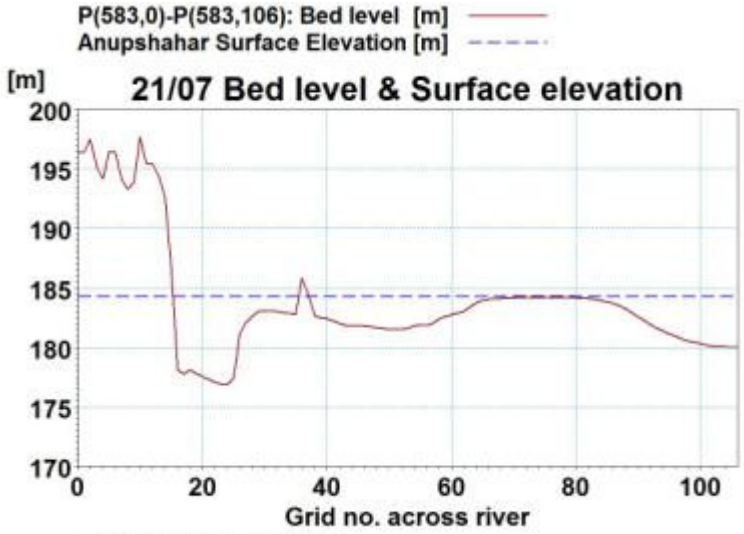
P(583,0)-P(583,106): Bed level [m]
Anupshahar Surface Elevation [m]
[m]
21/07 Bed level & Surface elevation
200
195
190
185
180
175
170
0
20
40
60
80
100
Grid no. across river
07/21/18 00:00:00:000

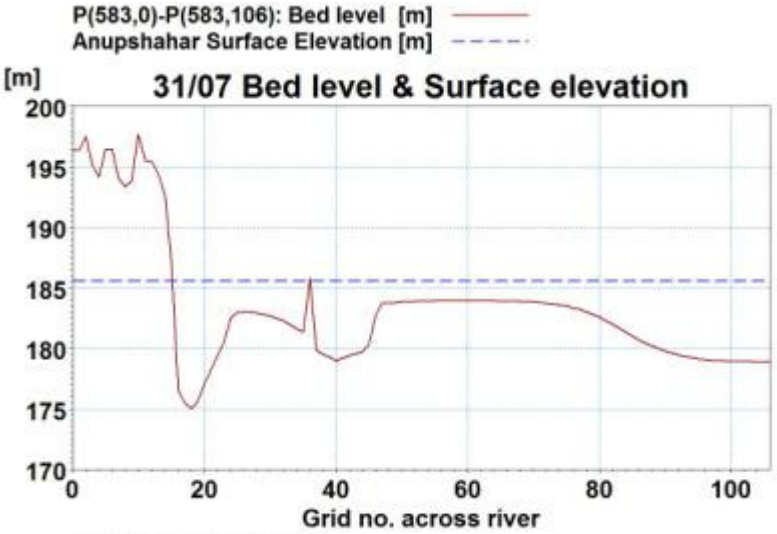
P(583,0)-P(583,106): Bed level [m]
Anupshahar Surface Elevation [m]
[m]
31/07 Bed level & Surface elevation
200
195
190
185
180
175
170
0
20
40
60
80
100
Grid no. across river
07/31/18 00:00:00:000

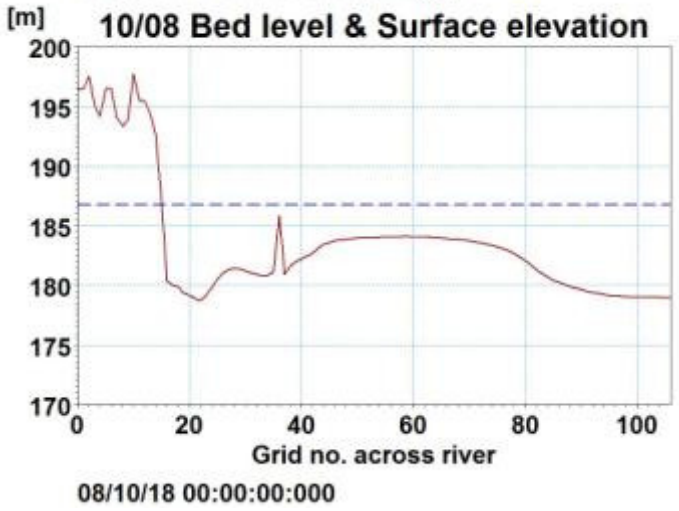
P(583,0)-P(583,106): Bed level [m]
Anupshahar Surface Elevation [m]
[m]
10/08 Bed level & Surface elevation
200
195
190
185
180
175
170
0
20
40
60
80
100
Grid no. across river
08/10/18 00:00:00:000

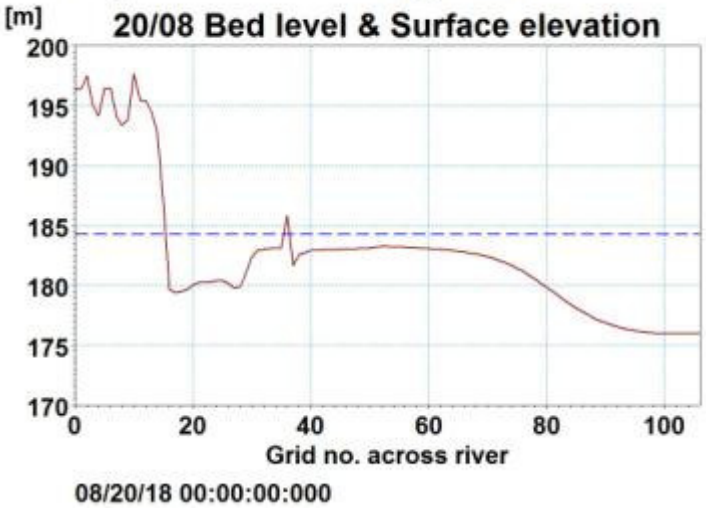
P(583,0)-P(583,106): Bed level [m]
Anupshahar Surface Elevation [m]
[m]
20/08 Bed level & Surface elevation
200
195
190
185
180
175
170
0
20
40
60
80
100
Grid no. across river
08/20/18 00:00:00:000

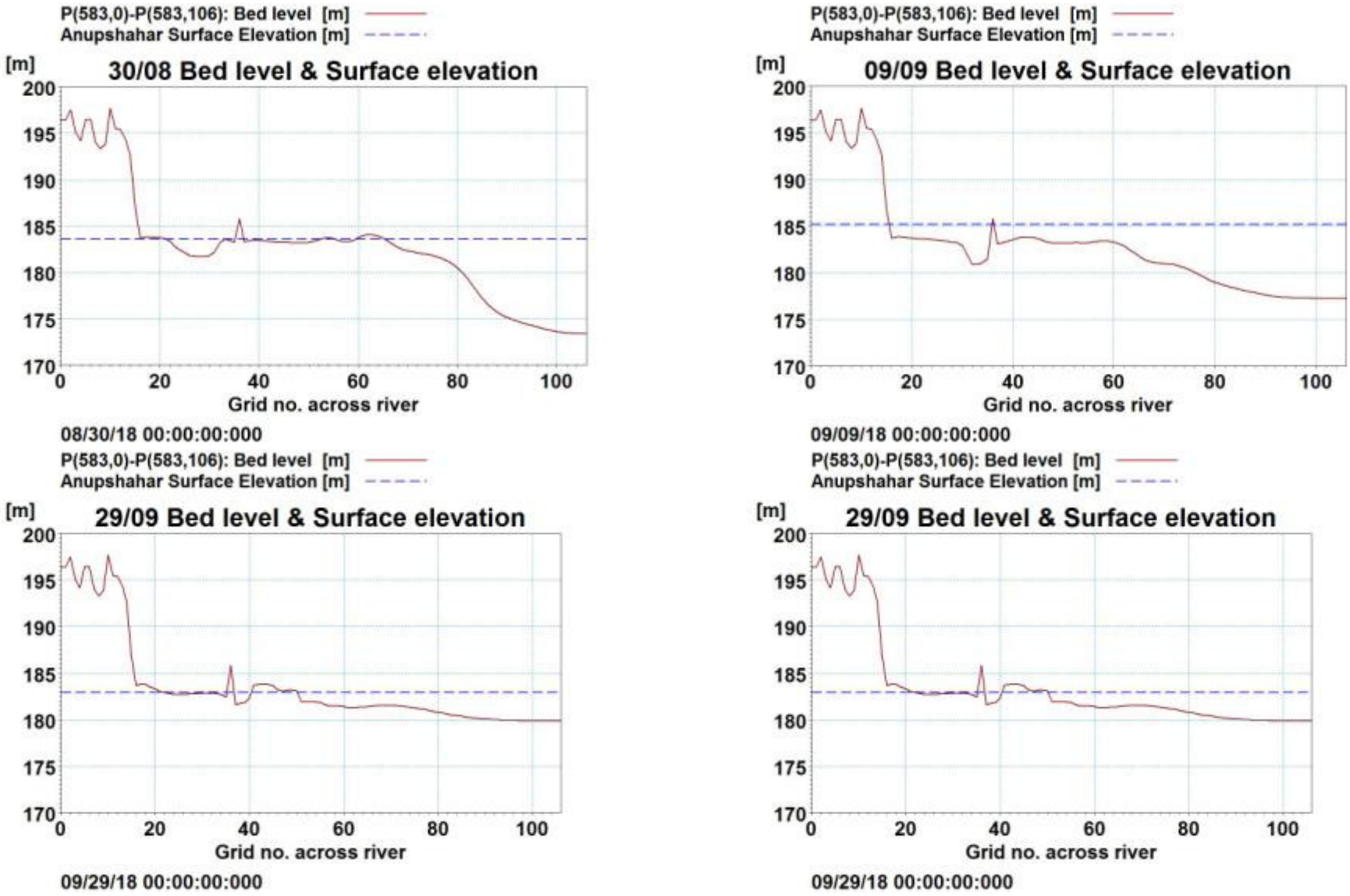

Figure 5.25: Temporal variation at 10 days interval of river section near Anupshahar (j=583) for 25-year flood.

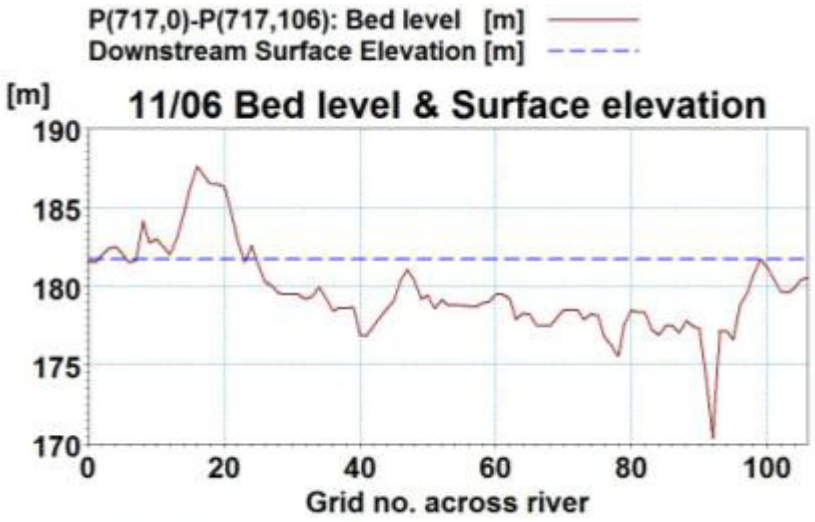
P(717,0)-P(717,106): Bed level [m]
Downstream Surface Elevation [m]
[m]
11/06 Bed level & Surface elevation
190
185
180
175
170
0
20
40
60
80
100
Grid no. across river
06/11/18 00:00:00:000

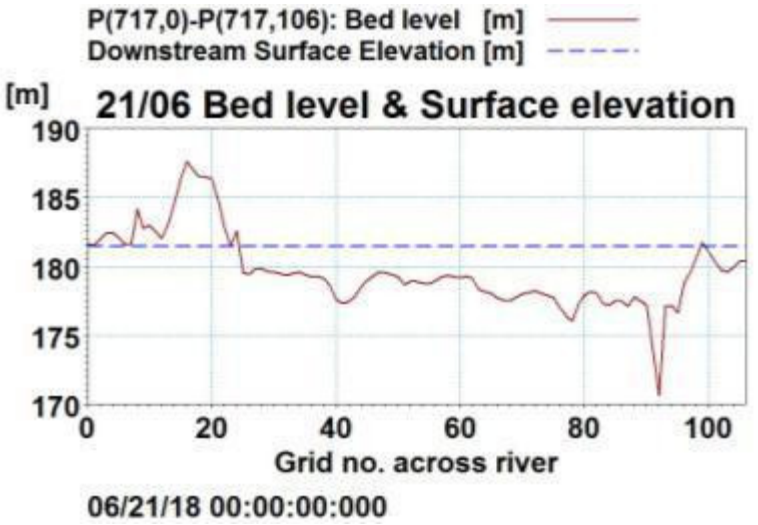
P(717,0)-P(717,106): Bed level [m]
Downstream Surface Elevation [m]
[m]
21/06 Bed level & Surface elevation
190
185
180
175
170
0
20
40
60
80
100
Grid no. across river
06/21/18 00:00:00:000

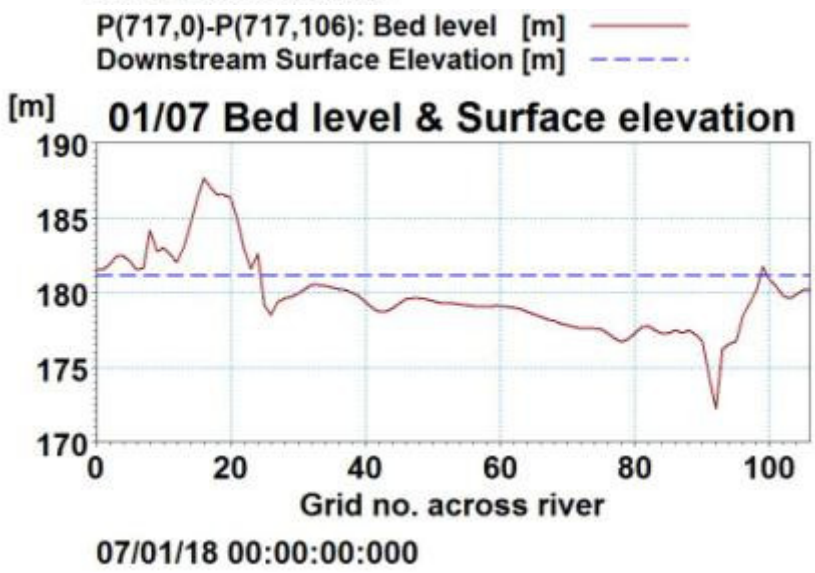
P(717,0)-P(717,106): Bed level [m]
Downstream Surface Elevation [m]
[m]
01/07 Bed level & Surface elevation
190
185
180
175
170
0
20
40
60
80
100
Grid no. across river
07/01/18 00:00:00:000

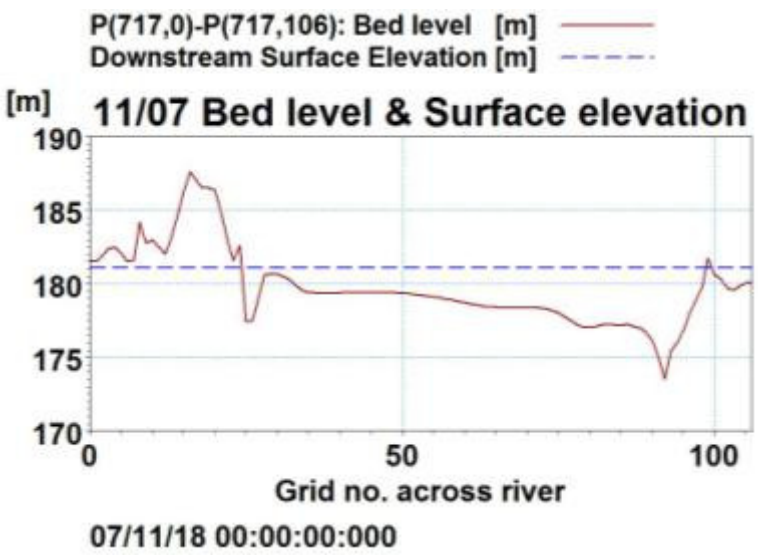
P(717,0)-P(717,106): Bed level [m]
Downstream Surface Elevation [m]
[m]
11/07 Bed level & Surface elevation
190
185
180
175
170
0
50
100
Grid no. across river
07/11/18 00:00:00:000

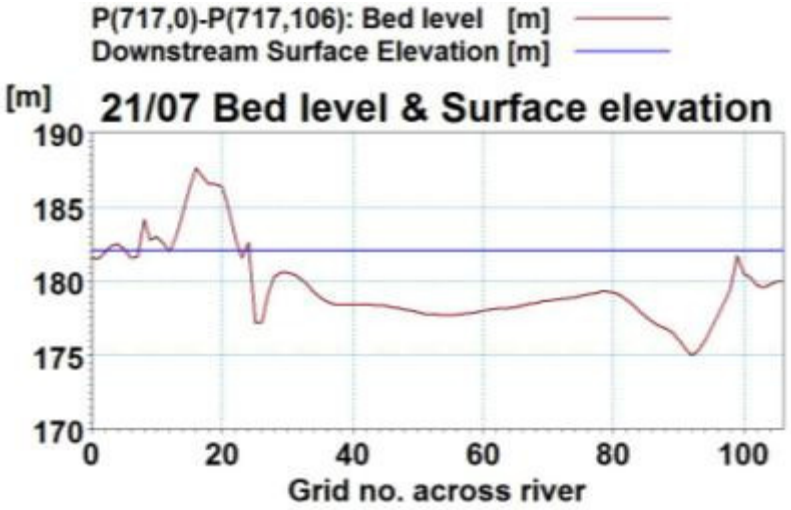
P(717,0)-P(717,106): Bed level [m]
Downstream Surface Elevation [m]
[m]
21/07 Bed level & Surface elevation
190
185
180
175
170
0
20
40
60
80
100
Grid no. across river
07/21/18 00:00:00:000

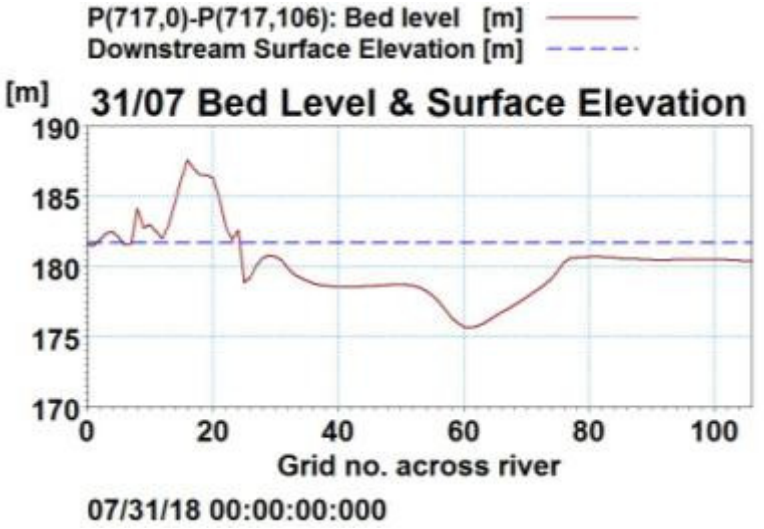
P(717,0)-P(717,106): Bed level [m]
Downstream Surface Elevation [m]
[m]
31/07 Bed Level & Surface Elevation
190
185
180
175
170
0
20
40
60
80
100
Grid no. across river
07/31/18 00:00:00:000

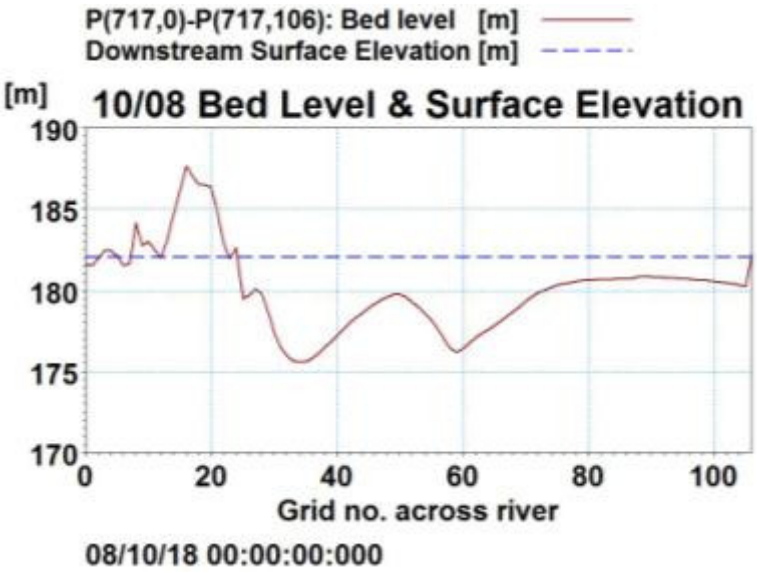
P(717,0)-P(717,106): Bed level [m]
Downstream Surface Elevation [m]
[m]
10/08 Bed Level & Surface Elevation
190
185
180
175
170
0
20
40
60
80
100
Grid no. across river
08/10/18 00:00:00:000

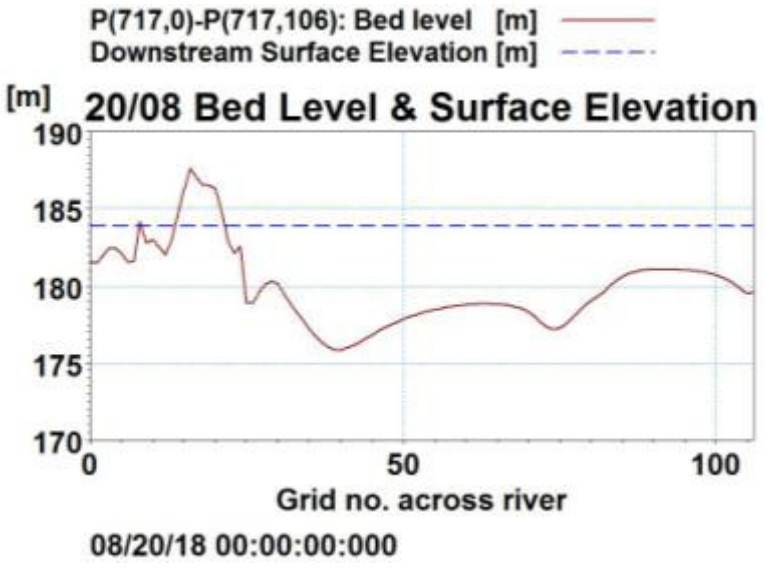
P(717,0)-P(717,106): Bed level [m]
Downstream Surface Elevation [m]
[m]
20/08 Bed Level & Surface Elevation
190
185
180
175
170
0
50
100
Grid no. across river
08/20/18 00:00:00:000

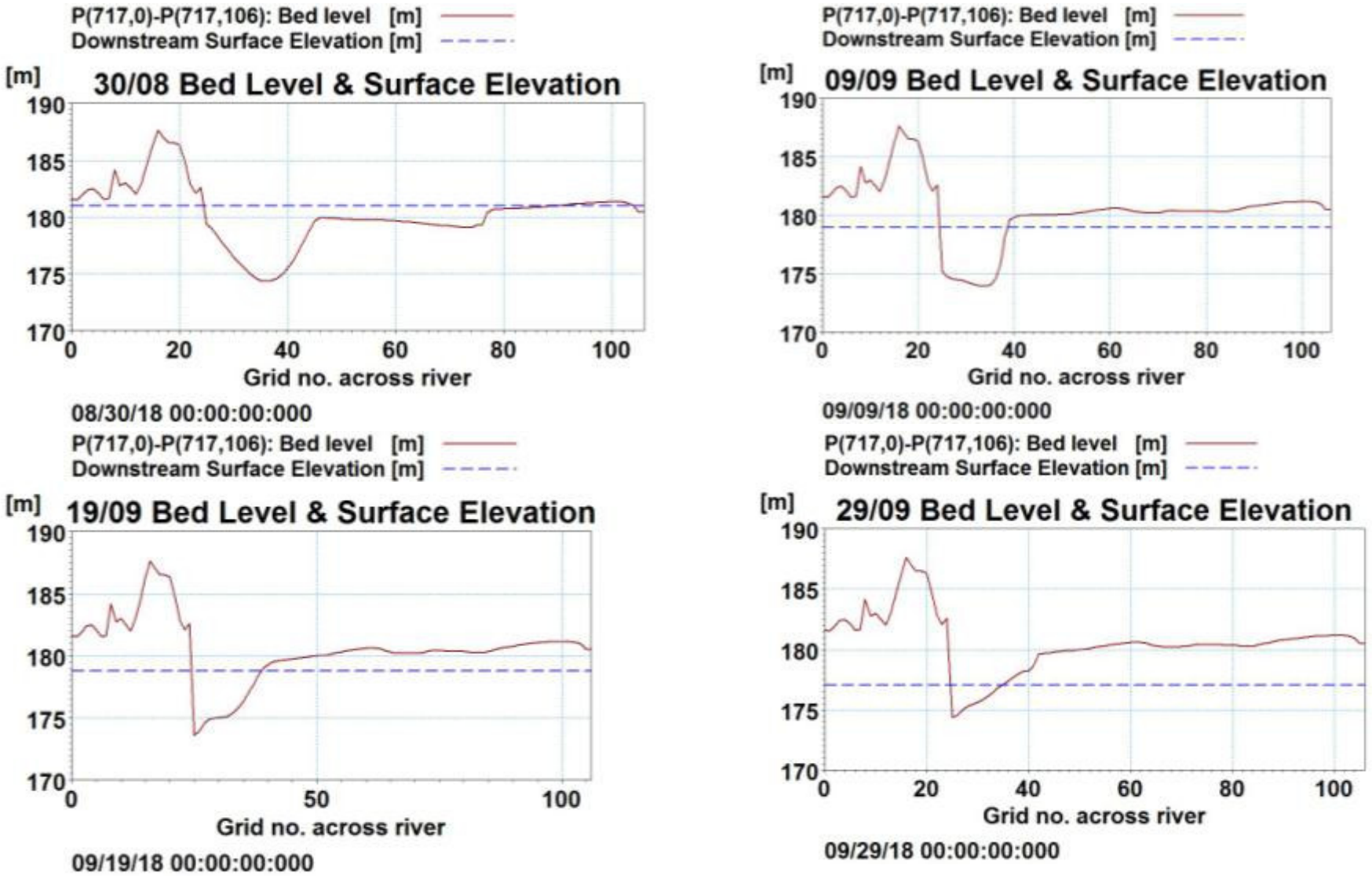

Figure 5.26: Temporal variation at 10 days interval of river section at downstream location (j=717) for 25-year flood.

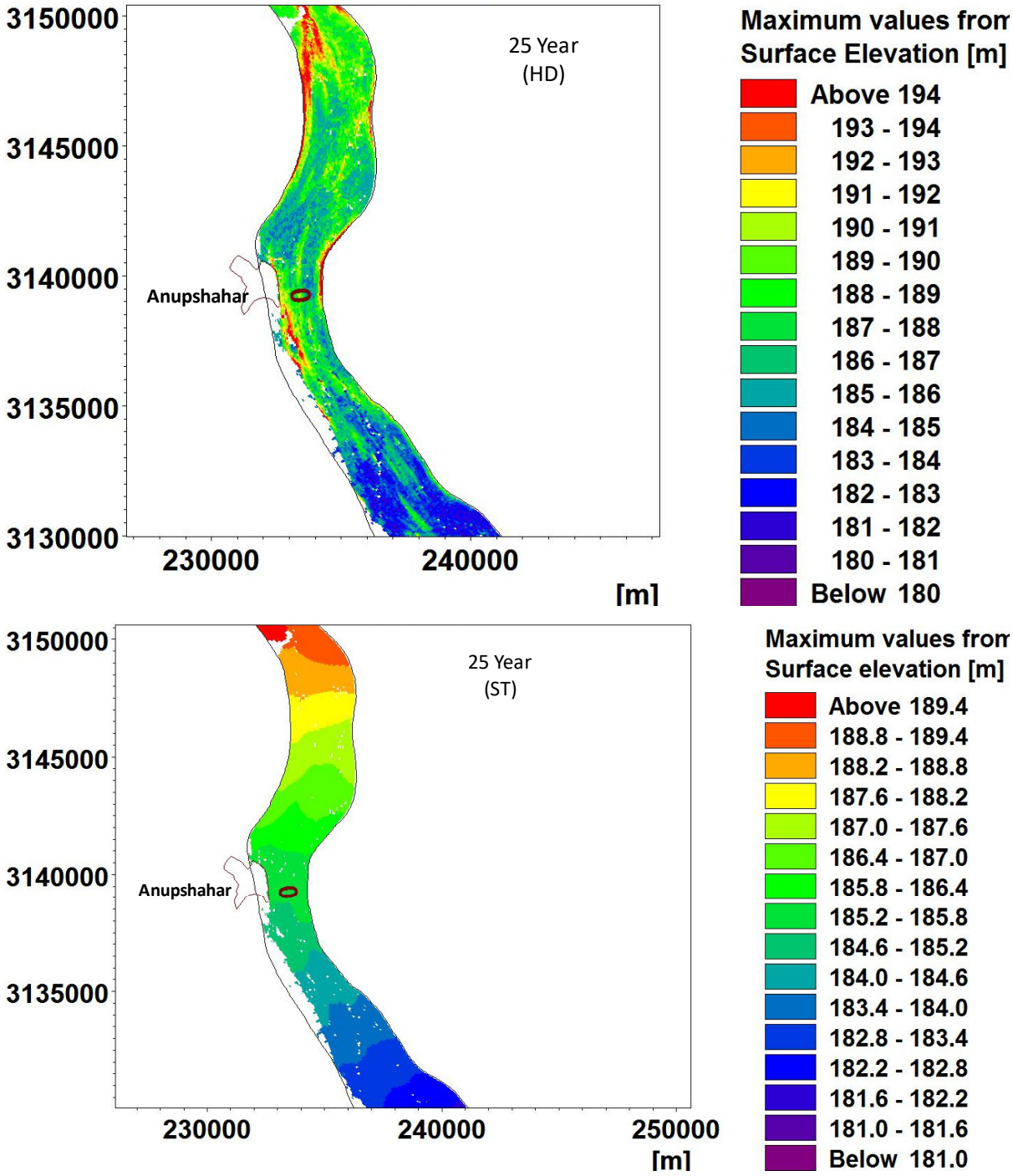

Figure 5.27: Maximum flood level map with and without sediment concentration for 25-year flood.

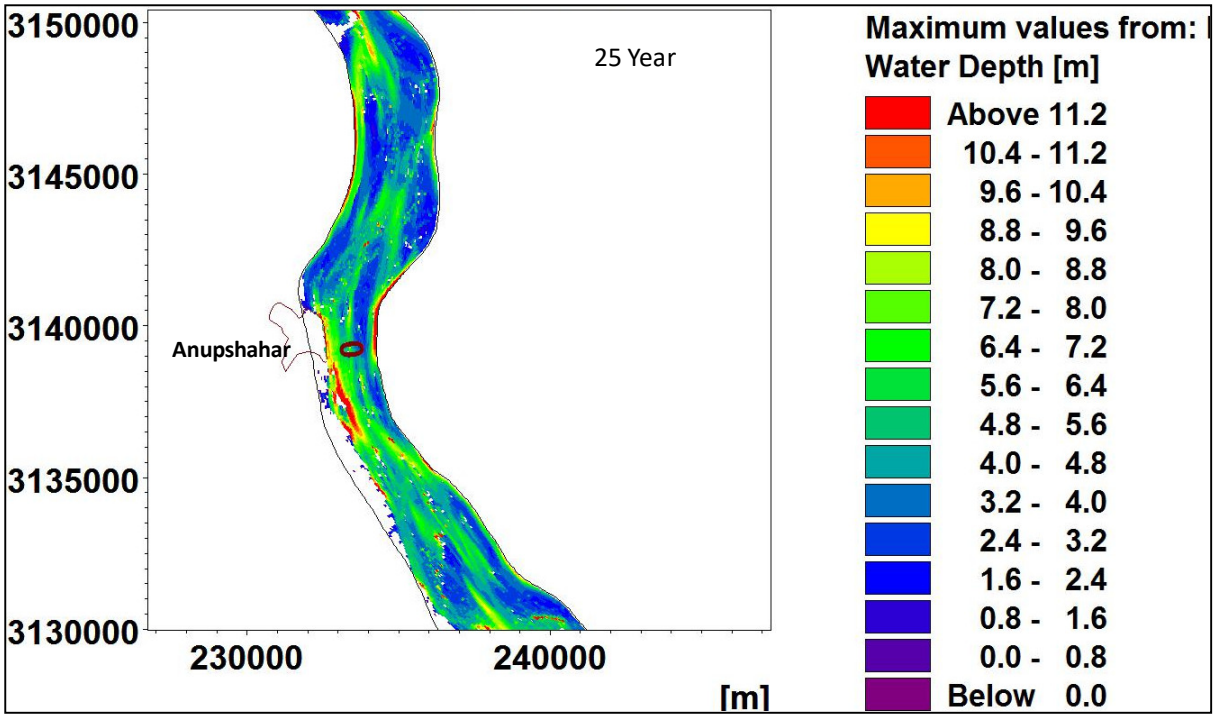

Figure 5.28: Map of maximum flooding depth for 25 year flood.

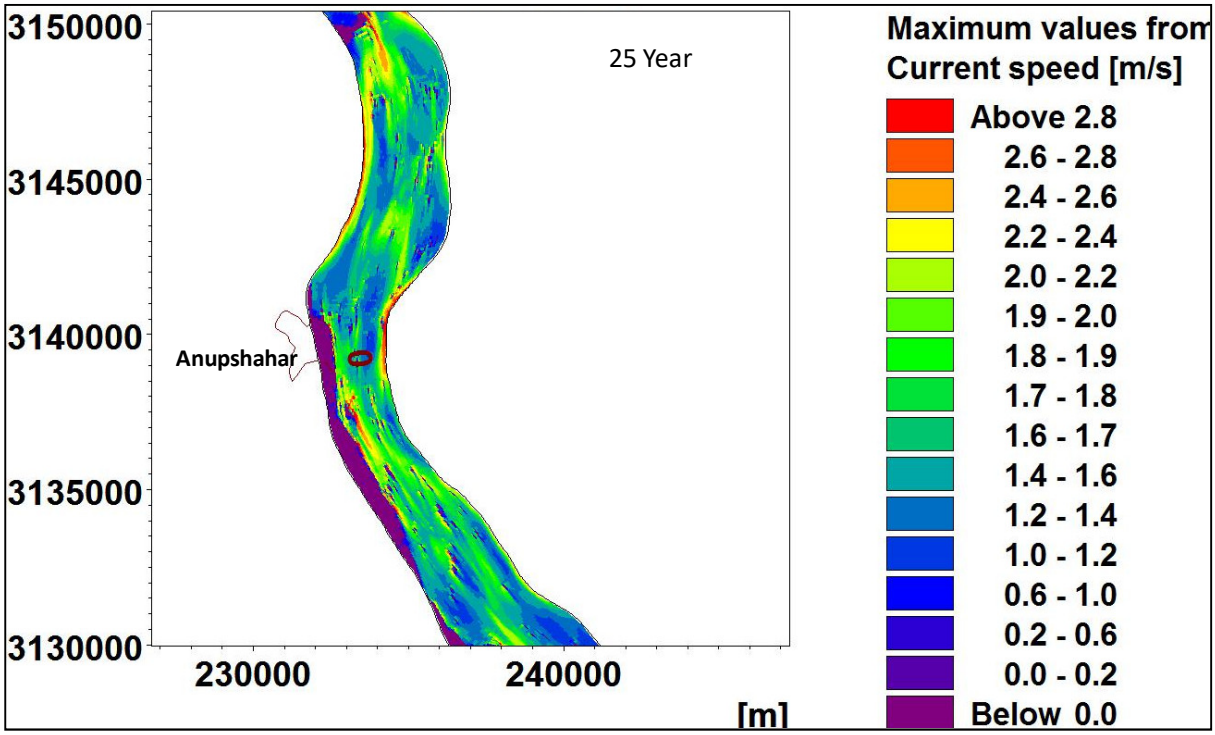

Figure 5.29: Map of maximum flow velocity for 25 year flood.

The ST model is further used to develop maps of maximum helical flow, sediment concentration and Sheer stress map. These flow attributes are needed when designing some anti-erosion work at the affected site. The maps of maximum helical flow, sediment

concentration and Sheer stress are shown in Figure 5.30, Figure 5.31 and Figure 5.32, respectively.

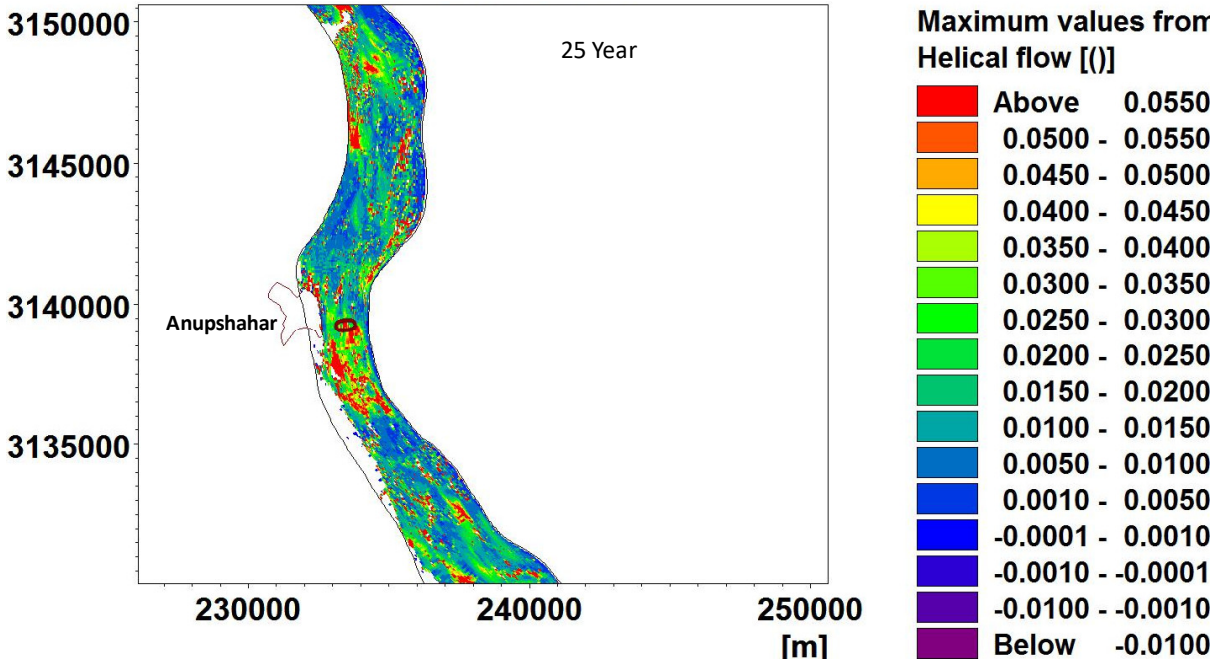

Figure 5.30: Map of the maximum helical flow for 25 year flood.

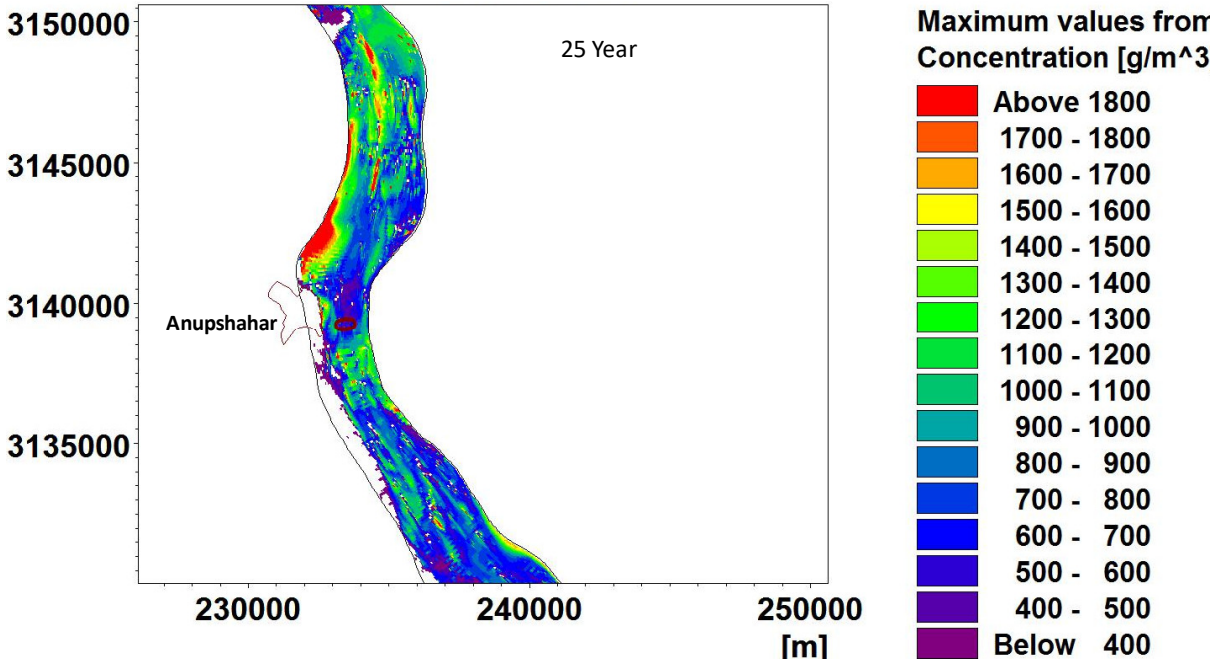

Figure 5.31: Map of maximum sediment concentration for 25 year flood.

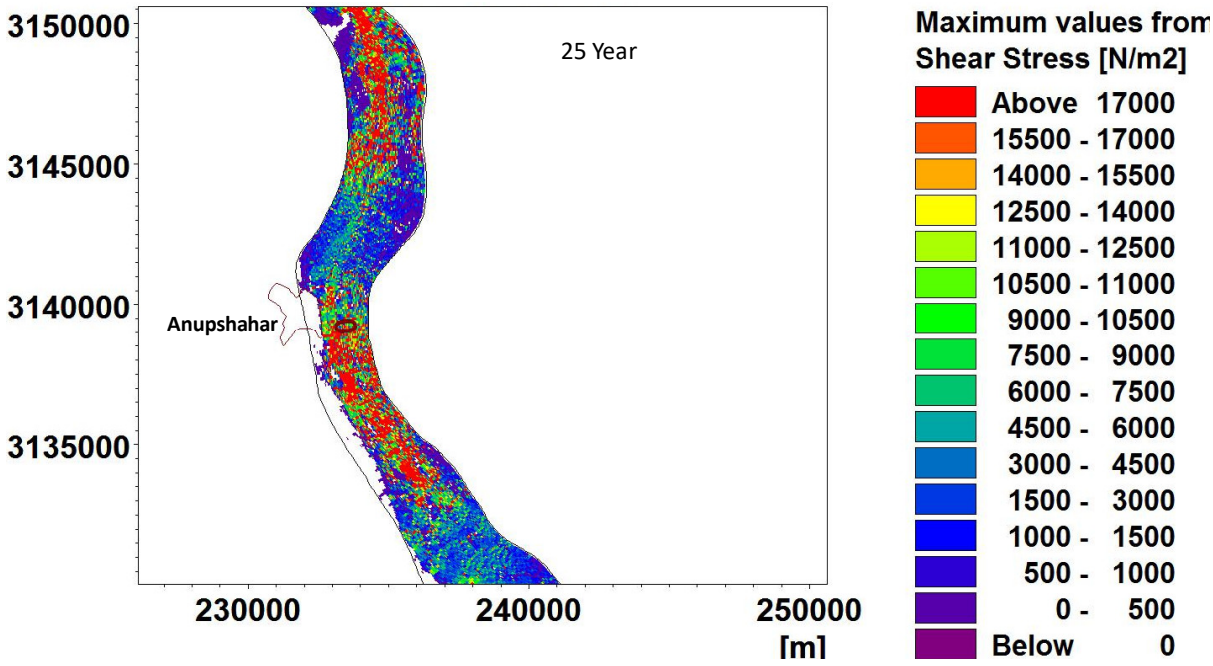

Figure 5.32: map of the maximum sheer stress for 25 year flood.

The flow direction can also be estimated from the modelling result. Such maps are useful in deciding the alignment of anti-erosion works for the affected site. The map of flow direction near Anupshahar, at the instant of maximum current is for 25-year flood is shown in Figure 5.33.

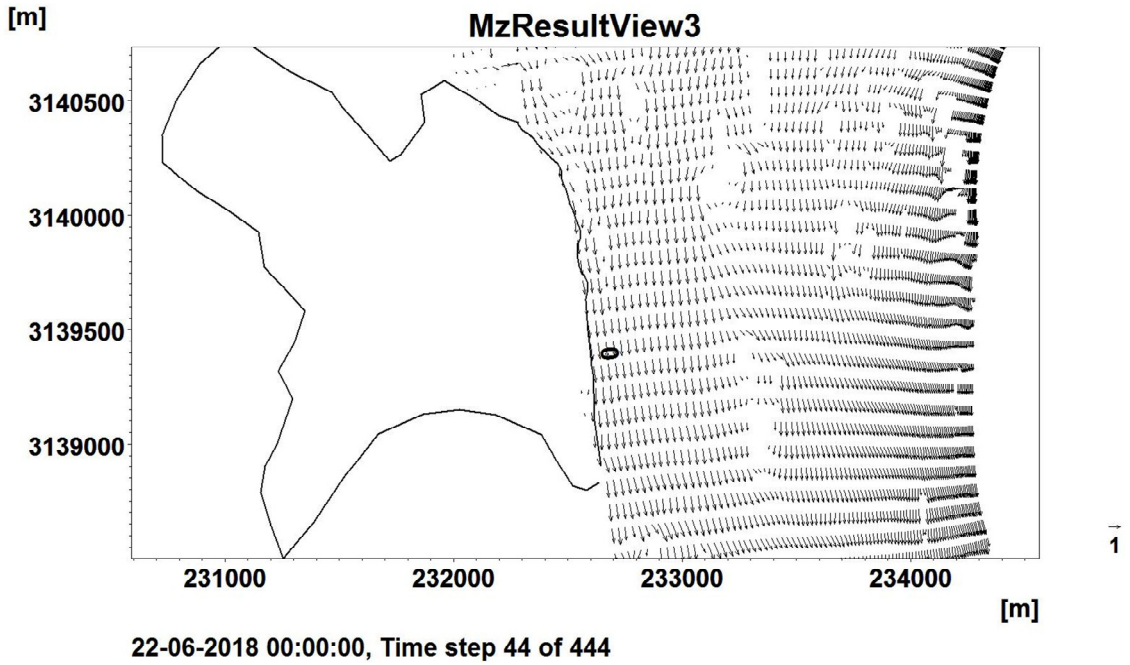

Figure 5.33: Direction of flow during maximum current near Anupshahar for 25-year flood.

Short term model prediction has been carried out for 25 year flood (during 21 june to 29 September). The monsoon (15th June to 15th October) of 2017 has been repeated three times to use as upstream inflow condition to the 2-D model. The morphological developments have been evaluated at specific time on the temporal scale over the period. During the simulation, the bed level changes at every grid is captures at an average interval of 10 days for duration of three months. The blue shade shows the erosion while the green shade shows the deposition. The movement of river bed erosion during 25 year flood shows that erosion occurs near Anupshahar site, however, it moves gradually in the downstream direction over a period of time.

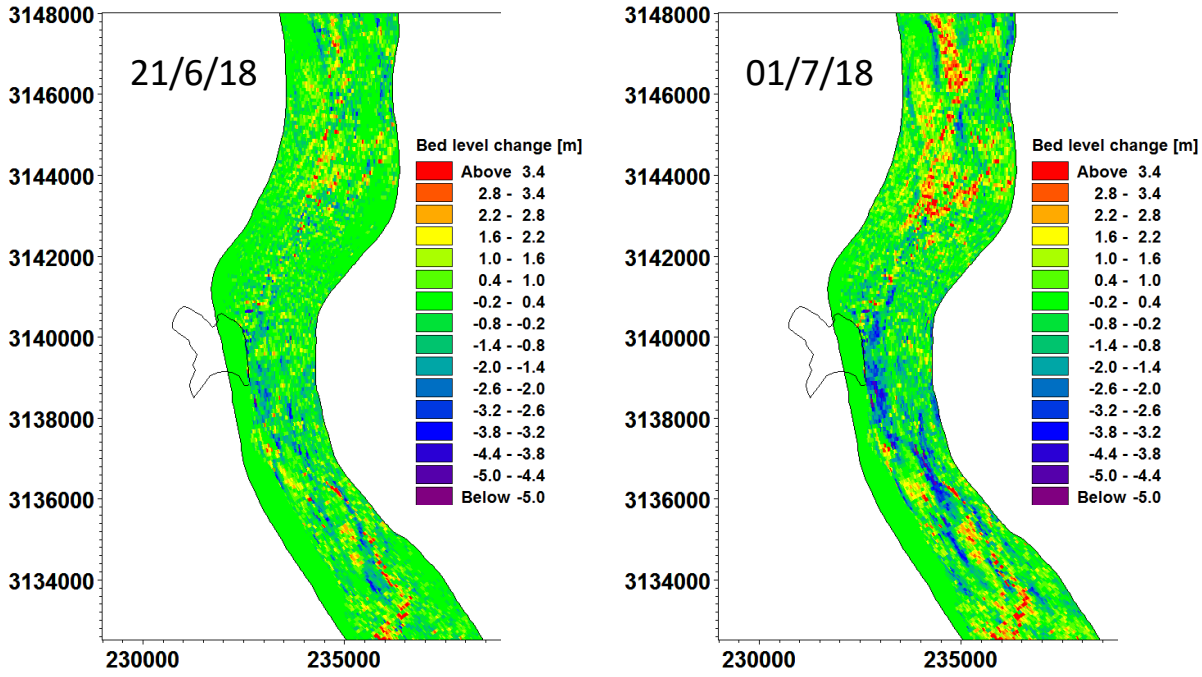

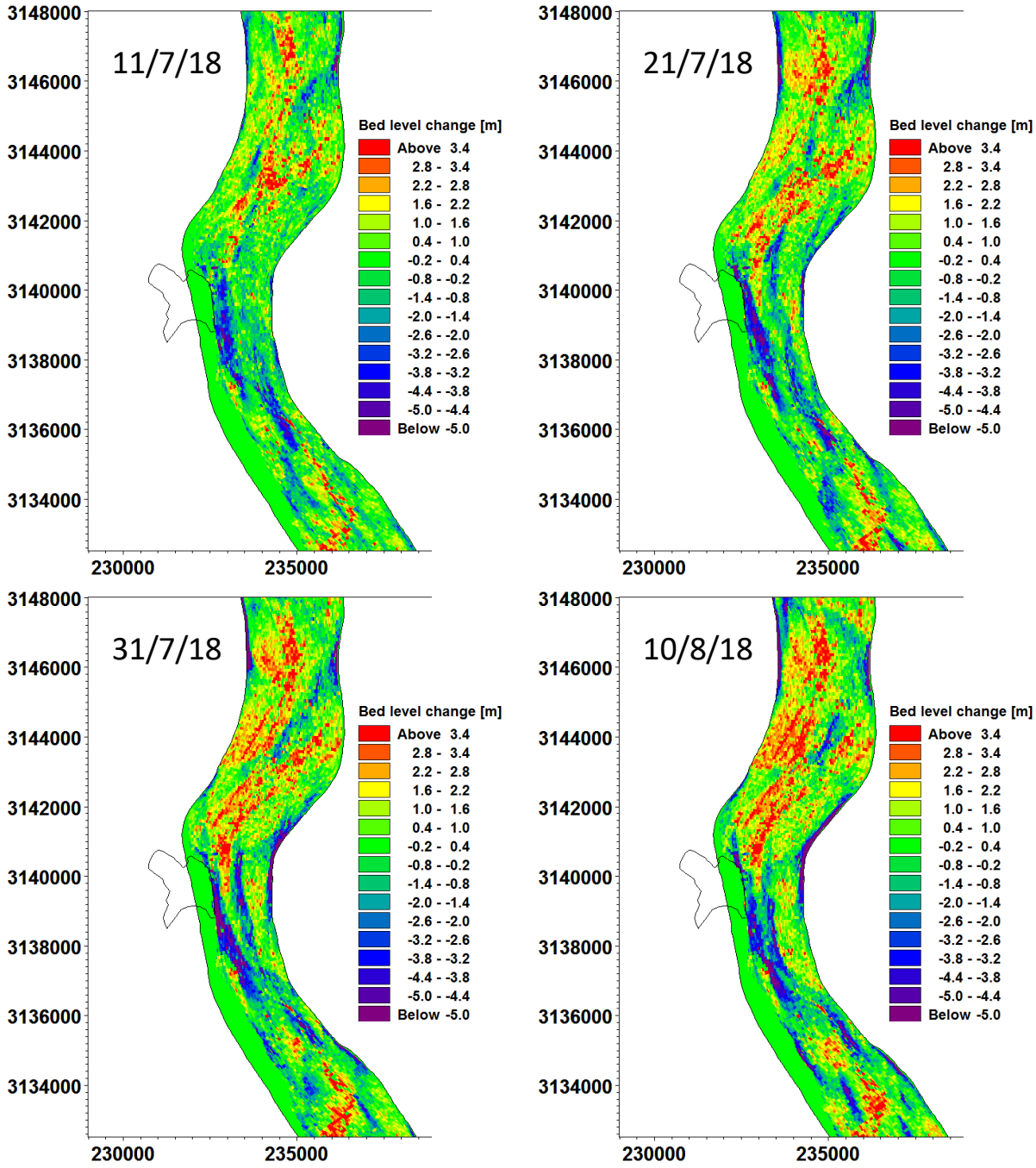
11/7/18
21/7/18
31/7/18
10/8/18
Bed level change [m]
Above 3.4
2.8 - 3.4
2.2 - 2.8
1.6 - 2.2
1.0 - 1.6
0.4 - 1.0
-0.2 - 0.4
-0.8 - -0.2
-1.4 - -0.8
-2.0 - -1.4
-2.6 - -2.0
-3.2 - -2.6
-3.8 - -3.2
-4.4 - -3.8
-5.0 - -4.4
Below -5.0
3148000
3146000
3144000
3142000
3140000
3138000
3136000
3134000
230000
235000

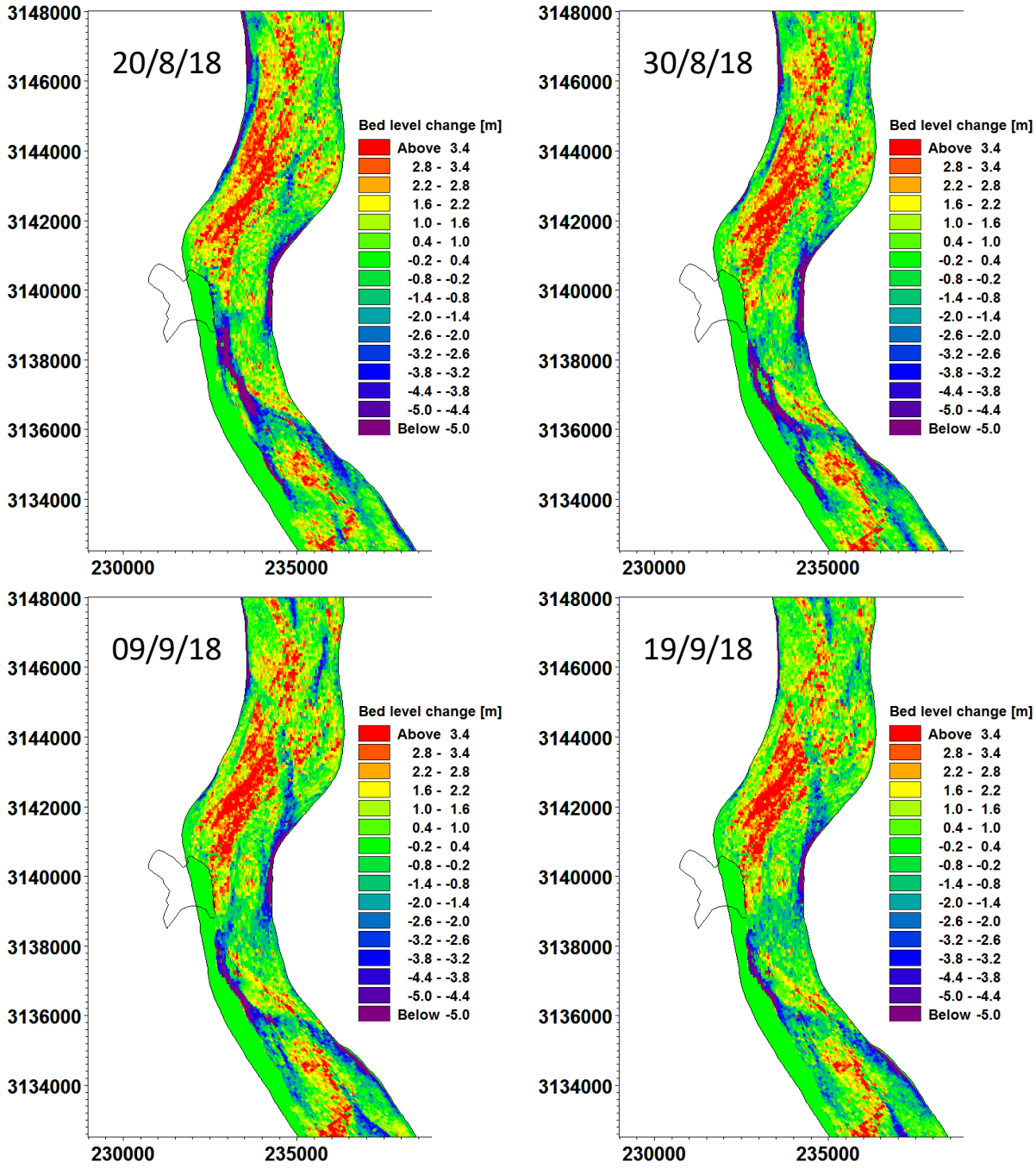

Figure 5.34: Short term morphological prediction for 25-year flood

5.3.6 Morpho-dynamic modelling for 100 year flood hydrograph

The MIKE 21C model is again simulated for 100 year return period flood and similar analysis was made. computes various flow attributes like water level, flow depth, velocity, sediment concentration, total sediment load, Net sediment/ erosion in spatial domain study reach. The flow characteristics are evaluated for two design flood condition as mentioned

In morphodynamic model, dynamic river bed is considered. With the progress of flow either erosion or deposition makes the changes in the bed level. To illustrate the changing bed level,

three locations have been identified, one upstream of Anupshahar (grid j=440), second at Anupshahar (grid j=583) and third downstream of Anupshahar (grid j=717). The river cross section profiles at these locations are plotted for an average interval of 10 days during the simulation. The river bed level profile for an upstream location (grid j=440) is shown in Figure 5.24. The figure shows the temporal changes of river bed level and flood level at this location. The movement of flow from right bank (grid k=0) towards left bank (grid k=107) can be visualised by comparing the temporal river section.

Similar movement of river flow from right bank towards left bank can be visualised for Anupshahar (grid j=583) and the downstream location (grid j=770) in Figure 5.35, Figure 5.36 AND Figure 5.37, respectively.

The MIKE 21C flow model is simulated for two condition, initially without considering the sediment flow and later on considering the sediment flow with mobile river bed. For both the cases, the maximum flood level maps for the area around Anupshahar are plotted as shown in Figure 5.27. The figure shows with hydrodynamic (HD) flow simulation the maximum flood level near Anupshahar is higher (of the order of 189-191 m) compared to maximum flood level (of the order of 185 m) for flow simulation with sediment transport (ST) and mobile bed consideration. With sediment transport model, the scouring of the river bed at every grid and time steps are included in the simulation and therefore lower value of the maximum flood level is estimated.

The maps of maximum flooding depth and maximum current (flow velocity) are also computed from HD simulation and are shown in Figure 5.38 and Figure 5.39, respectively.

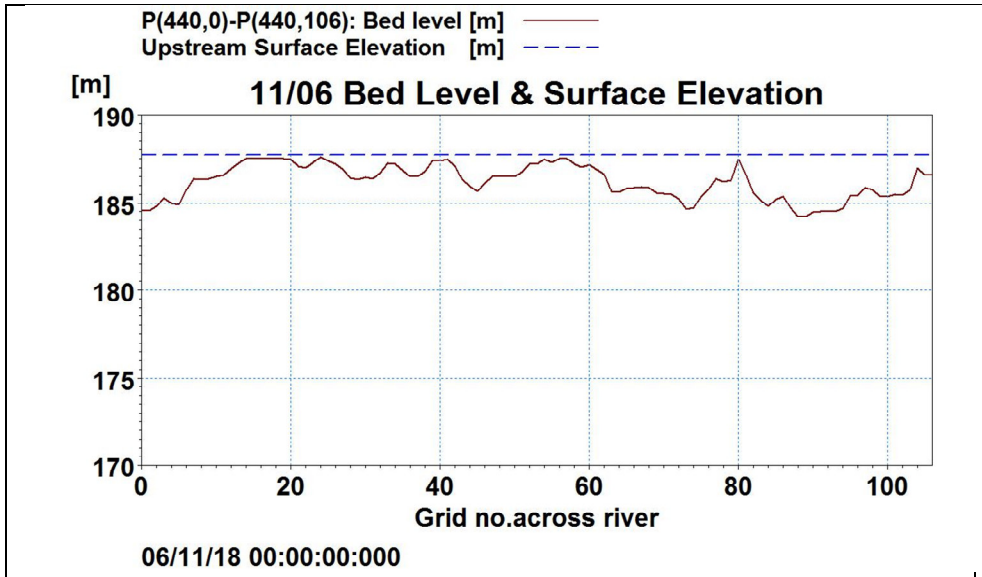
P(440,0)-P(440,106): Bed level [m]
Upstream Surface Elevation [m]
[m]
11/06 Bed Level & Surface Elevation
190
185
180
175
170
0
20
40
60
80
100
Grid no.across river
06/11/18 00:00:00:000

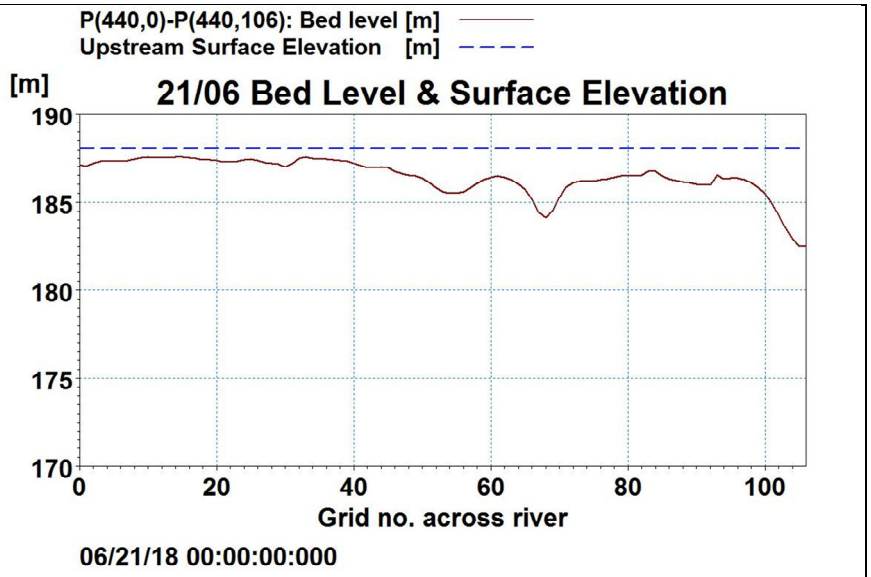
P(440,0)-P(440,106): Bed level [m]
Upstream Surface Elevation [m]
[m]
21/06 Bed Level & Surface Elevation
190
185
180
175
170
0
20
40
60
80
100
Grid no. across river
06/21/18 00:00:00:000

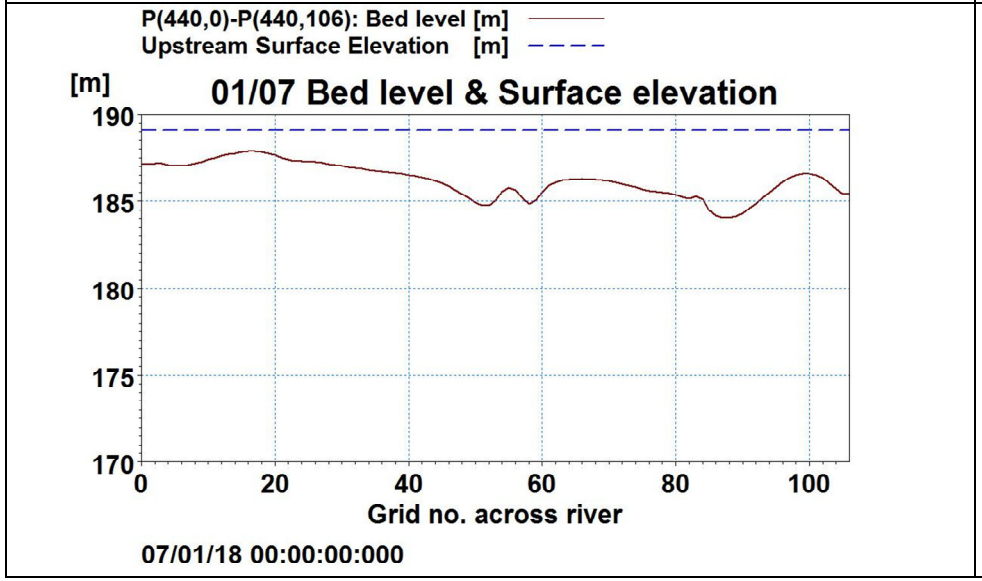
P(440,0)-P(440,106): Bed level [m]
Upstream Surface Elevation [m]
[m]
01/07 Bed level & Surface elevation
190
185
180
175
170
0
20
40
60
80
100
Grid no. across river
07/01/18 00:00:00:000

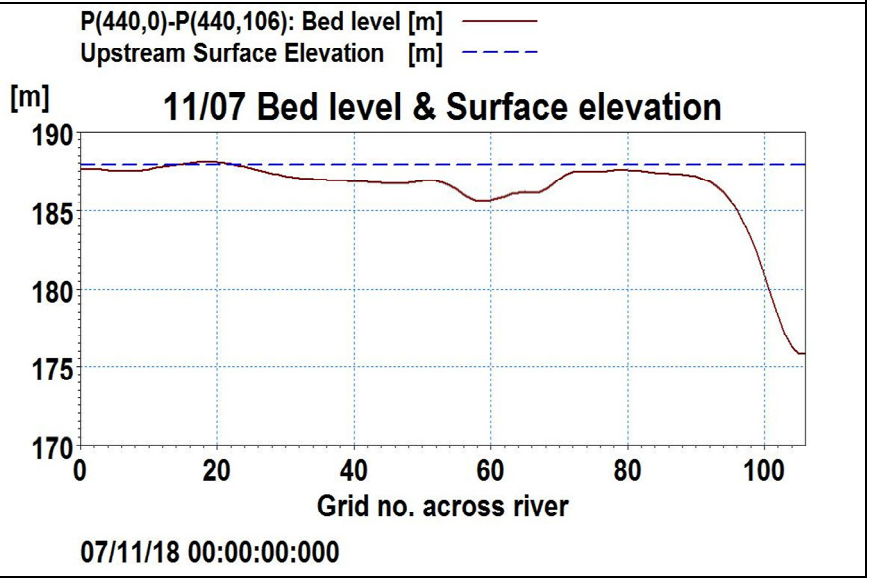
P(440,0)-P(440,106): Bed level [m]
Upstream Surface Elevation [m]
[m]
11/07 Bed level & Surface elevation
190
185
180
175
170
0
20
40
60
80
100
Grid no. across river
07/11/18 00:00:00:000

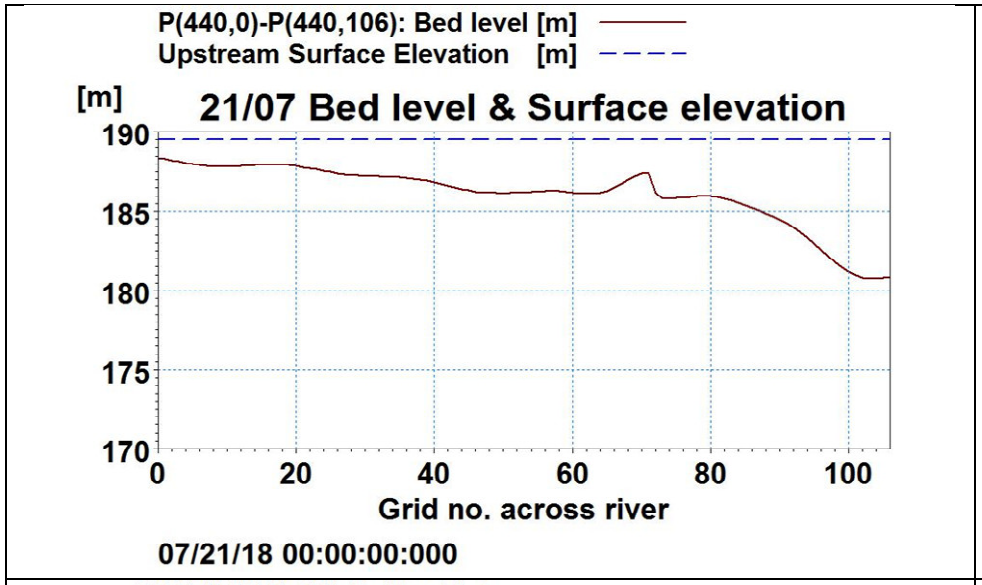
P(440,0)-P(440,106): Bed level [m]
Upstream Surface Elevation [m]
[m]
21/07 Bed level & Surface elevation
190
185
180
175
170
0
20
40
60
80
100
Grid no. across river
07/21/18 00:00:00:000

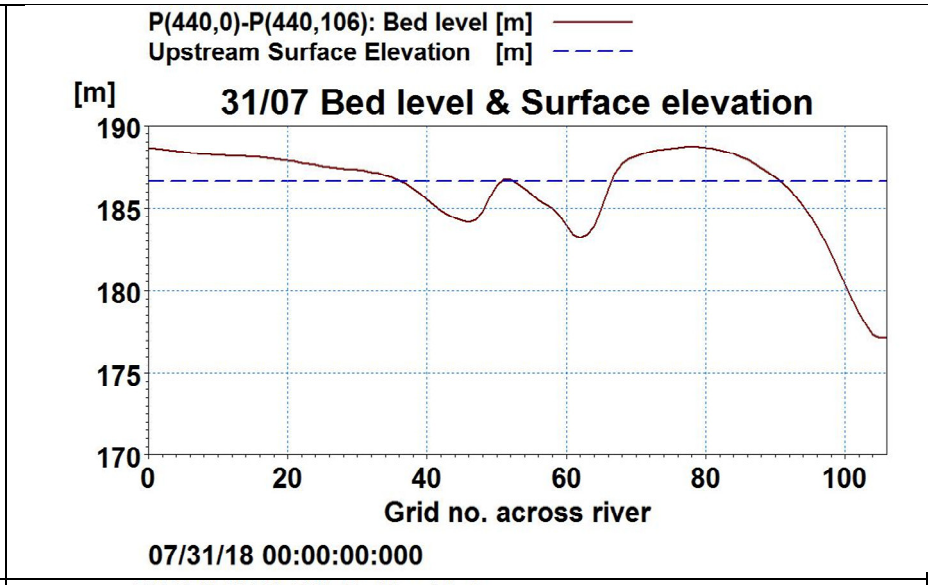
P(440,0)-P(440,106): Bed level [m]
Upstream Surface Elevation [m]
[m]
31/07 Bed level & Surface elevation
190
185
180
175
170
0
20
40
60
80
100
Grid no. across river
07/31/18 00:00:00:000

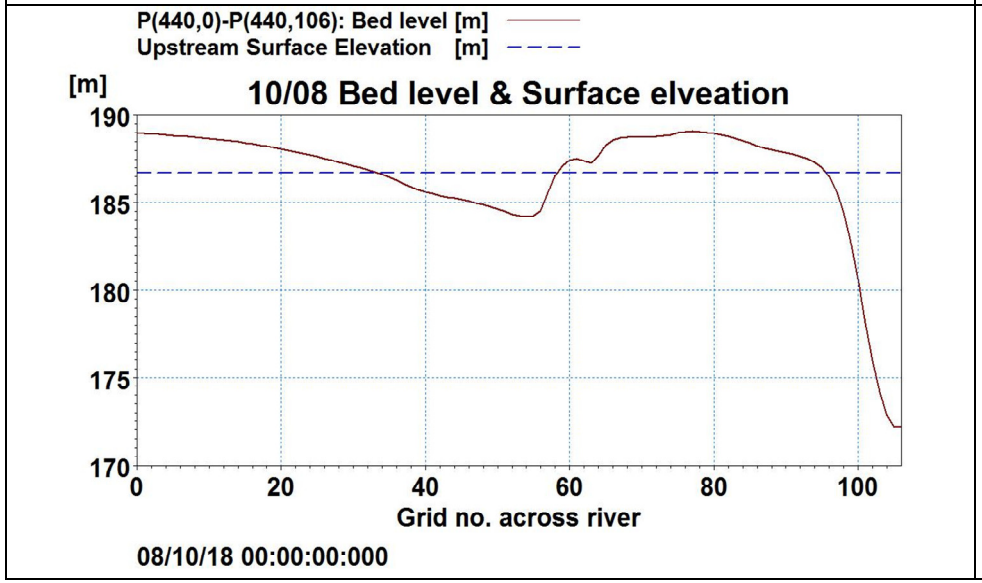
P(440,0)-P(440,106): Bed level [m]
Upstream Surface Elevation [m]
[m]
10/08 Bed level & Surface elveation
190
185
180
175
170
0
20
40
60
80
100
Grid no. across river
08/10/18 00:00:00:000

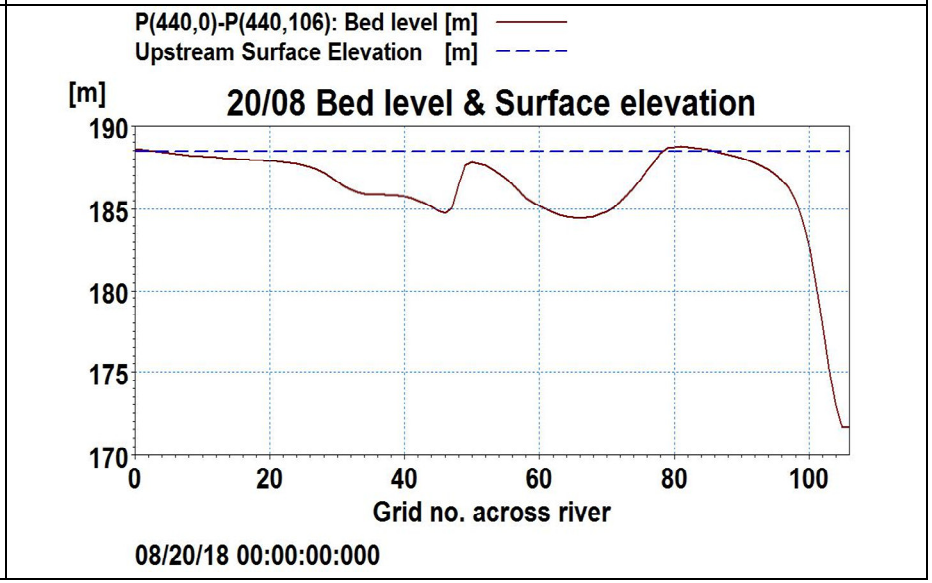
P(440,0)-P(440,106): Bed level [m]
Upstream Surface Elevation [m]
[m]
20/08 Bed level & Surface elevation
190
185
180
175
170
0
20
40
60
80
100
Grid no. across river
08/20/18 00:00:00:000

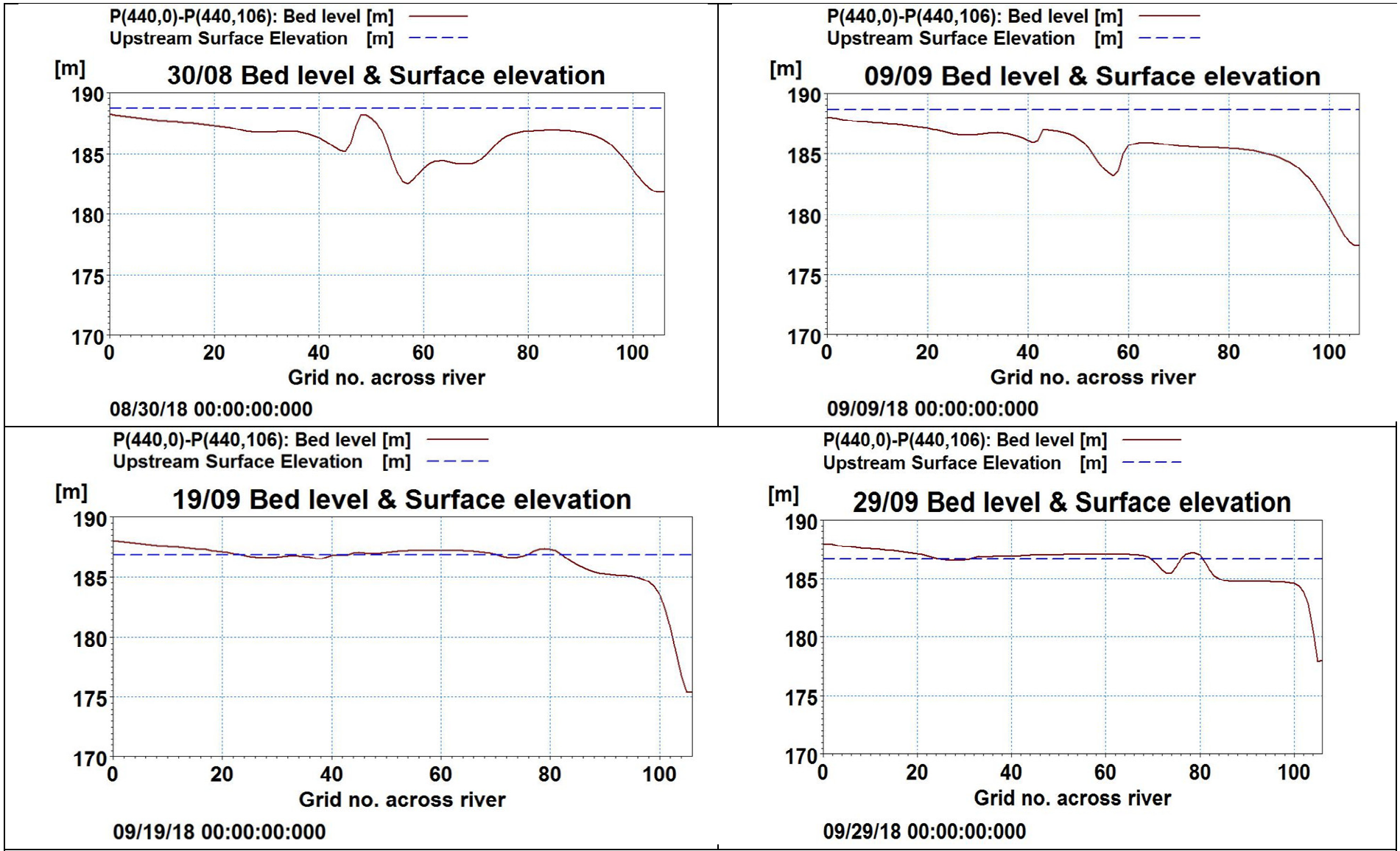

Figure 5.35: Temporal variation of river section at upstream location (j=440) for 100-year flood.

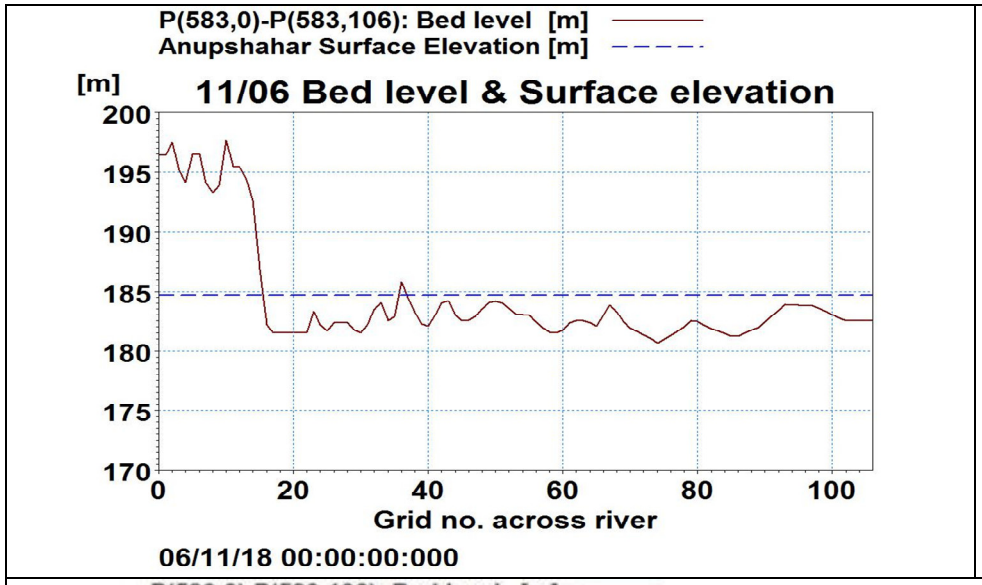
P(583,0)-P(583,106): Bed level [m]
Anupshahar Surface Elevation [m]
[m]
11/06 Bed level & Surface elevation
200
195
190
185
180
175
170
0
20
40
60
80
100
Grid no. across river
06/11/18 00:00:00:000

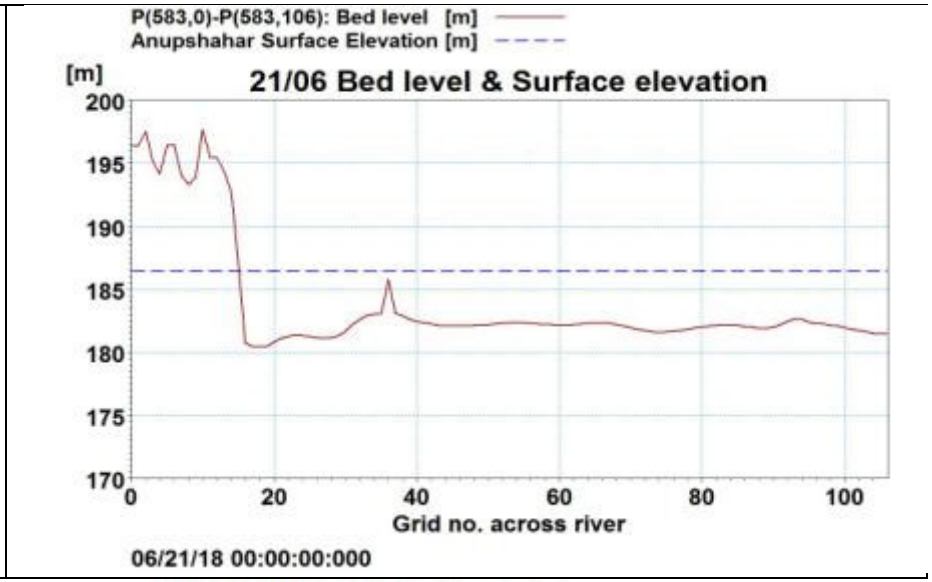
P(583,0)-P(583,106): Bed level [m]
Anupshahar Surface Elevation [m]
[m]
21/06 Bed level & Surface elevation
200
195
190
185
180
175
170
0
20
40
60
80
100
Grid no. across river
06/21/18 00:00:00:000

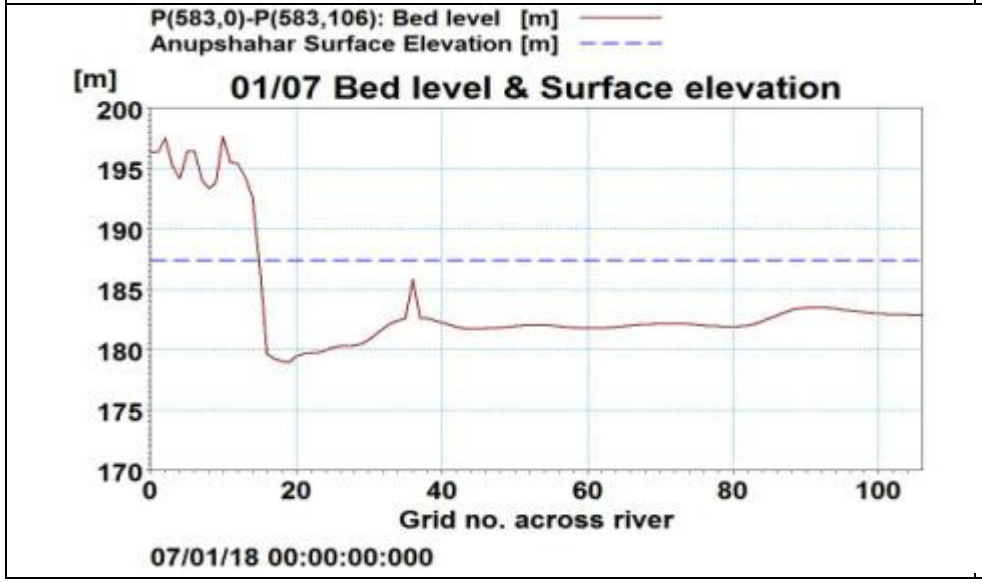
P(583,0)-P(583,106): Bed level [m]
Anupshahar Surface Elevation [m]
[m]
01/07 Bed level & Surface elevation
200
195
190
185
180
175
170
0
20
40
60
80
100
Grid no. across river
07/01/18 00:00:00:000

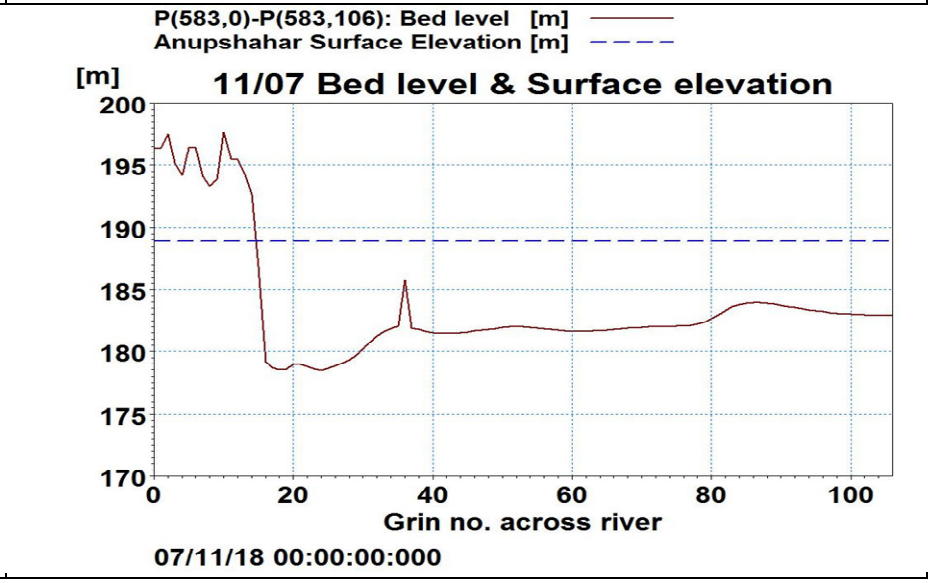
P(583,0)-P(583,106): Bed level [m]
Anupshahar Surface Elevation [m]
[m]
11/07 Bed level & Surface elevation
200
195
190
185
180
175
170
0
20
40
60
80
100
Grin no. across river
07/11/18 00:00:00:000

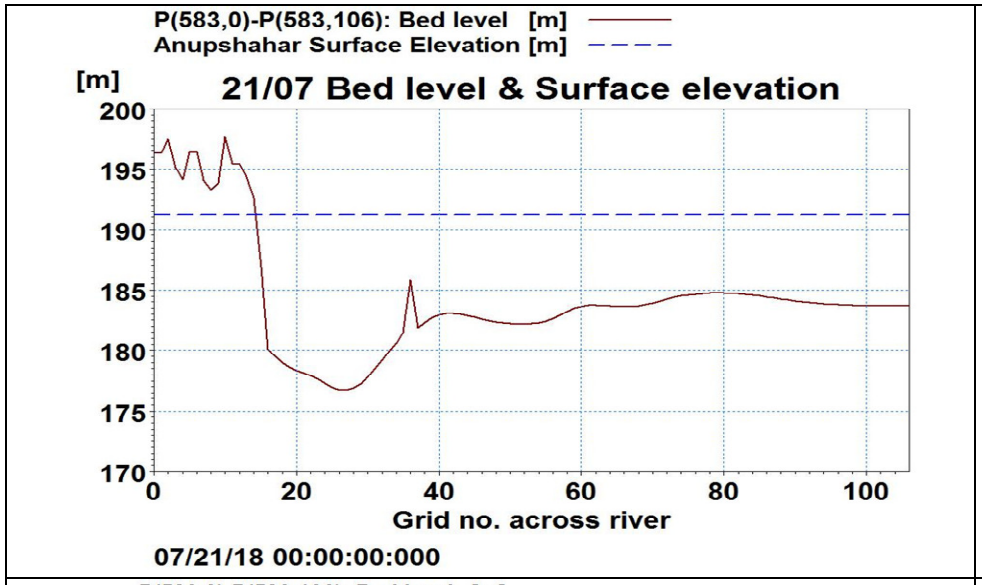
P(583,0)-P(583,106): Bed level [m]
Anupshahar Surface Elevation [m]
[m]
21/07 Bed level & Surface elevation
200
195
190
185
180
175
170
0
20
40
60
80
100
Grid no. across river
07/21/18 00:00:00:000

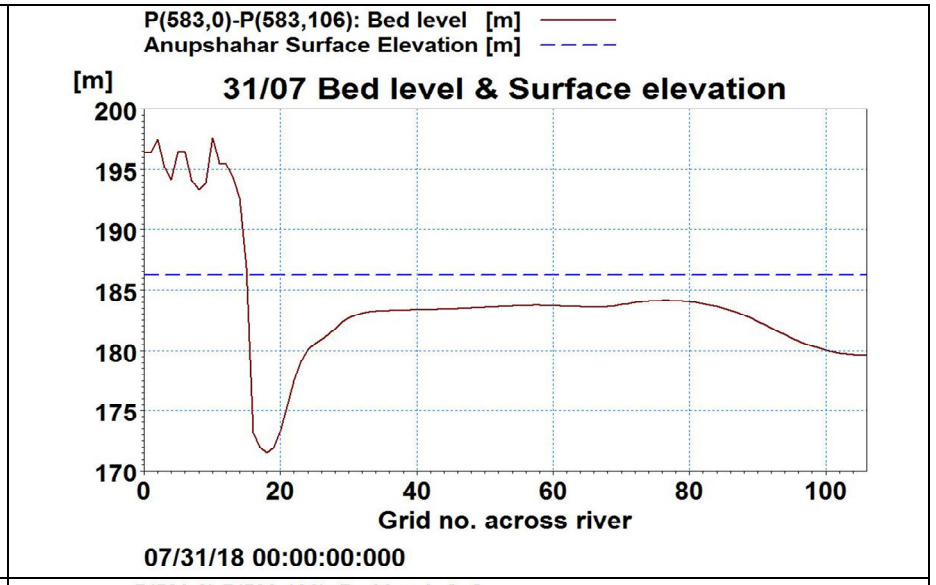
P(583,0)-P(583,106): Bed level [m]
Anupshahar Surface Elevation [m]
[m]
31/07 Bed level & Surface elevation
200
195
190
185
180
175
170
0
20
40
60
80
100
Grid no. across river
07/31/18 00:00:00:000

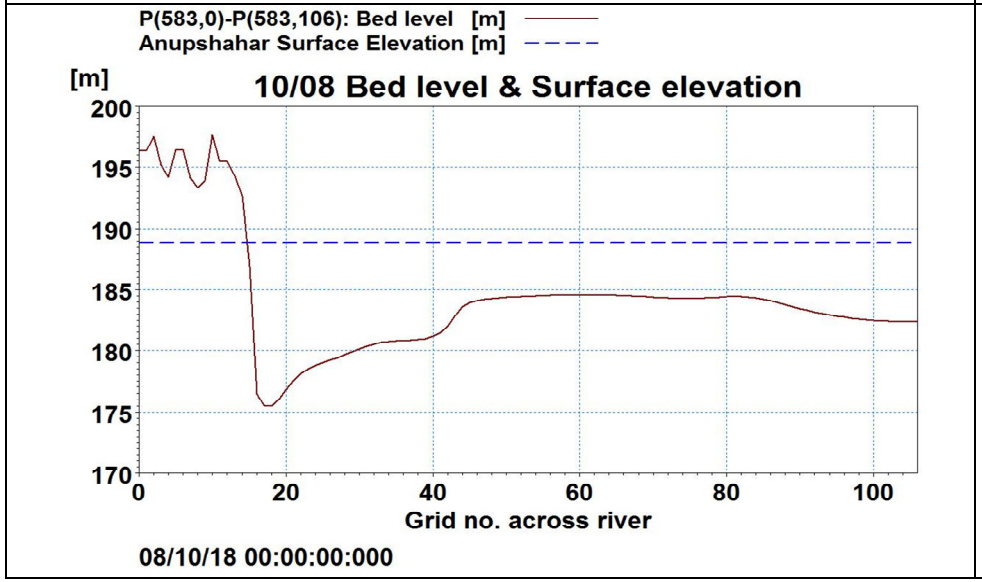
P(583,0)-P(583,106): Bed level [m]
Anupshahar Surface Elevation [m]
[m]
10/08 Bed level & Surface elevation
200
195
190
185
180
175
170
0
20
40
60
80
100
Grid no. across river
08/10/18 00:00:00:000

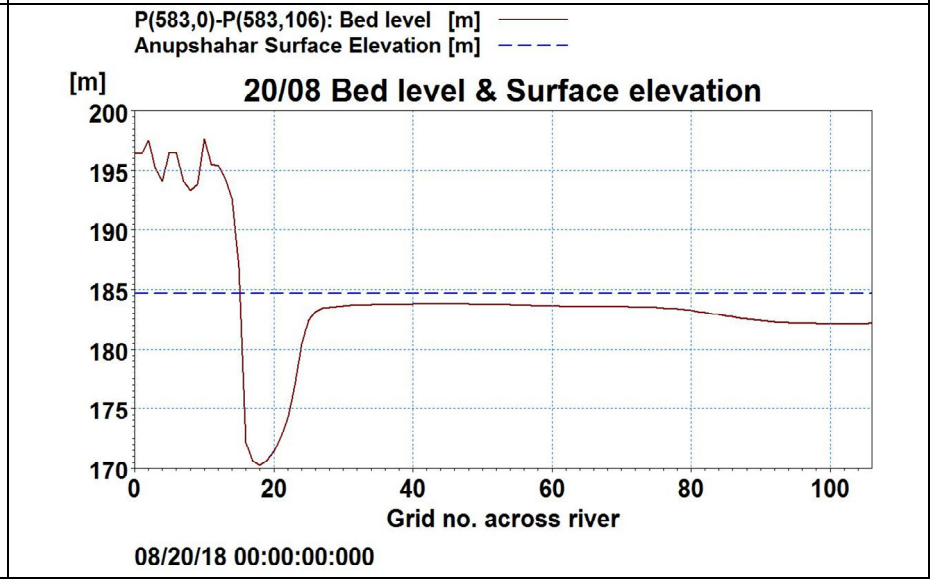
P(583,0)-P(583,106): Bed level [m]
Anupshahar Surface Elevation [m]
[m]
20/08 Bed level & Surface elevation
200
195
190
185
180
175
170
0
20
40
60
80
100
Grid no. across river
08/20/18 00:00:00:000

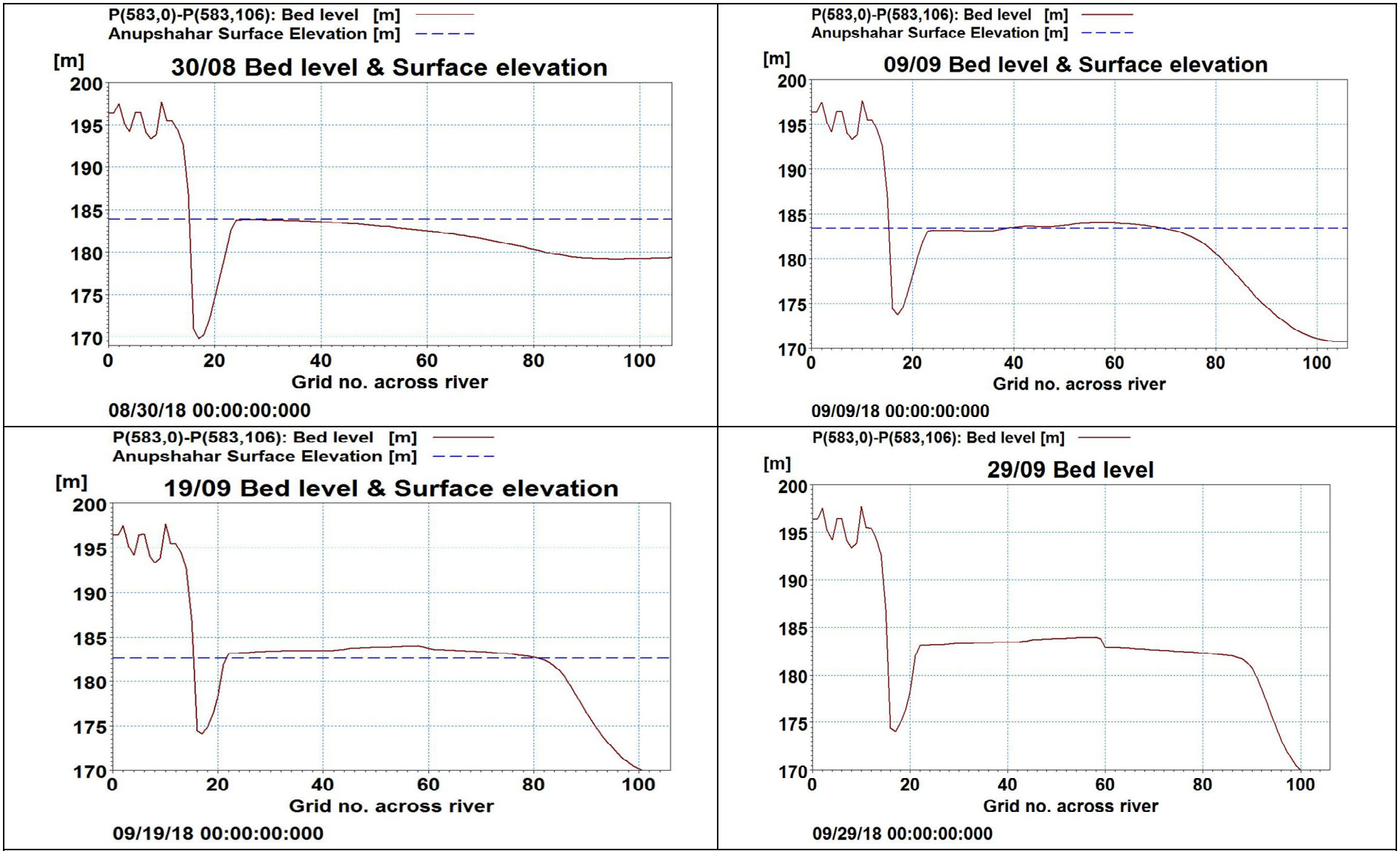

Figure 5.36: Temporal variation of river section near Anupshahar (j=583) for 100-year flood.

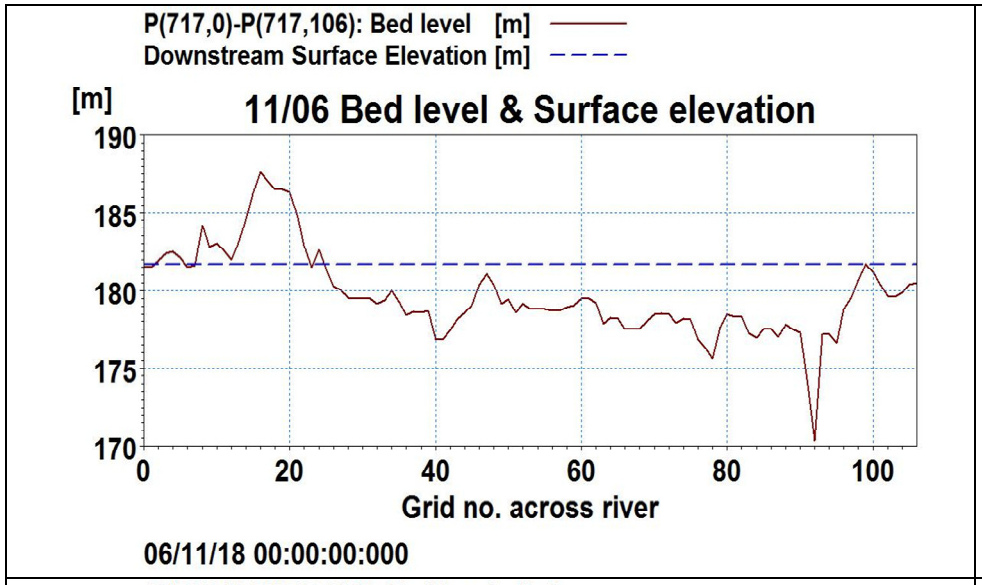
P(717,0)-P(717,106): Bed level [m]
Downstream Surface Elevation [m]
[m]
11/06 Bed level & Surface elevation
190
185
180
175
170
0
20
40
60
80
100
Grid no. across river
06/11/18 00:00:00:000

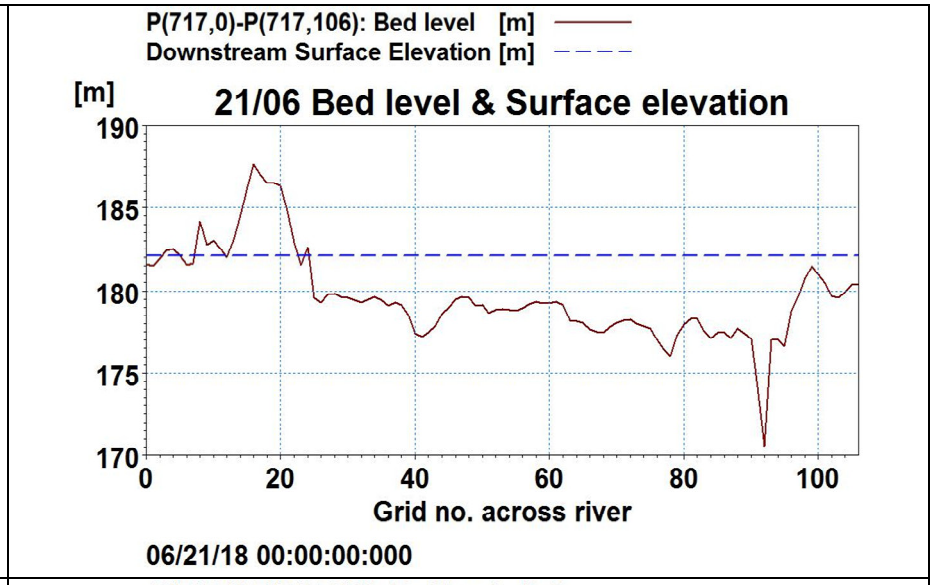
P(717,0)-P(717,106): Bed level [m]
Downstream Surface Elevation [m]
[m]
21/06 Bed level & Surface elevation
190
185
180
175
170
0
20
40
60
80
100
Grid no. across river
06/21/18 00:00:00:000

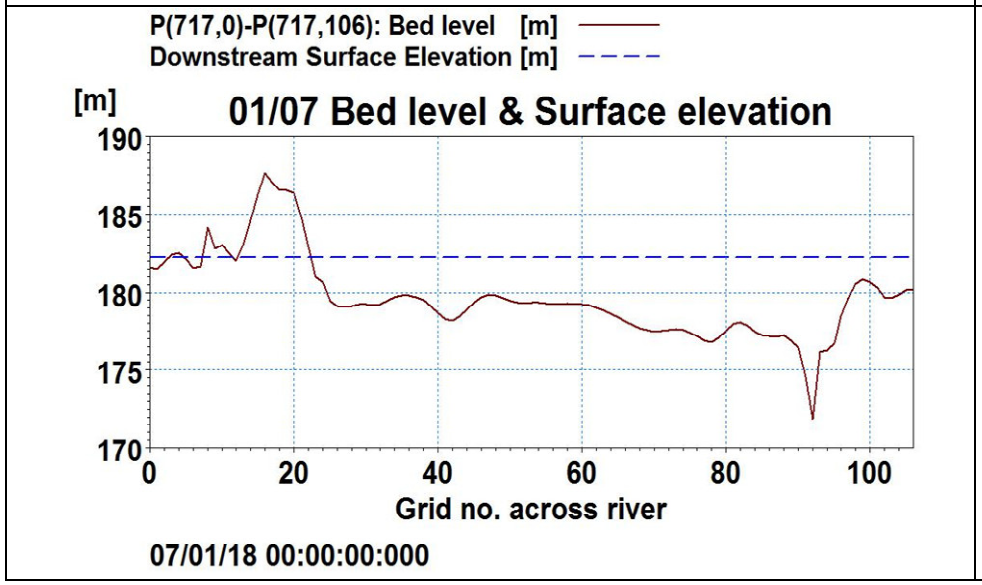
P(717,0)-P(717,106): Bed level [m]
Downstream Surface Elevation [m]
[m]
01/07 Bed level & Surface elevation
190
185
180
175
170
0
20
40
60
80
100
Grid no. across river
07/01/18 00:00:00:000

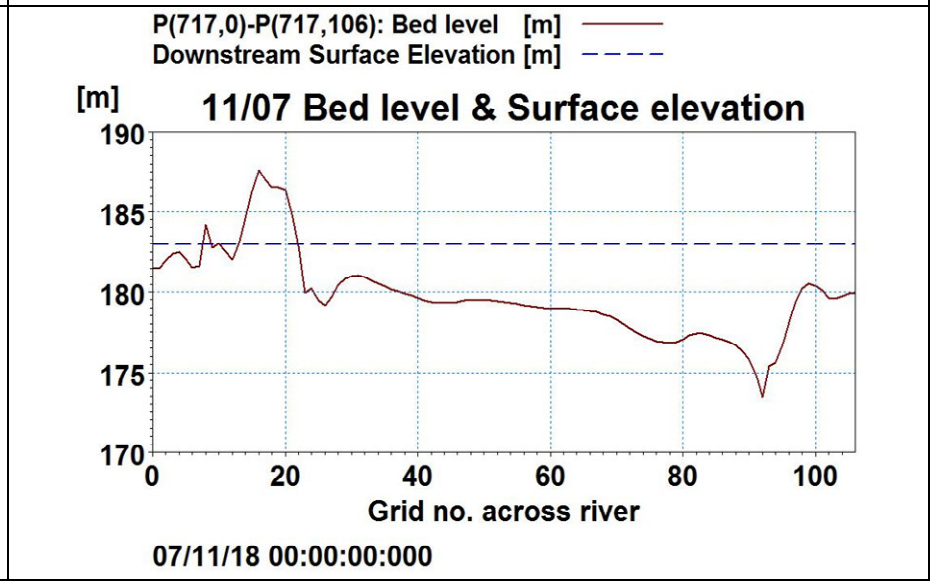
P(717,0)-P(717,106): Bed level [m]
Downstream Surface Elevation [m]
[m]
11/07 Bed level & Surface elevation
190
185
180
175
170
0
20
40
60
80
100
Grid no. across river
07/11/18 00:00:00:000

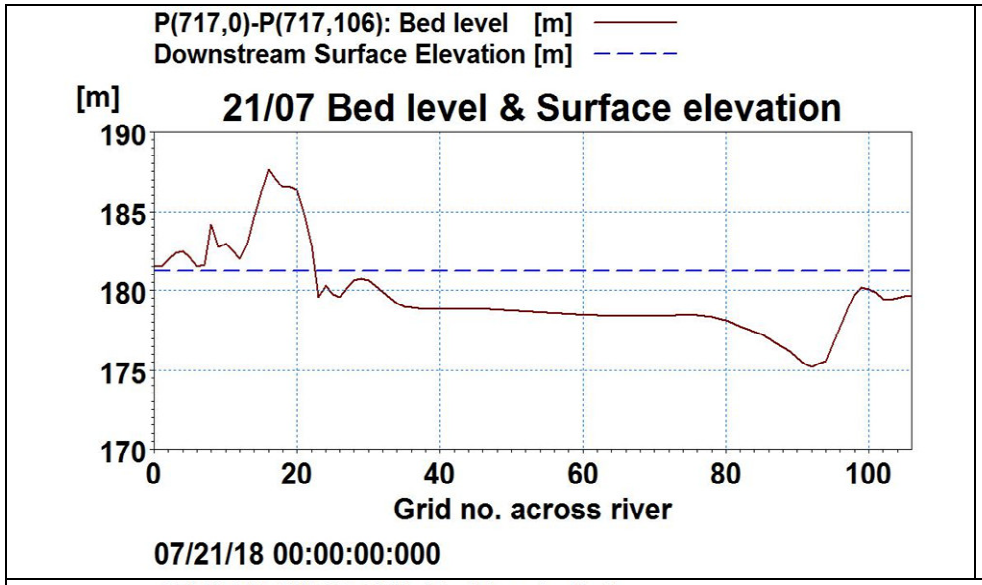
P(717,0)-P(717,106): Bed level [m]
Downstream Surface Elevation [m]
[m]
21/07 Bed level & Surface elevation
190
185
180
175
170
0
20
40
60
80
100
Grid no. across river
07/21/18 00:00:00:000

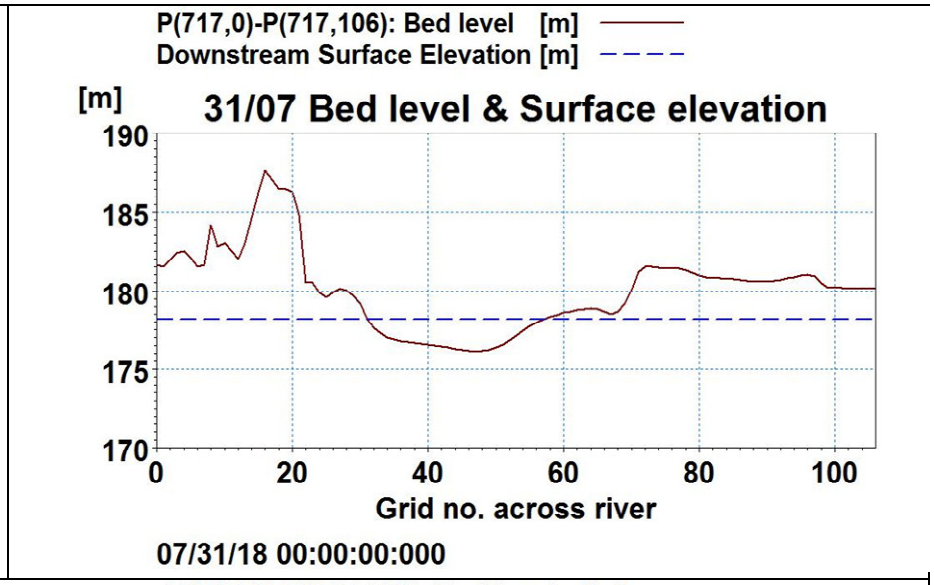
P(717,0)-P(717,106): Bed level [m]
Downstream Surface Elevation [m]
[m]
31/07 Bed level & Surface elevation
190
185
180
175
170
0
20
40
60
80
100
Grid no. across river
07/31/18 00:00:00:000

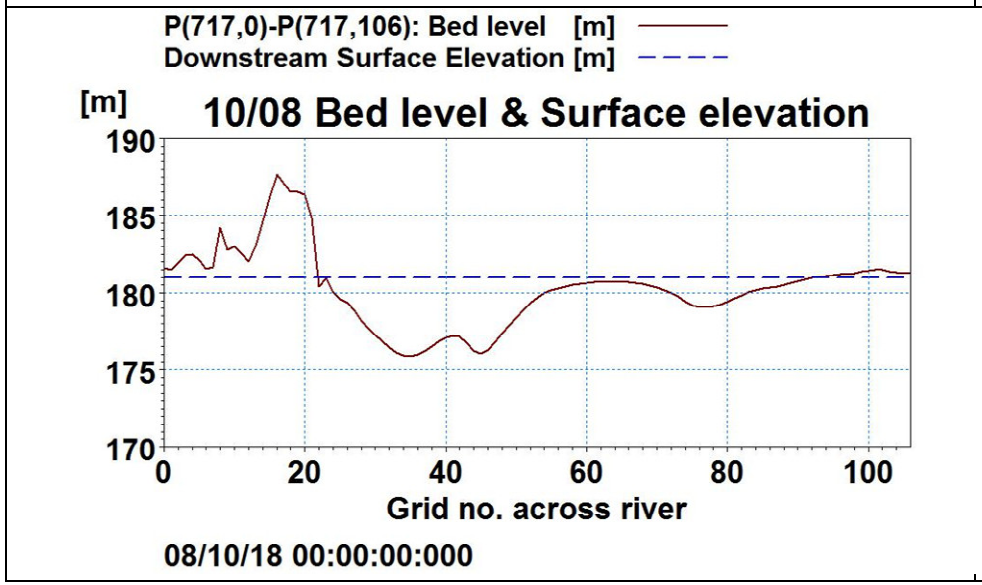
P(717,0)-P(717,106): Bed level [m]
Downstream Surface Elevation [m]
[m]
10/08 Bed level & Surface elevation
190
185
180
175
170
0
20
40
60
80
100
Grid no. across river
08/10/18 00:00:00:000

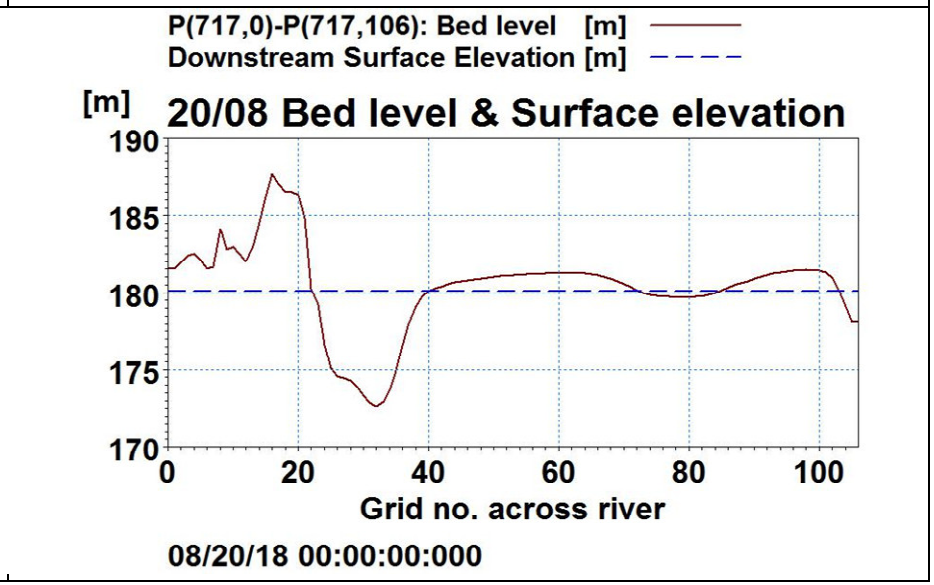
P(717,0)-P(717,106): Bed level [m]
Downstream Surface Elevation [m]
[m]
20/08 Bed level & Surface elevation
190
185
180
175
170
0
20
40
60
80
100
Grid no. across river
08/20/18 00:00:00:000

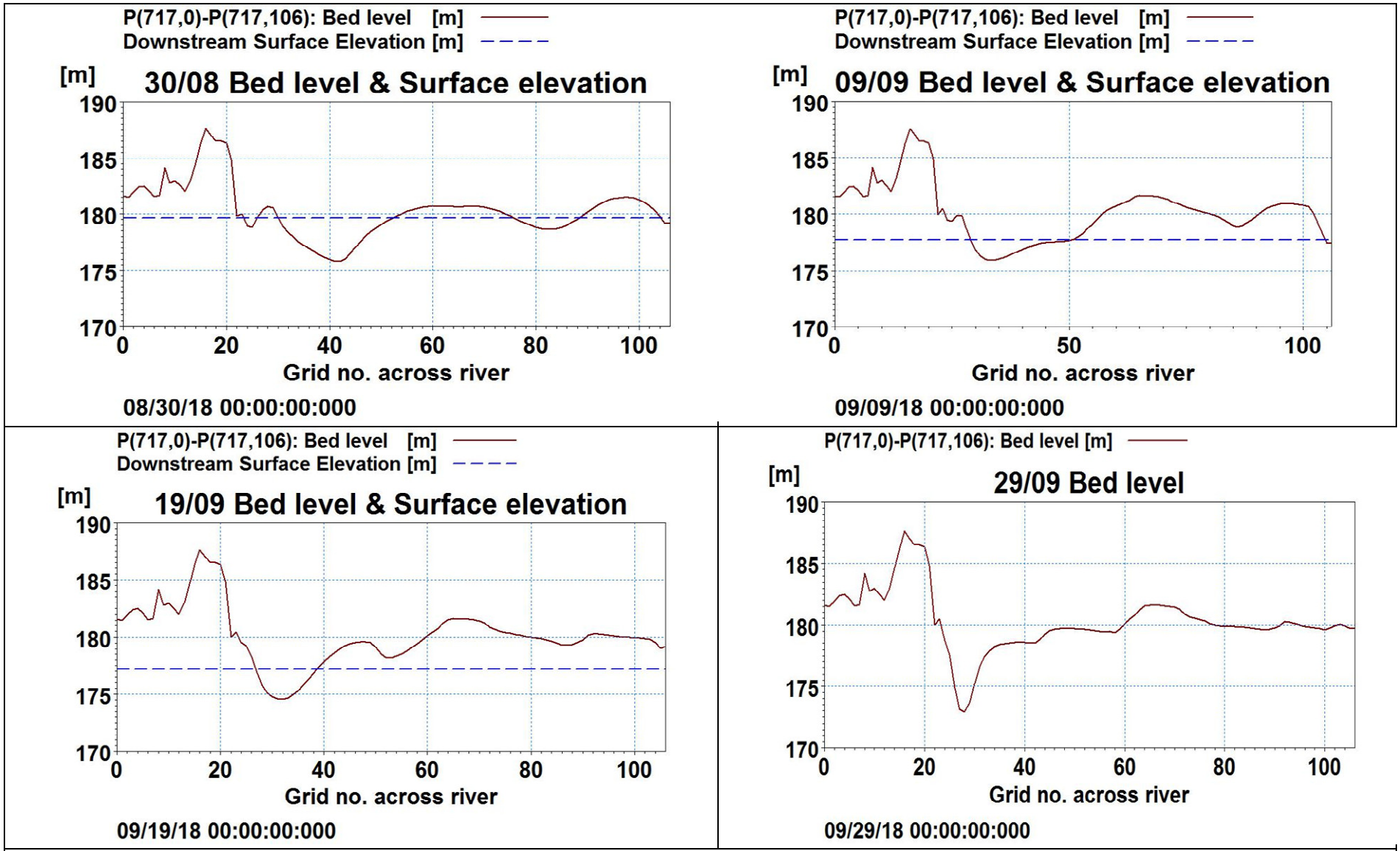

Figure 5.37: Temporal variation of river section at downstream location (j=717) for 100-year flood.

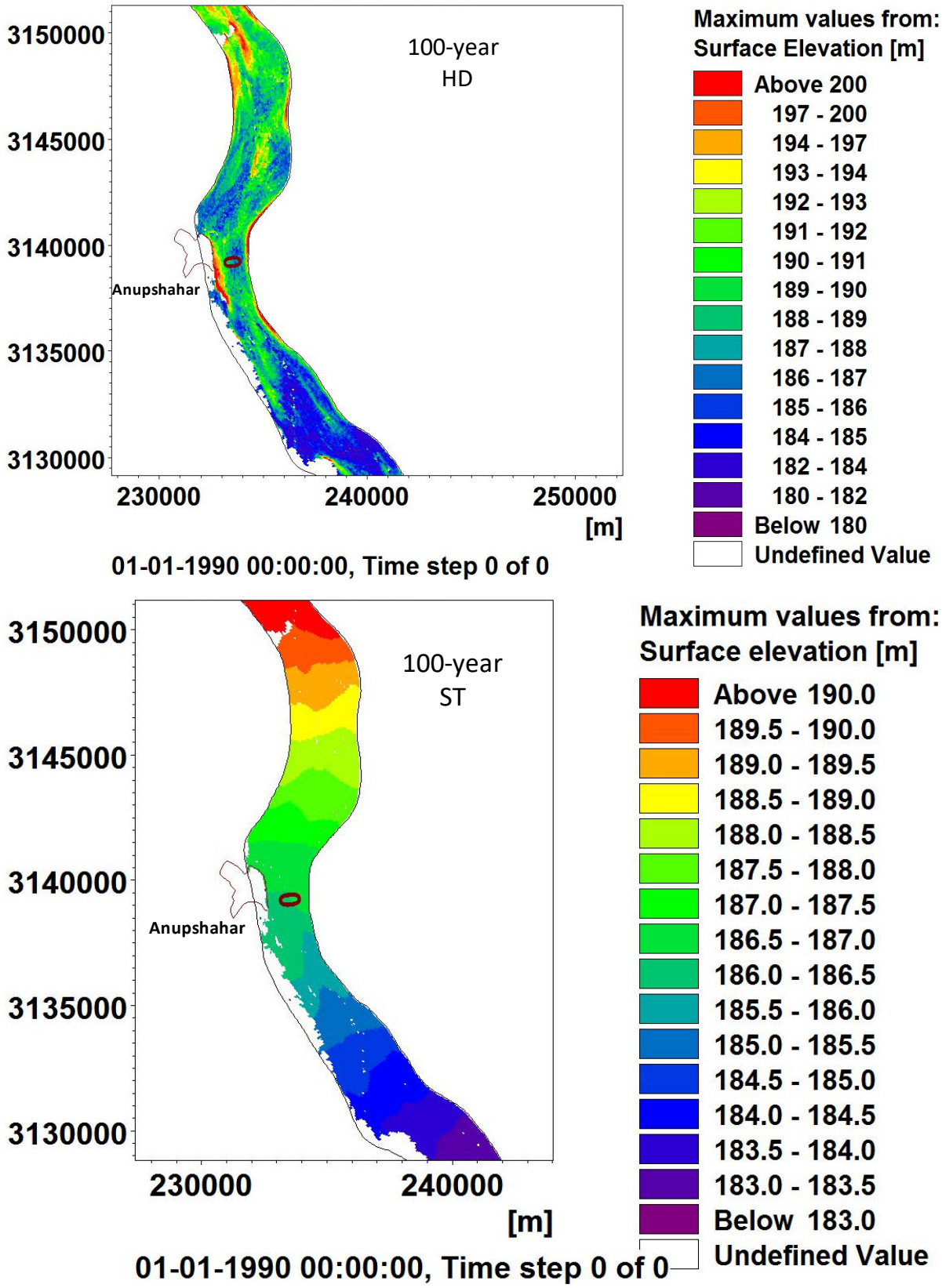

Figure 5.38: Maximum flood level map with and without sediment concentration for 100-year flood.

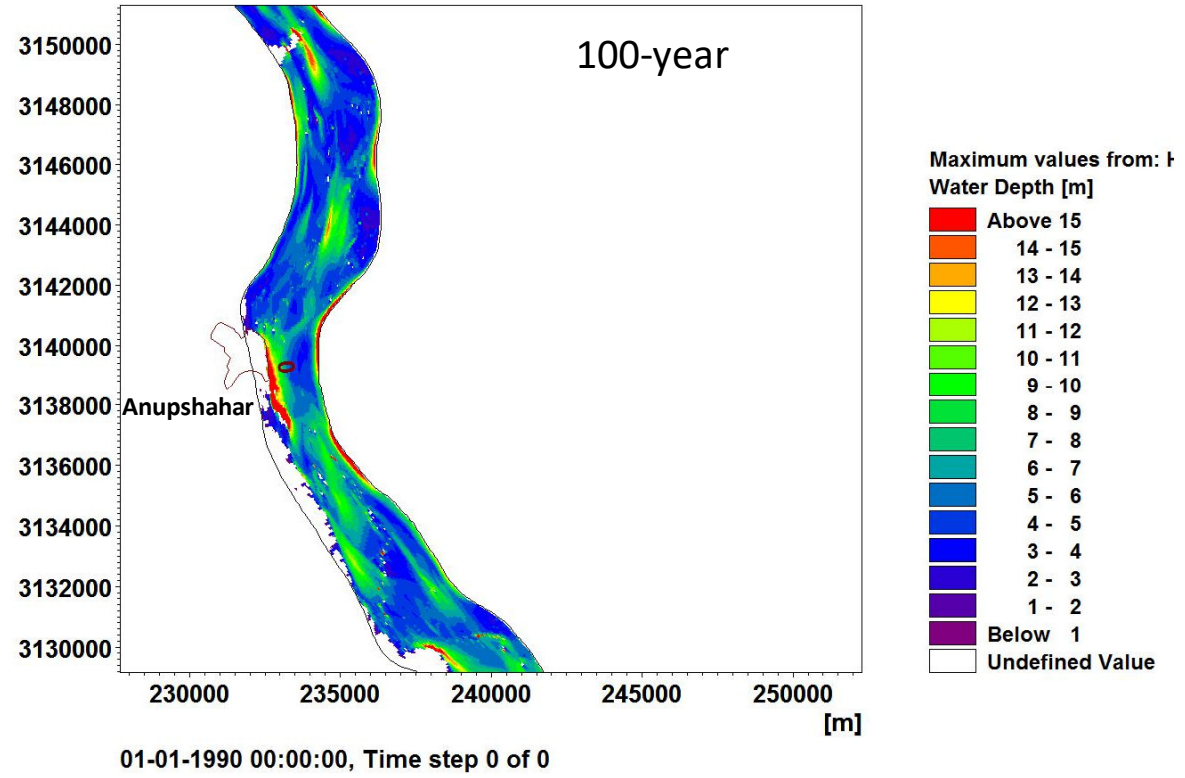

Figure 5.39: Map of maximum flooding depth for 100-year flood.

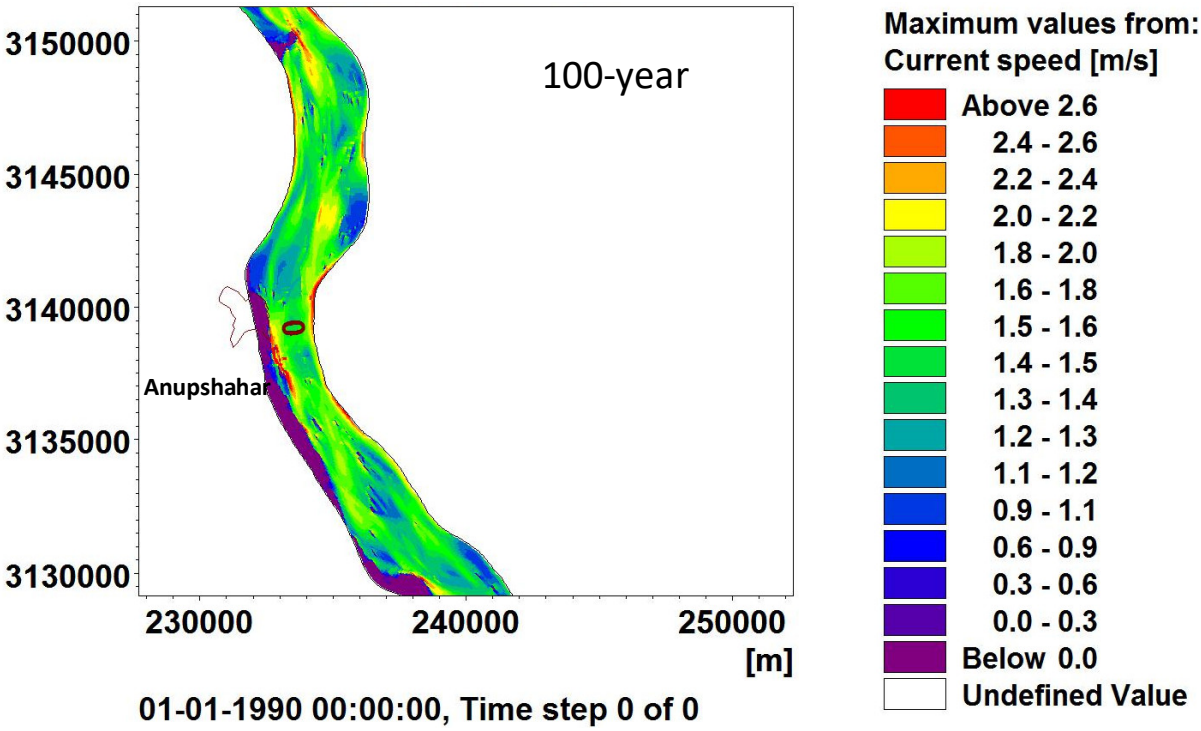

Figure 5.40: Map of maximum flow velocity for 100-year flood...

The ST model is further used to develop maps of maximum helical flow, sediment concentration and Sheer stress map. These flow attributes are needed when designing some

anti-erosion work at the affected site. The maps of maximum helical flow, sediment concentration and Sheer stress are shown in Figure 5.41, Figure 5.42 and Figure 5.43, respectively.

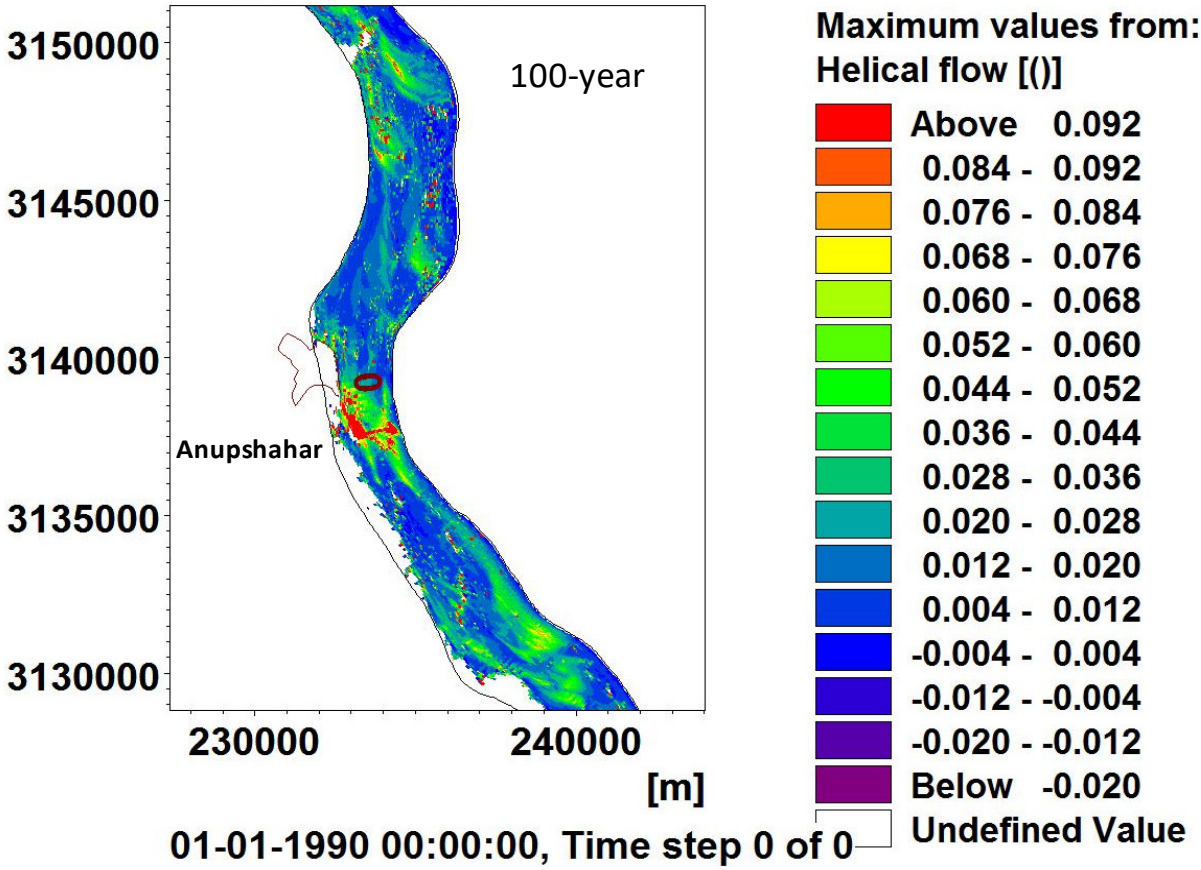

Figure 5.41: Map of the maximum helical flow for 100-year flood.

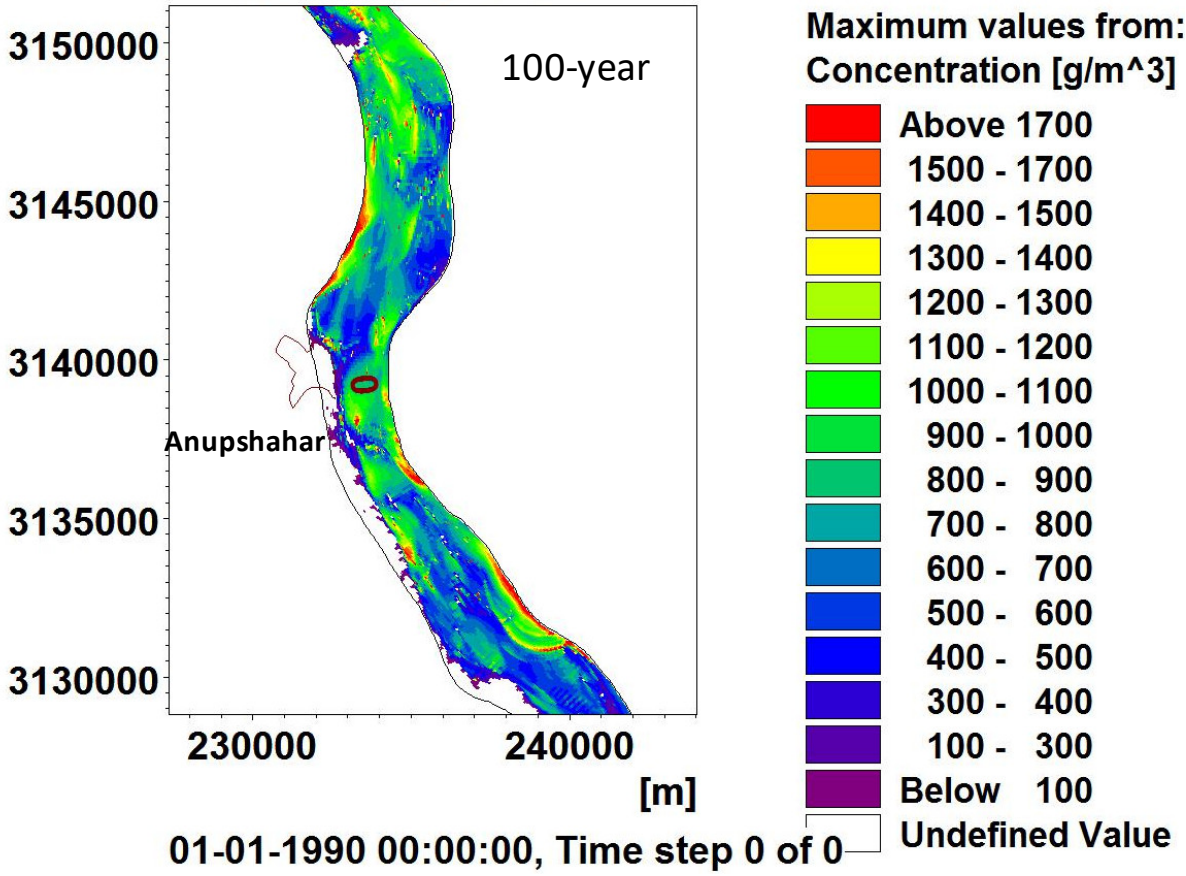

Figure 5.42: Map of maximum sediment concentration for 100-year flood.

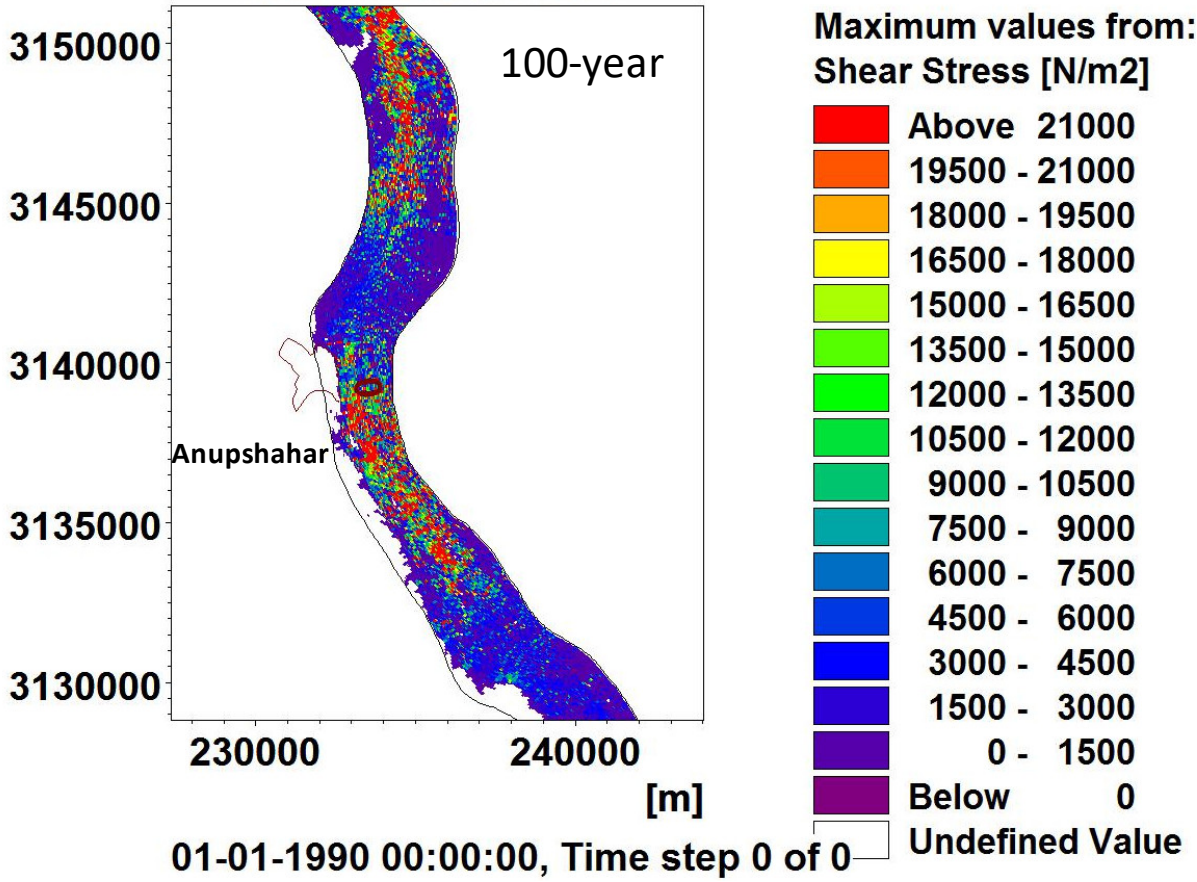

Figure 5.43: map of the maximum sheer stress for 100-year flood.

Short term model prediction has been carried out for 100 year flood (during 21 june to 29 September). The monsoon (15th June to 15th October) of 2017 has been repeated three times to use as upstream inflow condition to the 2-D model. The morphological developments have been evaluated at specific time on the temporal scale over the period. During the simulation, the bed level changes at every grid is captures at an average interval of 10 days for duration of three months (Figure 5.44). The blue shade shows the erosion while the green shade shows the deposition. The movement of river bed erosion during 100 year flood shows that erosion occurs near Anupshahar site, however, it moves gradually in the downstream direction over a period of time.

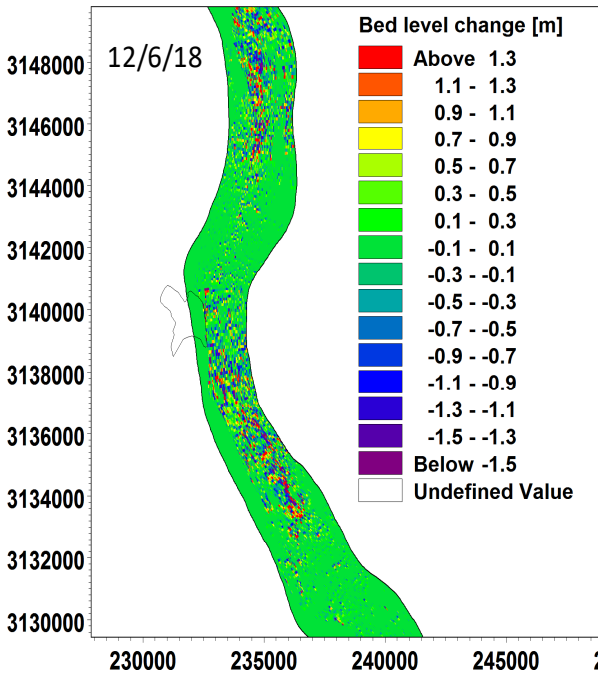
12/6/18
Bed level change [m]
Above 1.3
1.1 - 1.3
0.9 - 1.1
0.7 - 0.9
0.5 - 0.7
0.3 - 0.5
0.1 - 0.3
-0.1 - 0.1
-0.3 - -0.1
-0.5 - -0.3
-0.7 - -0.5
-0.9 - -0.7
-1.1 - -0.9
-1.3 - -1.1
-1.5 - -1.3
Below -1.5
Undefined Value
3148000
3146000
3144000
3142000
3140000
3138000
3136000
3134000
3132000
3130000
230000
235000
240000
245000

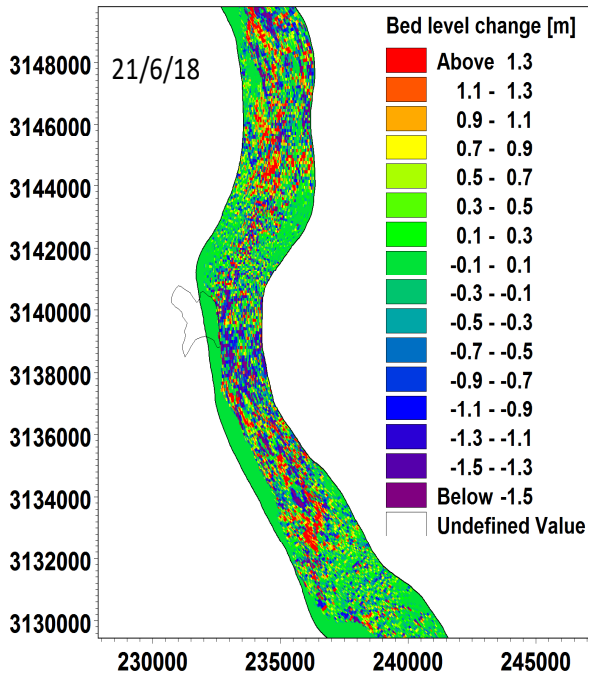
21/6/18
Bed level change [m]
Above 1.3
1.1 - 1.3
0.9 - 1.1
0.7 - 0.9
0.5 - 0.7
0.3 - 0.5
0.1 - 0.3
-0.1 - 0.1
-0.3 - -0.1
-0.5 - -0.3
-0.7 - -0.5
-0.9 - -0.7
-1.1 - -0.9
-1.3 - -1.1
-1.5 - -1.3
Below -1.5
Undefined Value
3148000
3146000
3144000
3142000
3140000
3138000
3136000
3134000
3132000
3130000
230000
235000
240000
245000

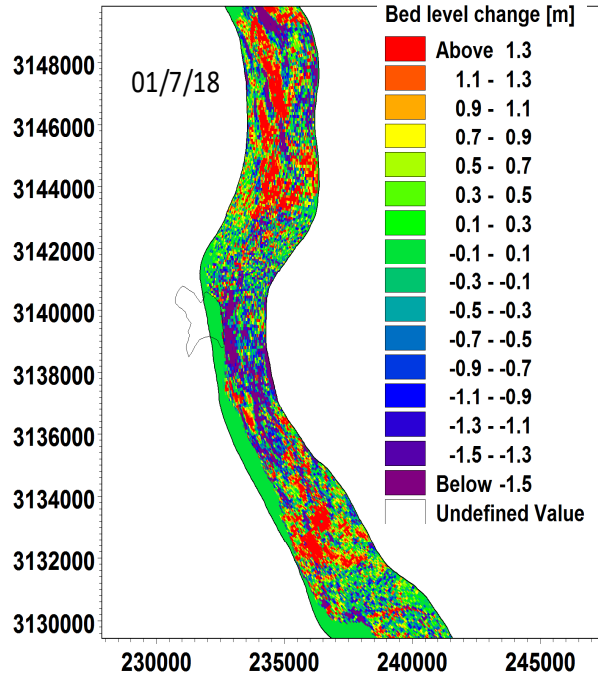
01/7/18
Bed level change [m]
Above 1.3
1.1 - 1.3
0.9 - 1.1
0.7 - 0.9
0.5 - 0.7
0.3 - 0.5
0.1 - 0.3
-0.1 - 0.1
-0.3 - -0.1
-0.5 - -0.3
-0.7 - -0.5
-0.9 - -0.7
-1.1 - -0.9
-1.3 - -1.1
-1.5 - -1.3
Below -1.5
Undefined Value
3148000
3146000
3144000
3142000
3140000
3138000
3136000
3134000
3132000
3130000
230000
235000
240000
245000

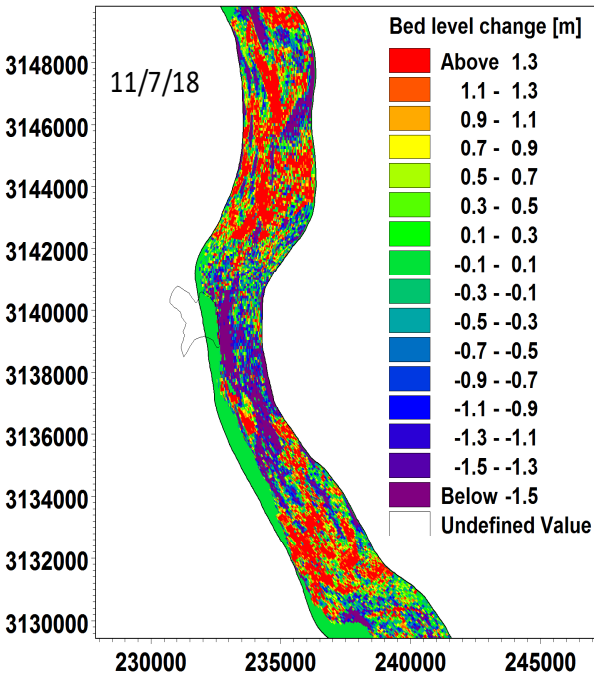
11/7/18
Bed level change [m]
Above 1.3
1.1 - 1.3
0.9 - 1.1
0.7 - 0.9
0.5 - 0.7
0.3 - 0.5
0.1 - 0.3
-0.1 - 0.1
-0.3 - -0.1
-0.5 - -0.3
-0.7 - -0.5
-0.9 - -0.7
-1.1 - -0.9
-1.3 - -1.1
-1.5 - -1.3
Below -1.5
Undefined Value
3148000
3146000
3144000
3142000
3140000
3138000
3136000
3134000
3132000
3130000
230000
235000
240000
245000

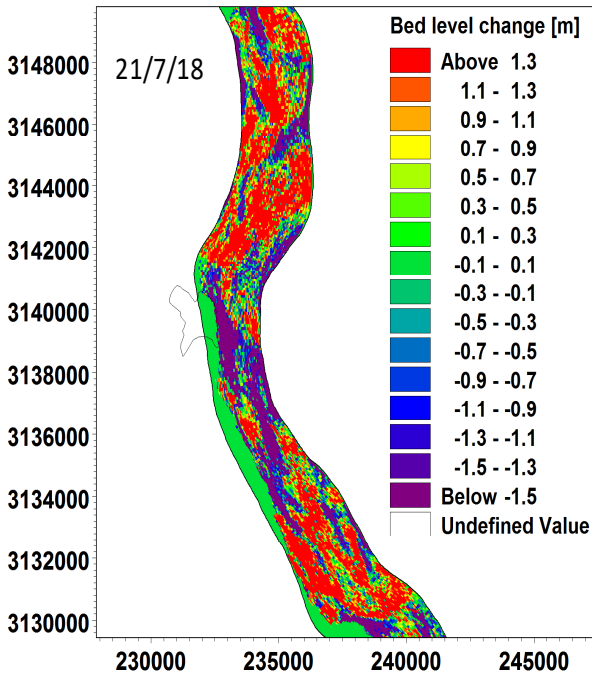
21/7/18
Bed level change [m]
Above 1.3
1.1 - 1.3
0.9 - 1.1
0.7 - 0.9
0.5 - 0.7
0.3 - 0.5
0.1 - 0.3
-0.1 - 0.1
-0.3 - -0.1
-0.5 - -0.3
-0.7 - -0.5
-0.9 - -0.7
-1.1 - -0.9
-1.3 - -1.1
-1.5 - -1.3
Below -1.5
Undefined Value
3148000
3146000
3144000
3142000
3140000
3138000
3136000
3134000
3132000
3130000
230000
235000
240000
245000

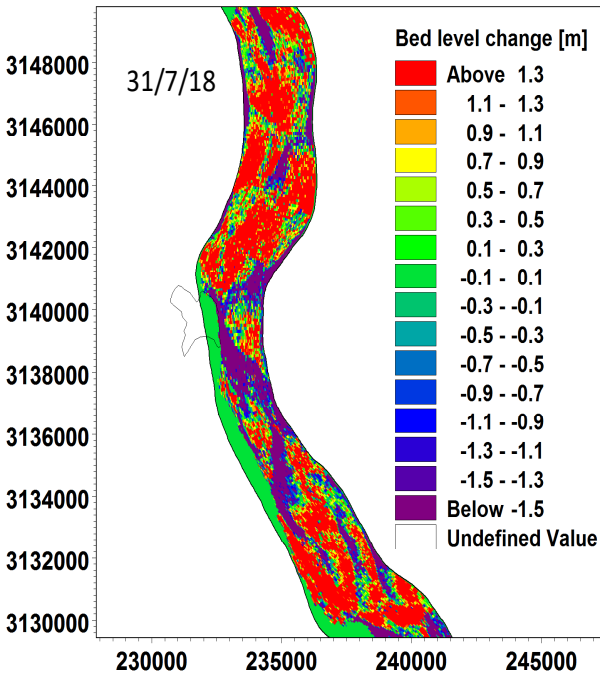
31/7/18
Bed level change [m]
Above 1.3
1.1 - 1.3
0.9 - 1.1
0.7 - 0.9
0.5 - 0.7
0.3 - 0.5
0.1 - 0.3
-0.1 - 0.1
-0.3 - -0.1
-0.5 - -0.3
-0.7 - -0.5
-0.9 - -0.7
-1.1 - -0.9
-1.3 - -1.1
-1.5 - -1.3
Below -1.5
Undefined Value
3148000
3146000
3144000
3142000
3140000
3138000
3136000
3134000
3132000
3130000
230000
235000
240000
245000

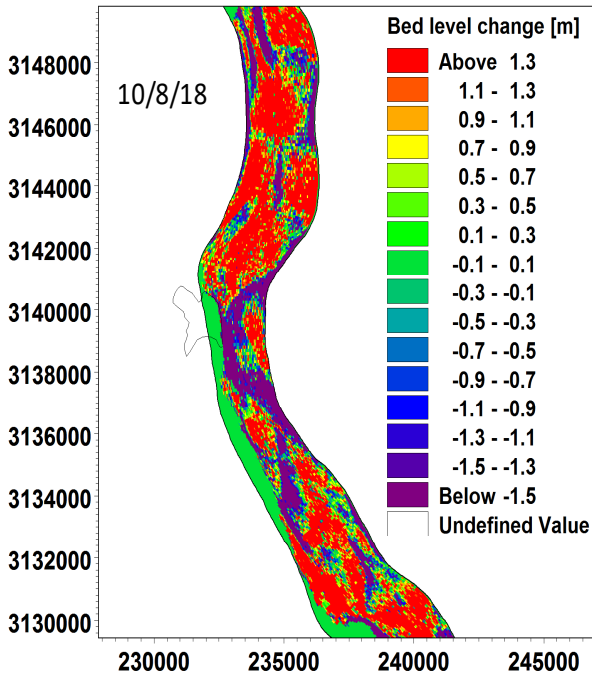
10/8/18
Bed level change [m]
Above 1.3
1.1 - 1.3
0.9 - 1.1
0.7 - 0.9
0.5 - 0.7
0.3 - 0.5
0.1 - 0.3
-0.1 - 0.1
-0.3 - -0.1
-0.5 - -0.3
-0.7 - -0.5
-0.9 - -0.7
-1.1 - -0.9
-1.3 - -1.1
-1.5 - -1.3
Below -1.5
Undefined Value
3148000
3146000
3144000
3142000
3140000
3138000
3136000
3134000
3132000
3130000
230000
235000
240000
245000

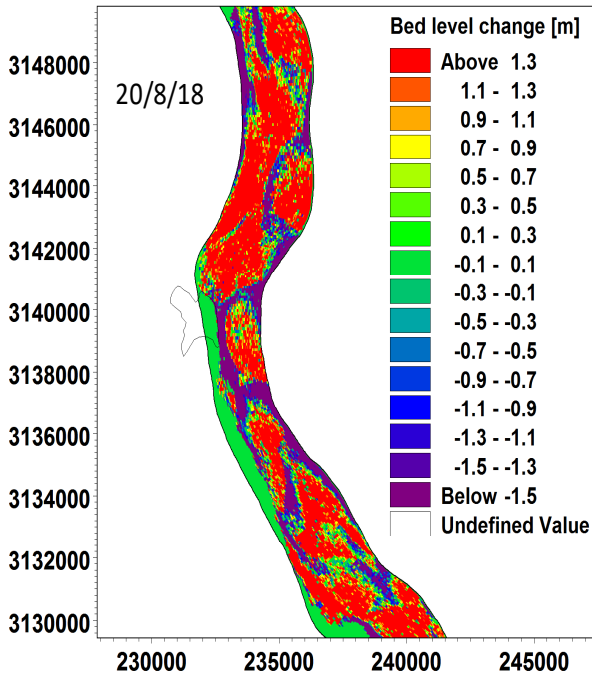
20/8/18
Bed level change [m]
Above 1.3
1.1 - 1.3
0.9 - 1.1
0.7 - 0.9
0.5 - 0.7
0.3 - 0.5
0.1 - 0.3
-0.1 - 0.1
-0.3 - -0.1
-0.5 - -0.3
-0.7 - -0.5
-0.9 - -0.7
-1.1 - -0.9
-1.3 - -1.1
-1.5 - -1.3
Below -1.5
Undefined Value
3148000
3146000
3144000
3142000
3140000
3138000
3136000
3134000
3132000
3130000
230000
235000
240000
245000

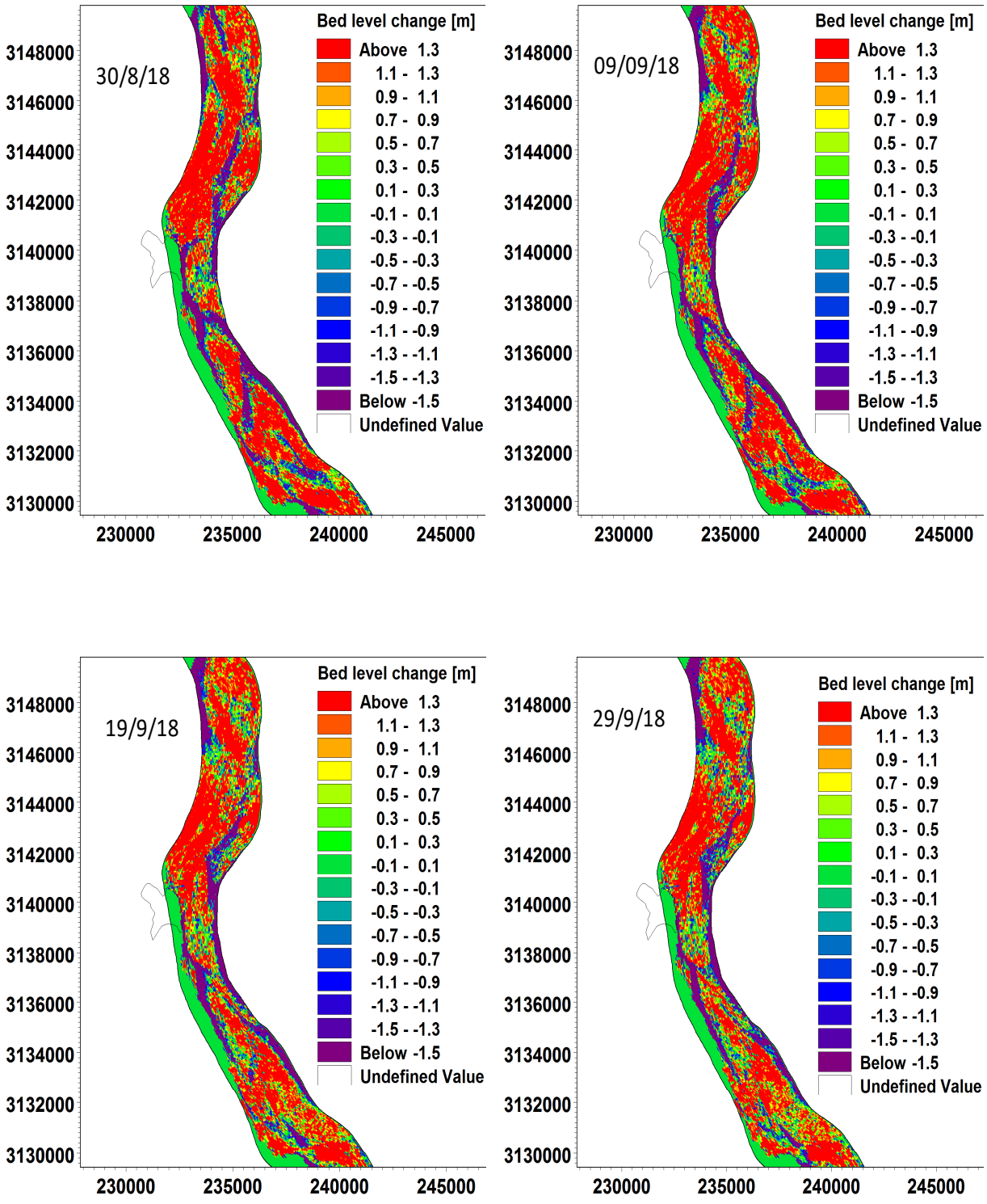

Figure 5.44: Short term morphological prediction for 100-year flood

6 CONCLUSION

1. Remote sensing images are very useful information for study of temporal behaviour of river course over a period of time.
2. Image processing and GIS tools are helpful in analysis remote sensing data, extracting information and its analysis for river shifting study.
3. Eight critical locations namely; Alamgirpur, Pooth, Alapur, Mandu, Ahar, Anupshahar, Sherpur and Karanwas are identified where the river has shifted considerably and for which detailed shifting analysis has been carried out.
4. The maximum shift at Alamgirpur is computed as 897 m, at Pooth 705 m, at Alapur 200 m, at Mandu 212 m, at Ahar 948 m, at Anupshahar 400 m, at Sherpur 783 m, and at Karanwas 662 m. All locations other than Anupshahar is rural settlement and therefore small population is affected. However agricultural activities at these locations are affected significantly.
5. Anupshahar being urban settlement, small amount of erosion is also critical. The shifting trend analysis shows that at Anupshahar, river is shifting 23 m per year.
6. 1D river flow model has been developed in MIKE 11 and 25 year and 100-year flood hydrograph is simulated to compute the maximum flood level, flood inundation and maximum flow velocity near Anupshahar. The maximum flood level for 25- and 100- year flood at Anupshahr is computed as 182.07m and 182.68 m, respectively. The maximum flow velocity for 25- and 100- year flood is computed as 1.8 m/s.
7. The curvilinear grid based morphodynamic model is developed in MIKE 21C for the study area with 1486x107 grids. The monsson data for year 2013 is used to calibrate and validate the model.
8. The sediment balance analysis has been carried out for 2013 flow data and river reach of erosion/ deposition have been identified and the quantitative sediment balance is estimated.
9. MIKE 21C model is simulated for 25-and 100- year flood and various flow attributes like, temporal variation of river bed at selected river sections, maximum flood level, maximum flood depth and maximum flow velocity for HD flow simulation is computed. Considering the sediment transport, the maximum flood level, helical flow, sediment

concentration, and sheer stress has been computed.

10. The results shows that with the inclusion of sediment transport, the lower values of maximum flood level is computed compared to HD modelling. This is due to inclusion of scour and mobile bed in sediment transport model.

11. For 25- and 100- year flow model the short term morphological changes/ behaviour of river has been simulated and temporal maps are presented.

REFERENCES

Ahmed, A. A., & Fawzi, A. (2011). Meandering and bank erosion of the River Nile and its environmental impact on the area between Sohag and El-Minia, Egypt. Arabian Journal of Geoscience, 4, 1–11.

Ashraf, M., Bhatti, M. T., & Shakir, A. (2016). River bank erosion and channel evolution in sand-bed braided reach of River Chenab: Role of floods during different flow regimes. Arabian Journal of Geoscience, 9, 140.

Baki, A. B. M., & Gan, T. Y. (2012). Riverbank migration and island dynamics of the braided Jamuna river of the Ganges– Brahmaputra basin using multi-temporal Landsat images. Quaternary International, 263, 148–161.

Bandyopadhyay, S., Ghosh, K., & De, S. K. (2014). A proposed method of bank erosion vulnerability zonation and its application on the River Haora, Tripura, India. Geomorphology, 224, 111–121.

Banerjee, S.N. & Chakraborty, P. (1983), Some observations on recent trends of shifting of the Ganga between Rajmahal and Ahiron, Journal of the Geological Society of India, 24, pp 318-321.

Bartley, R., Keen, R. J., Hawdon, A. A., Hairsine, P. B., Disher, M. G., & Kinsey-Henderson, A. E. (2008). Bank erosion and channel width change in a tropical catchment. Earth Surface Processes and Landforms, 33, 2174–2200.

Barton, I. and Bathols, J.: 1989, Monitoring floods with AVHRR**,** International Journal of Remote Sensing 10**(**12), 1873–1892.

Bates, P. D., Lane, S. N. and Ferguson, R. I. 2005. Computational Fluid Dynamics: Applications in Environmental Hydraulics. *John Wiley & Sons Ltd*.

Bednarz, Sarah Witham. Impact and success: Evaluating a GIS training institute. Proceedings, 19th Annual ESRI User Conference. July, San Diego, California. http://gis.esri.com/library/user-conf/proc99/proceed/papers/pap895/p895.htm. Last visited August 30, 2002.

Bhakal, L., Dubey, B., & Sarma, A. K. (2005). Estimation of bank erosion in the river Brahmaputra near Agyathuri by using geographic information system. Journal of the Indian Society of Remote Sensing, 33(1), 81–84

Bhowmik, M., & Pan, N. D. (2014). Qualitative assessment of bank erosion hazard in a part of the Haora River, West Tripura District. In M. Singh (Ed.), Landscape ecology and water management (pp. 193–203). Tokyo: Springer.

Chatterjee, C. Forster, S and Bronstert A. 2008. Comparison of hydrodynamic models of different complexities to model floods with emergency storage areas. *Hydrol. Process.* 22, 4695–4709 (2008)

Christensen B. B., Jirinec P., Larsen Ole and Paetsch M. 2006. MIKE 21C – Morphological and Hydrodynamic Modeling Software and its application on River Loire and Labe,

Clarke, K. C., 1986. Advances in geographic information systems, computers, environment and urban systems, Vol. 10, pp. 175–184.

Clarke, K. C., 1986. Advances in geographic information systems, computers, environment and urban systems, Vol. 10, pp. 175–184.

Crampton, J. (1995). The Ethics of GIS. Cartography and Geographic Information Systems 22(1): 84-89.

Cunge, J. A., Holly, F. M. and Verwy, A. 1980. Practical Aspects of Computational River Hydraulics. Pitman, London.

CWC, (2012). Handbook of flood protection, anti-erosion and river training works, Flood Management Organisation, Central Water Commission, New Delhi.

Dehghani, M. & Afrazi, M. (2014). Choosing the best route variants base on Environmental parameters by means of remote sensing and GIS.3rd International conference on recent advances in, railway engineering.

Dhondia, Z. and Stelling, G. 2002. Application of one-dimensional - two-dimensional integrated hydraulic model for flood simulation and damage assessment. *Intl. Conf. on Hydroinformatics, Cardiff, UK, Proc*. 5: 265-276.

Forster, S., Chatterjee, C. and Bronstert A. 2008. Hydrodynamic simulation of the operational management of a proposed flood emergency storage area at the middle Elbe river. River Research Application 24: 900–913 (2008).

Geographic Information Systems as an Integrating Technology: Context, Concepts, and Definitions". Kenneth E. Foote and Margaret Lynch, The Geographer's Craft Project, Department of Geography, The University of Colorado at Boulder. Retrieved21 Apr. 2015.

Geographic Sciences and Natural Resources Research,CAS,Beijing 100101);Preliminary Establishment of the GIS Platform of Water Cycle of the River Basin[J];Progress In Geography;2003-05

Goodchild, Michael F (2010). "Twenty years of progress: GIScience in 2010".Journal of Spatial Information Science (1). doi:10.5311/JOSIS.2010.1.2. "Arcgis homepage″. Arcgis.com. Retrieved 2015-07-26.

Horritt, M. S. and Bates, P. D. 2002. Evaluation of 1D and 2D numerical models for predicting river flood inundation. *J. of Hydrology*. 268: 87-99.

https://www.researchgate.net/publication/269694554_Bank_shifting_of_river_Ganga_in_the_downstream_of_Bhagalpur_Vikramshila_Setu [accessed Jul 6, 2017].

Maliene V, Grigonis V, Palevičius V, Griffiths S (2011). "Geographic information system: Old principles with new capabilities". Urban Design International. pp. 1–6. doi:10.1057/udi.2010.25.

Mani, P., Chatterjee, C. and Kumar, R. 2014. Flood hazard assessment with multiparameter approach derived from coupled 1D and 2D hydrodynamic flow model. Nat. Hazards, 70: 1553–1574.

Mani, P., Kumar, R., & Chatterjee, C. (2003). Erosion study of a part of Majuli River-Island using remote sensing data. Journal of the Indian Society of Remote Sensing, 31(1), 12–18

Morianou, G. G., Kourgialas, N. N. and Karatzas, G. P. 2016b Comparison between curvilinear and rectilinear grid based hydraulic models for river flow simulation.

Morianou, G. G., Kourgialas, N. N., Karatzas, G. P. and Nikolaidis, N. P. 2016a Hydraulic and sediment transport simulation of Koiliaris River using the MIKE 21 C model.

Moriaou, G. G., Kourgialas N. N., Karatzas G. P. and Nikolaidis N. P, 2017 Assessing hydro-morphological changes in Mediterranean stream using curvilinear grid modelling approach – climate change impact.

Mukherjee, R., Bilas, R., Biswas, S.S. et al. Bank erosion and accretion dynamics explored by GIS techniques in lower Ramganga river, Western Uttar Pradesh, India. Spat. Inf. Res. 25, 23–38 (2017). https://doi.org/10.1007/s41324-016-0074-2

Nardi, L., Campo, L., & Rinaldi, M. (2013). Quantification of riverbank erosion and application in risk analysis. Natural Hazards, 69, 869–887.

Ngunyi, J., Mundia, C., & Gachari, M. (2017). Analysis of Standard Gauge Railway Using GIS and Remote Sensing.American Journal of Geographic Information System,6(2), 54-63.

Pal, R., Biswas, S. S., Pramanik, M. K., & Mondal, B. (2016). Bank vulnerability and avulsion modeling of the BhagirathiHugli river between Ajay and Jalangi confluences in lower Ganga Plain, India. Modeling Earth Systems and Environment, 2(2), 65.

Patro, S, Chatterjee C, Mohanty S, Singh R and Raghuwanshi N. S. 2009. Flood inundation modeling using MIKE FLOOD and remote sensing data, *Journal of the Indian Society of Remote Sensing.* 37(1):107-118.

Pramanik N, Panda R. K. and Sen D. J. 2010. One dimensional hydrodynamic modeling of river flow using DEM extracted river cross-sections, *Water Resources Management.* 24(5):835-852

Rana, N. K., Kumar, R., & Kumar, D. (2009). Nature of channel shifting of foothills Fed river in alluvial setting: A case study of River Rapti, India. Indian Journal of Geomorphology, 13-14, 83–98.

Rungo, M. and Olesen, K. W. 2003. Combined 1- and 2- dimensional flood modelling. *4th Iranian Hydraulic Conference*, 21-23 Oct, Shiraz, Iran.

Sarma, J. N., & Acharjee, S. (2012). A GIS based study on bank erosion by the river Brahmaputra around Kaziranga National Park, Assam, India. Earth System Dynamics Discussions, 3(2), 1085–1106

Sarma, J. N., Bora, D., & Goswami, U. (2007). Change of river channel and bank erosion of the Burhi Dihing river (Assam), assessed using remote sensing data and GIS. Journal of the Indian Society of Remote Sensing, 35, 93–100.

Sen D. J. and Garg N. K. 1998. Efficient solution technique for dendritic channel networks, *J. of Hydrologic Engineering.* 124: 831-839.

Singh, D. S., & Awasthi, A. (2011). Natural hazards in the Ghaghara River area, Ganga Plain, India. Natural Hazards, 57(2), 213–225

Sinha, R., & Ghosh, S. (2012). Understanding dynamics of large rivers aided by satellite remote sensing: A case study from Lower Ganga plains, India. Geocarto International, 27(3), 207–219

Sinha, R., Sripriyanka, K., Jain, V., & Mukul, M. (2014). Avulsion threshold and planform dynamics of the Kosi River in north Bihar (India) and Nepal: A GIS framework.Geomorphology,216, 157-170.

Tayade B.S., Oak A.R., Isaac N., Sohoni S.V., 2016 Application of 2D modelling for design of anti erosion works for a braided river – a case study.

Thakur, P. K., Laha, C., & Aggarwal, S. P. (2012). River bank erosion hazard study of river Ganga, upstream of Farakka barrage using remote sensing and GIS. Natural Hazards, 61(3), 967–987.

Tingsanchali, T. and Karim, M. F. 2005. Flood hazard and risk analysis in the southwest region of Bangladesh. *Hydrological Processes*. 19(10): 2055-2069.

Usul, N and Turan B. 2006. Flood forecasting and analysis within the Ulus Basin, Turkey, using geographic information systems, *Natural Hazards.* 39(2):213-229

Winterbottom, S. J., & Gilvear, D. J. (2000). A GIS-based approach to mapping probabilities of river bank erosion: Regulated River Tummel, Scotland. Regulated Rivers: Research ad Management, 16, 127–140